THE THERMOPOWER AND RESISTIVITY OF NEARLY MAGNETIC DILUTE ALLOYS

by

Constantin Wassilieff

Submitted for the degree of Doctor of Philosophy in Physics at Victoria University of Wellington, 1982.

TABLE OF CONTENTS

ABSTRACT

In some nearly magnetic dilute alloys, in which the host and impurity are transition metals of similar electronic structure, the thermopower is observed to form a "giant" peak at about the spin fluctuation temperature T_{sf} deduced from resistivity measurements. Two explanations for these peaks have been postulated: the first is that the peaks are a diffusion thermopower component involving scattering off localized spin fluctuations (LSF) at the impurity sites; the second is that they are an LSF drag effect.

We examine the thermopower and resistivity of two nearly magnetic alloy systems: Rh(Fe) and Pt(Ni).

In the first part of this thesis we describe measurements of the low temperature thermopower and resistivity of several Rh(Fe) alloys to clarify discrepancies in previous measurements and we show, by using a modified Nordheim-Gorter analysis, that the observed thermopower peaks are a diffusion and not a drag effect.

In the second part of the thesis we describe measurements of the low temperature thermopower and resistivity of Pt(Ni), for which no previous data had been available. The Pt(Ni) samples are manufactured as thin, evaporated films on glass substrates. However, due to the difficulty encountered in controlling the very high residual resistivity of these samples, we are not able to draw definite conclusions regarding either the thermopower or the resistivity.

ACKNOWLEDGEMENTS

I wish to thank the following people for assistance given in the course of this work:

David Beaglehole, Dave Gilmour, Peter Gilberd, Alan Kaiser, Peter Schroeder, Joe Trodahl, Bjorn Vartik and anyone else whom I may have forgotten.

INTRODUCTION

The first part of this thesis is concerned with the long-standing problem of the thermopower of dilute Rh(Fe) alloys at low temperatures. The oustanding problems, which we successfully resolve, are as follows:

1) The temperature at which a "giant", negative peak has been observed to occur has not been certain.
2) The concentration-dependence of the peak magnitude is apparently opposite to that observed in the similar LSF alloys Pd(Ni) and Ir(Fe).
3) The mechanism responsible for the peak could either be a diffusion effect or a spin fluctuation drag effect, the latter proposed by Kaiser (1976).

In Chapter One we discuss magnetic and nearly magnetic impurities in metals. A quasi-historical account is given which forms the basis of a discussion of localized spin fluctuations and their effect upon the resistivity of alloys containing nearly magnetic impurities.

In Chapter Two we present a discussion of the thermopower of alloys with transition metal impurities, concluding with an account of spin fluctuation drag thermopower.

Pertinent experimental details are described in Chapter Three. We describe the design of cryostats for measuring the thermopower and resistivit- of wire samples and present an account of the measurement process.

The analysis of experimental data is described in Chapter Four, in which we modify the traditional Nordheim-Gorter Rule for the addition of diffusion thermopowers so that it is capable of application in the case of samples whose host residual resistivity is not constant from sample-to-sample, the latter condition being necessary for the application of the traditional Nordheim-Gorter Relation. In fact we deliberately alter the host residual resistivity as part of our method to distinguish diffusion and drag mechanisms. We review previously published data on the resistivity and thermopower of Pd(Ni), Ir(Fe) and Rh(Fe) and conclude the first part of the thesis with an analysis of our Rh(Fe) resistivity and thermopower data, by which means we resolve the problems mentioned previously, showing that the observed thermpower peaks are a diffusion and not a drag effect.

In the second part of the thesis we describe the manufacture and the low temperature measurements of the resistivity and thermopower of thin film samples of Pt(Ni). We compare these measurements with those of wire samples of Pt(Ni). As Pt(Ni) should be an alloy of the LSF type its resistivity and thermopower should have similar characteristics to those of other LSF alloys. We seek to do three things:

1) Determine T_{sf} from the resistivity measurements.
2) Look for possible features in the thermopower connected with LSF at the Ni impurity sites.
3) If visible, determine whether these features are a diffusion or a spin fluctuation drag effect, as we do in the first part of the thesis.

However, physical characteristics such as the residual resistivity of the films prove to be difficult to control and we are unable to achieve our objectives with these samples. Definitive resistivity and thermopower data on Pt(Ni) films have yet to appear.

Chapter One

THE FORMATION OF LOCAL MAGNETIC MOMENTS

1.1 Freidel's Virtual Bound State

To visualize Freidel's concept, let us add a transition metal impurity, characterized by an incomplete d-shell, to a metal host whose electronic states are approximated by the free electron gas model. Let us suppose that the energy of the impurity d-level lies within approximately $k_B T$ of the Fermi level E_F of the host so that it can contribute to the electronic properties of the alloy. We find that the conduction electrons mix with the d-electrons to broaden the d-level. If the d-level was buried well down below the conduction band it would not be able to interact with the conduction electrons at all and hence would have an infinite lifetime. It would be a bound state characterized by an infinitely narrow energy width. With the former case a conduction electron can temporarily occupy the vacant d-state and escape again into the conduction band states that are near to it in energy. The lifetime of the state is thus limited and hence it is broadened in energy. It is not a bound state but a virtually bound state (VBS), after Freidel (1958) who first introduced the concept.

The energy of the VBS in a particular host is determined by the excess charge ΔZ on the impurity since the Fermi level of the host remains unchanged (charge neutrality condition). The effect of this may be seen as we consider a succession of 3-d impurities in a simple metal host, for example, Al. There is room for 2 x (21 + 1) = 10 electrons of both spins in a d-level. Hence when $\Delta Z = 5$ we would expect the VBS to occur at E_F where half of the d-states are on either side of E_F.

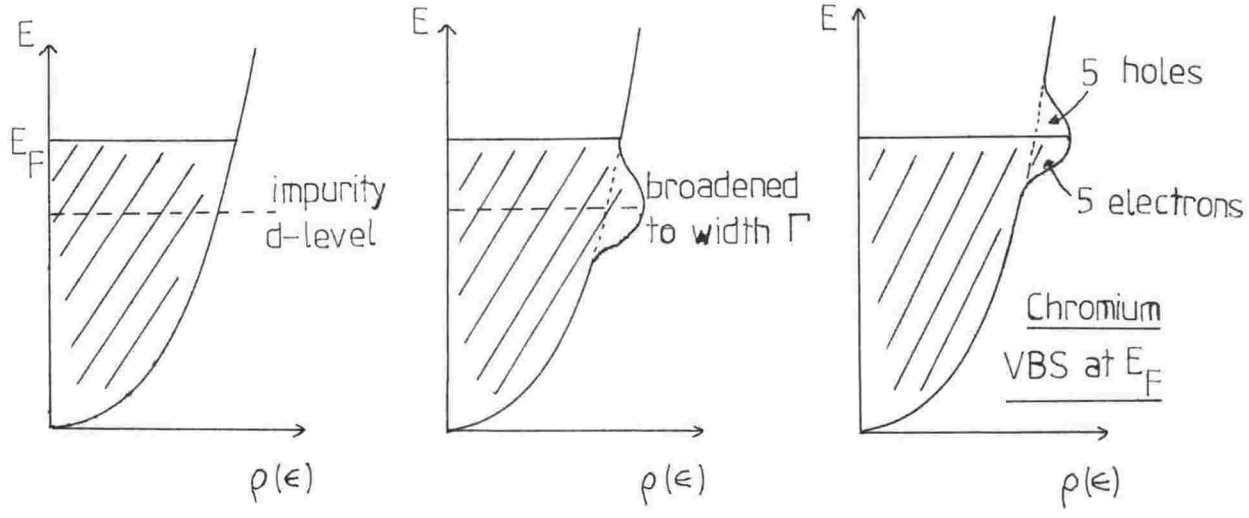

This situation is met in Al(Cr) with atomic Cr having 5 d-electrons. Now, since the VBS is at E_F, the maximum number of conduction electrons can interact with (scatter off) the VBS and hence the residual restivity will be a maximum, with 3-d elements to the left of Cr ($\Delta Z<5$) and to the right ($\Delta Z>5$) having a smaller residual resistivity as the VBS is correspondingly above and below E_F.

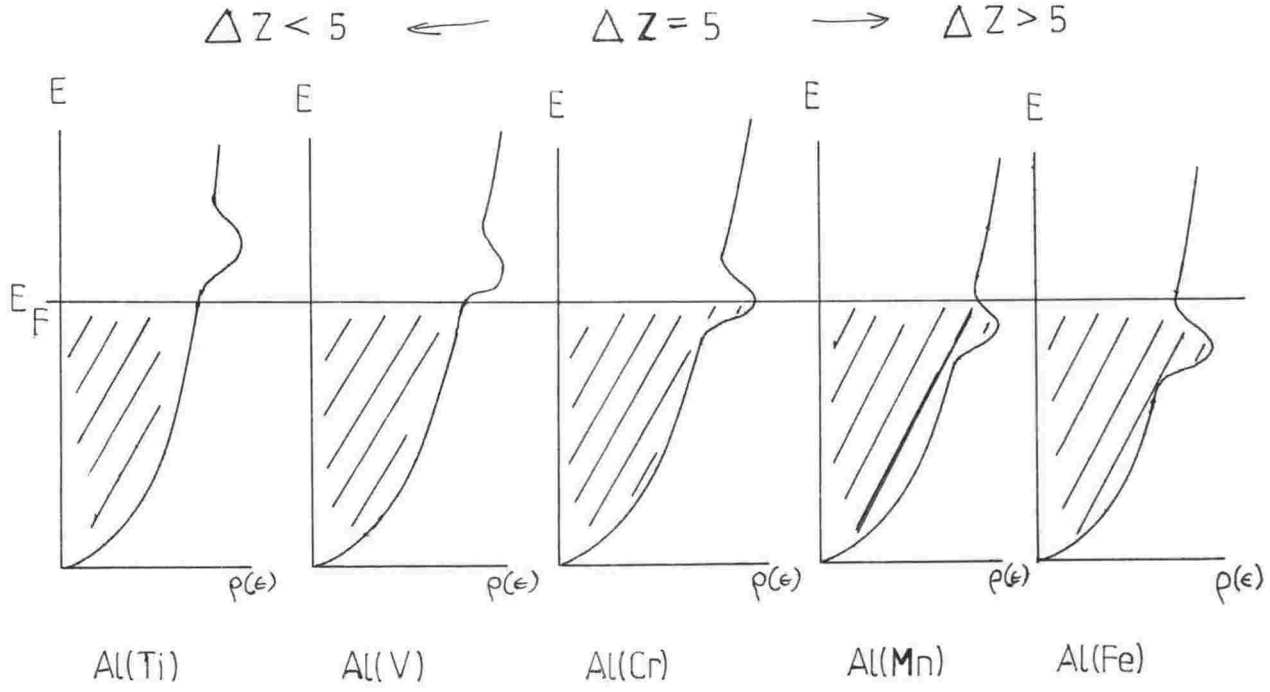

In terms of conduction electron phase shifts, $\delta_e = \frac{\pi}{2}$ for Cr, when the VBS is at the E_F.

Now, in addition to the broadening of the d-levels of the impurity by s-d mixing, they are also split into spin up and spin down components separated in energy as follows. Since parallel spin electrons are kept apart as a consequence of the Pauli Principle it follows that opposite spin electrons are able to approach more closely and hence experience a greater Coulomb repulsion U above that felt between parallel spin electrons. Hence spin up and spin down VBS components differ in energy by U where U depends upon the number of electrons in the d-level.

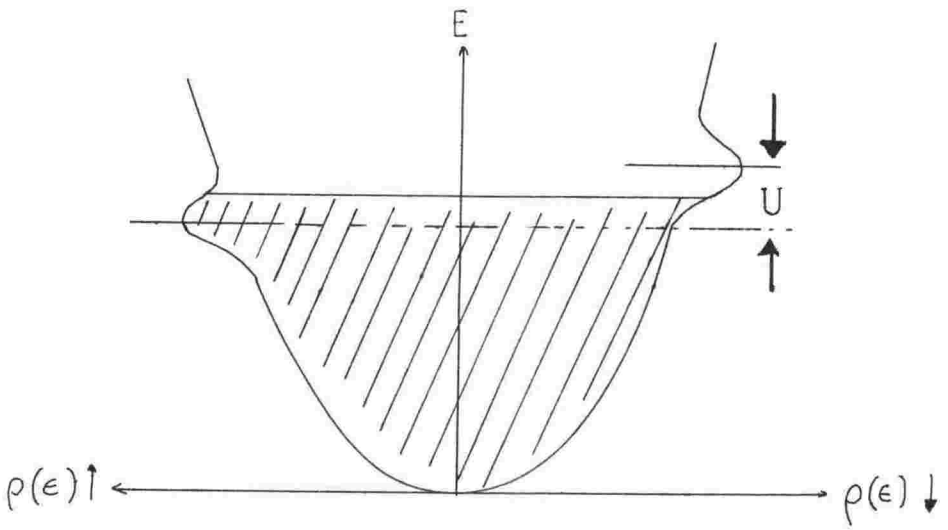

From the diagram it can immediately be seen that there are now more spin up electrons than spin down ones. Hence there is now a nett magnetic moment on the impurity. By magnetic moment we mean the susceptibility χ now has a Curie-Weiss temperature-dependent component.

If the width Γ of the VBS components is greater than U the spin up and spin down components coalesce into a non-magnetic state where the average occupation of both states is the same. Γ depends on the Fermi energy. In the case of an Al host (E_F ~ 12 eV) Γ is such that the 3-d impurities are non-magnetic. With a Cu host however with E_F ~ 7 eV we find that Cr, Mn and Fe are magnetic whereas Ni and Co are not since the number of d-electrons is too small for $U>\Gamma$.

As ΔZ increases across the 3-d row two VBS will cross the Fermi level. As a result we may expect a plot of residual resistivity vs. atomic number to exhibit two maxima. cf. Al(3d) with one broad maximum centred about Al(Cr).

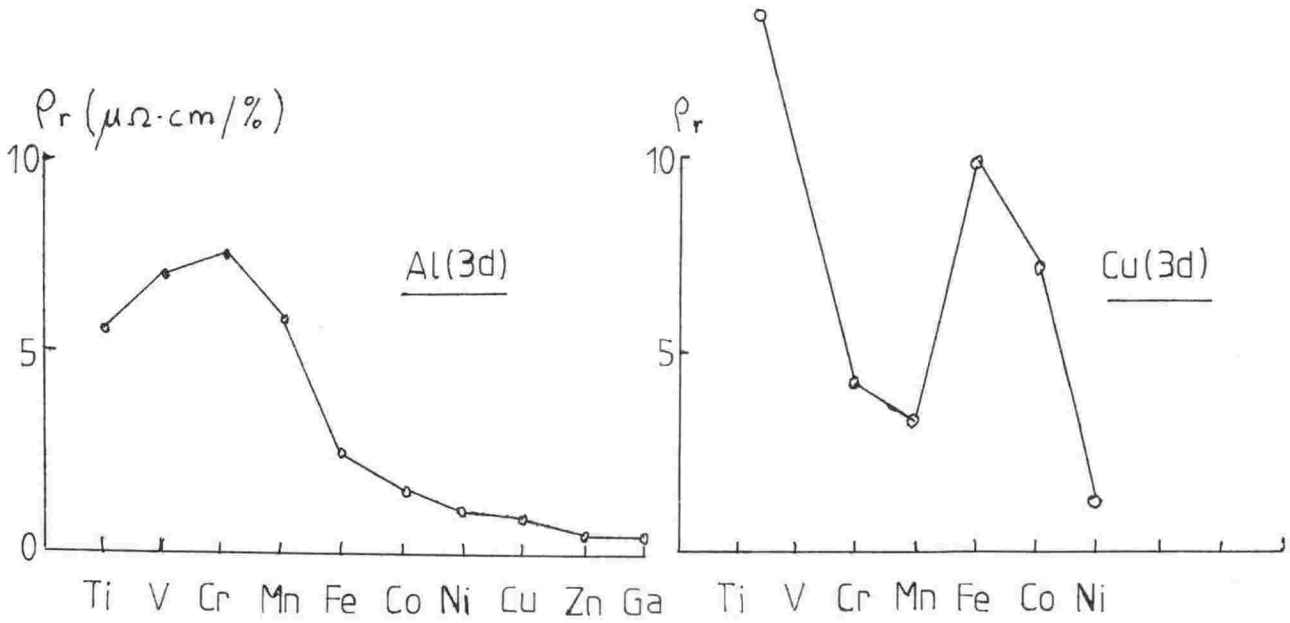

Residual resistivities for 3-d impurities in Al and Cu (After Freidel).

1.2 Anderson's Model

Anderson (1961) put Freidel's qualitative ideas on a more quantitative footing. Anderson's approach to the causes of local moment formation was to assume a local moment exists and to consider the conditions under which it can survive.

Anderson's model for the electronic states of the alloy system is appropriate for impurity atoms with an unfilled or partly filled d-shell in a host whose conduction band states are extended e.g. a sea of s-electrons. We shall only consider 3d transition-metal impurities i.e. Fe group, in this discussion.

Since we assume a local moment exists the spin up d-state will be full, and at an energy E below the Fermi level, and a spin down electron attempting to occupy it will feel the full Coulomb repulsion U between it and the electron (up) already on the impurity. It can only occupy a state whose energy is E + U, which is empty since we assume a local moment exists already, and hence must lie above E_F.

Now, the conduction electrons can mix with the electrons in the local d-level and cause that state to become broadened. The effective number of spin up electrons has been reduced since it can "escape" temporarily into the conduction band. Similarly the broadening of the spin down state allows it to become partially filled, since the broadened state now overlaps the Fermi level, and hence increase the number of spin down electrons. This

has the effect of decreasing the repulsion U. The energy of the spin up state moves up and that of the spin down state moves down. If the s-d mixing is sufficiently strong, the states will eventually coalesce, the occupancy of both states will be equal and the moment cannot be maintained.

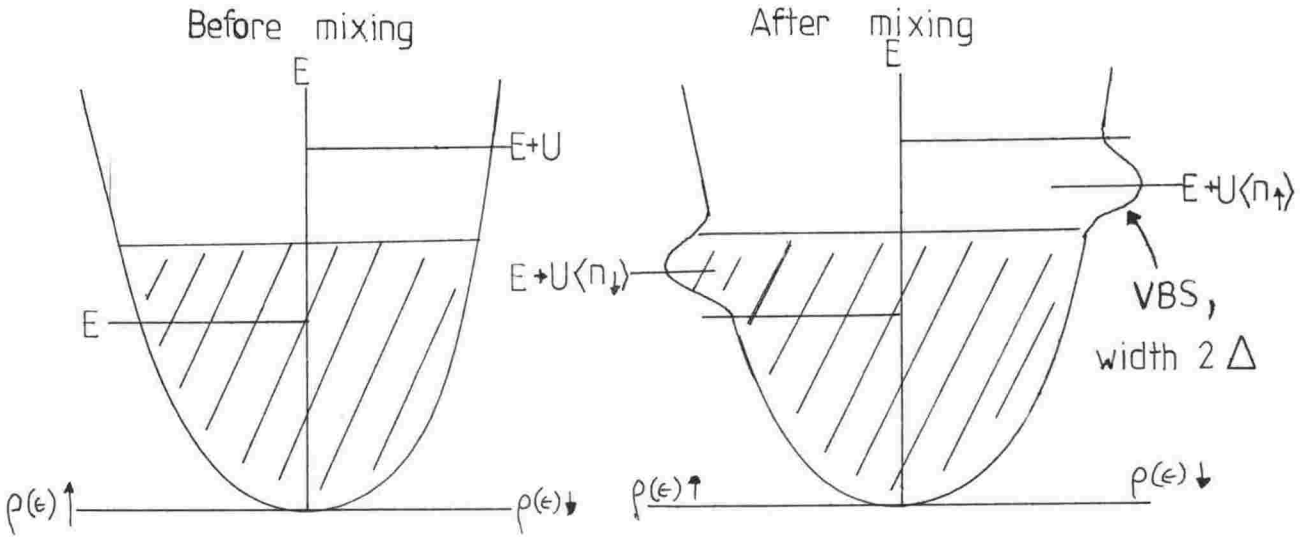

Calculation of the energy shifts of the spin up and down states depends upon the numbers of up and down electrons which is computed from the shaded areas of the (what turn out to be) virtual bound states, below E_F. As the number of electrons, in turn, depends upon the energy shifts the calculation must be performed self-consistently, the solution of which leads to a transition curve where there appears to be a sharp transition from magnetic to non-magnetic behaviour,

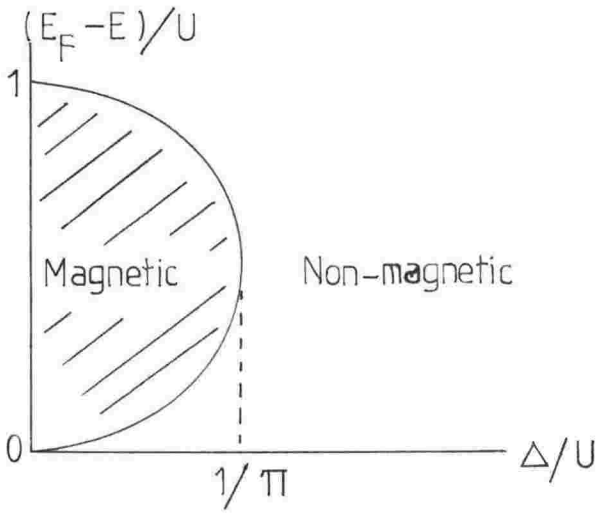

Regions of Magnetic and Non-magnetic Behaviour

The transition curve is given by

$$U\rho_d(E_F) = 1$$

where $\rho_d(E_F)$ is the density of impurity d-states for both spins. Now when $\pi\Delta<U$ (and $(E_F-E)/U$ is about the middle of the curve) the impurity will be

magnetic. We can see that the condition for magnetism depends more critically upon Δ/U than $(E_F - E)/U$.

As in Freidel's picture the Al-3d system is non-magnetic as is Cu-Ni and Cu-Co.

The magnetic limit of Anderson's model has been shown by Schrieffer and Wolff (1966) to be equivalent to the exchange Hamiltonian of Kondo (1964). Kondo made the first successful effort to understand the cause of the resistance minimum which appears in many dilute alloys with transition metal impurities. It was already known that the resistance minimum was associated with the impurities and not a property of the metal itself. Kondo's approach was to assume a local spin $\tilde{S}$ on the impurity which interacted with the conduction electrons of the host, with spin $\tilde{s}$, via an exchange interaction J. J was assumed to be -ve i.e. anti-ferromagnetic, coupling spins of opposite sign. Kondo's Hamiltonian was

$$H = -J\ \tilde{S}.\tilde{s}$$

Calculations using this Hamiltonian, going beyond first order Born approximation, gave a logarithmic resistivity term of the form

$$\rho = \rho_o(1 + 2J\ N(E_F)\ \ln\ \frac{T}{T_k})$$

where ρ_o is a constant and $N(E_F)$ is the conduction electron density of states per spin per host atom at the E_F. T_K is at present simply a parameter in the theory. This logarithmic term, when added to the electron-phonon resistivity, gives the observed resistance minimum.

From the start it was obvious that as $T \rightarrow 0$ the resistivity diverged to infinity. Experimentally this is not observed in metals or alloys suggesting that something was happening to the impurity spin below the characteristic temperature T_K. It is generally thought that below T_K there exists a quasi-bound state where the local moment surrounds itself with a compensating cloud of conduction electrons of opposite spin to itself thus eventually canceling the moment completely at T = 0. This is commonly referred to as the Nagaoka bound state after Nagaoka (1967) who, among others, postulated the existence of such a state thus removing the difficulty posed by Kondo's treatment. The Kondo temperature is defined as

$$T_K = T_F \exp\left[-\frac{1}{JN(E_F)}\right]$$

where $T_F = E_F/K_B$

It has been shown (Anderson 1973; Wilson 1974) that below T_K the exchange "constant" J tends to infinity hence as we reduce T to below T_K the impurity spin traps a conduction electron of opposite spin and is locked into a singlet state i.e. S = 0. For an infinite -ve J the impurity traps a conduction electron of opposite spin and is thereby locked into a singlet state of zero nett spin. Any attempt to break the singlet by transferring an electron in or out of the impurity site takes an infinite amount of energy. That particular impurity is thus out of the way as far as exchange scattering is concerned. For the conduction electrons it acts as a non-magnetic, infinitely repulsive impurity and hence we have Nagaoka's bound state. It turns out that the residual resistivity (i.e. the resistivity at T = 0) has a maximum value which is uniquely related to ΔZ. This maximum value is called the unitarity limit (where the conduction electron phase shift is $\pi/2$) and it is believed that this limit is approached in all Kondo systems as $T \rightarrow 0$. Nozières (1974) calculated the resistivity below T_K and found that it approached T = 0 as $1 - aT^2$. Experimentally, Cu(Fe) is found to have a -ve T^2 dependence at low temperatures (Star *et al.* 1972).

The Non-magnetic Limit

Rather than the true non-magnetic limit, far from the transition curve, we shall consider rather the nearly-magnetic case close to the transition curve.

An alloy, such as Al(Mn), which does not possess an impurity susceptibility of Curie-Weiss form at low temperatures (although the susceptibility is enhanced above that in the host due to the presence of a VBS near the Fermi level), due to the average occupation of the spin up and down virtual states being the same, has a resistivity reminiscent of magnetic scattering i.e. resistivity decreasing with increasing temperature from T = 0 as in Kondo alloys. Although the impurity possesses no permanent local moment there can be a nett instantaneous moment which is periodically destroyed by s - d mixing with the conduction electrons i.e. if the impurity has an unpaired d-electron an electron of opposite spin can hop onto the impurity and reduce the spin to zero. Thus the impurity spin fluctuates between spin up (1/2) and zero. This is termed a localized spin fluctuation.

Observed for a long enough period of time the VBS appears to have an equal number of spin up and down electrons so the impurity appears non-magnetic. When the nett impurity spin fluctuates at a greater rate than it would due to thermal fluctuations alone the impurity appears non-magnetic. At higher temperature where many thermal fluctuations occur in the time occupied by one spin fluctuation, the impurity behaves as well defined local moment i.e. the conduction electron retains its spin between one impurity and another and so it "sees" the impurity as magnetic. If the conduction electron has its spin changed by some other scattering process between collisions with the impurities it will see the impurity as non-magnetic; the scattering does not depend on the spin. So a local moment can only be observed above a certain characteristic temperature i.e. T_K. This is the view taken by Rivier and Zlatic (1972) who assume that the appearance of a logarithmic term in their localized spin fluctuation resistivity calculations implies a magnetic moment at the impurity. Anderson (1968) supports this point of view.

With some alloys previously thought to be non-magnetic, such as Al(Mn) and Cu(Ni), it has been shown that at higher temperatures a split VBS appears implying the existence of a local moment (Gruner 1972; Kaiser and Gilberd 1976). Cooper and Miljak (1976), while not actually observing a Curie-Weiss law in $\chi(T)$ in Al(Mn), conclude that there is evidence for such a behaviour although experimentally the law is masked by changes in the $\chi(T)$ of Al upon alloying and the changes in thermal expansion of Al, which causes T_K to change, reducing the temperature - dependence of χ.

1.3 Wolff Model Wolff (1961)

Wolff's approach to the problem of local moment formation was to consider the alloy's electronic states as a one-band model which was equivalent to assuming that the wave function on the impurity is similar to those of the host conduction electrons. The impurity is represented by a potential V which was allowed to be spin-dependent. If V for spin up electrons is different from V for spin down electrons then a local moment exists on the impurity. Although the impurity d-state wave function is similar to those of the conduction electrons there obviously must be sufficient difference for an impurity potential to exist. The structure of Wolff's model is in fact rather similar to Anderson's, the essential criterion for local moment formation being the existence of a relatively sharp virtual level near the Fermi level.

Both the models of Anderson and Wolff where devised to explain the occurrence of local moments in 4-d hosts containing Fe as the impurity. Anderson's model is more applicable at the beginning of the 4-d series; Wolff's model at the end where the host and impurity are more or less isoelectronic.

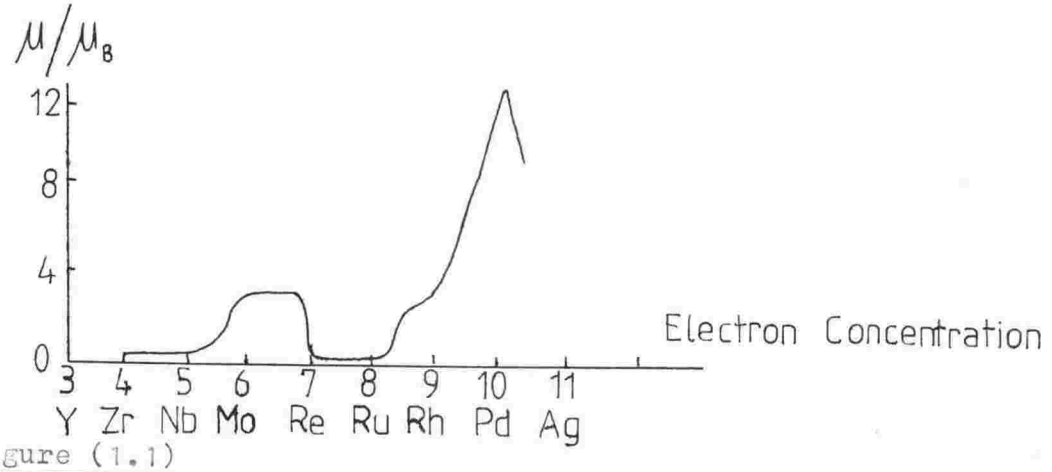

Figure (1.1)

Magnetic moment of Fe dissolved in various 4-d (and 5-d in the case of Re) transition metals as a function of electron concentration.

Varying the electron concentration of the host varies the width of the virtual level and the position of the Fermi level. A local moment occurs when the virtual level is close to the Fermi level and the virtual level is sufficiently narrow (after Clogston *et al.* (1962), and Matthias *et al.* (1960)).

The striking feature of Figure (1.1) is the "giant" moment at Pd. This comes about because Pd is, what is termed, a "nearly-magnetic" metal with a susceptibility about 10 times greater than that given by the Pauli susceptibility calculated from the band structure density of states. 3 Bohr magneton's worth of the effective moment comes from unpaired spins in the outer shells of Pd; the other 9 or so is made up of ferromagnetically aligned moments (each of about $0.05\mu_B$) that are induced on about 200 Pd ions within the Fe's vicinity (Low and Holden 1966).

The enhanced susceptibility is a manifestation of spin fluctuations occurring in the d-band of Pd. We shall discuss these in the next section.

1.4 Spin Fluctuations

It is found that in the transition metals Pd and Pt the magnetic susceptibility χ is higher than the value given from the Pauli susceptibility calculated from the band structure density of states.

$$\chi_o = \mu_B^2 \rho(E_F)$$

where $\rho(E_F)$ is the density of states at the Fermi level and μ_B is the Bohr magneton i.e. the magnetic moment on one electron.

This susceptibility enhancement may be understood as follows. Since parallel spin electrons are kept apart as a consequence of the Pauli exclusion principle there is a greater Coulomb repulsion U between opposite spin electrons since there is no such restriction keeping them apart. Hence the spin band splitting upon the application of a magnetic field H is greater than $2\mu_B H$ the ordinary Zeeman splitting of the spins. Hence there are more spin up electrons aligned with the field than in the Pauli case; thus the susceptibility is enhanced.

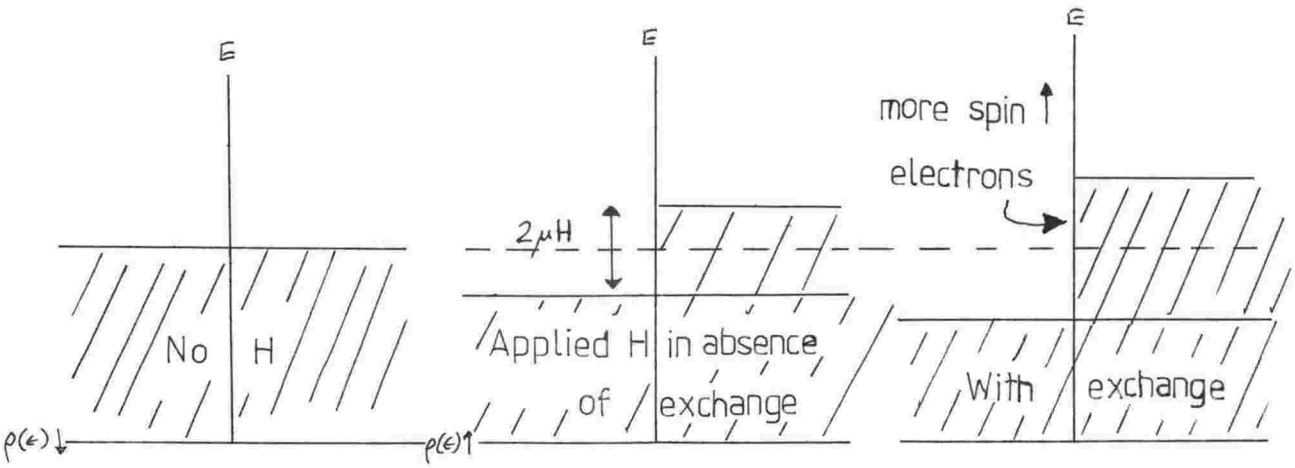

In terms of the mean field approximation, where each electron experiences a field proportional to the magnetization, we can qualitatively derive an expression for the enhanced susceptibility (see Stoner 1938; Izuyama, Kim and Kubo 1963). Starting with the assumption that the exchange field H_E is linearly proportional to the magnetization of the electrons M via the mean field constant where

$$H_E = \lambda M$$

where λ is equivalent to U (see Magnetism Vol. 4, p. 280), we get

$$\chi = \frac{\chi_o}{1 - U\chi_o} \qquad \textbf{Equation (1.1)}$$

The factor $\alpha = \frac{1}{1 - U\chi_o}$ is called the Stoner enhancement factor.

When $U\chi_o = 1$ the electron system becomes ferromagnetic i.e. a permanent magnetic moment on an atom can exist even in zero applied magnetic field. In the case of Pd $\chi/\chi_o = 10$ so evidently $U\chi_o \sim 0.9$ (Lederer and Mills 1968).

Although we have only talked about the static susceptibility enhancement equation (1.1) also holds in the low frequency case for the frequency-dependent susceptibility $\chi(q,\omega)$ where q,ω are the wave vector and frequency of the applied magnetic field. When $U\chi_o = 1$ we get spontaneous magnetic moments in the electron system even in the absence of any external disturbance such as a magnetic field. When $U\chi_o < 1$ there can be no such permanent alignment of parallel spins in the absence of any external disturbance since it is energetically unfavourable. However an external disturbance is always present in the form of thermal energy (except at $T = 0$) and this excites temporary alignments over small regions of the electron system. Since it is energetically unfavourable for spins to remain permanently aligned for $U\chi_o < 1$ as a result we find the average occupation of both spin bands and the same i.e. the electron system is non-magnetic in the sense that the susceptibility is less than infinite and is temperature dependent i.e. no Curie contribution.

These temporary spin alignments are called spin fluctuations or paramagnons by analogy with the name magnons given to spin waves in a ferromagnetic system. Spin fluctuations can be looked upon as critically damped spin waves.

Now at $T = 0$ there can be no spin fluctuations since there is no thermal energy. Hence we would expect spin fluctuations to obey Bose-Einstein statistics (since they are thermal excitations) and this fact is reflected in the resistivity of spin fluctuation alloys.

The spectral distribution of the spin fluctuations would be expected to be related to the frequency response of the susceptibility $\chi(\tilde{q},\omega)$ since spin fluctuations manifest themselves in an enhanced susceptibility. Just as the energy absorbed from an electrical disturbance is given by the imaginary part of the dielectric constant (essentially the electrical susceptibility) the absorptive part of the magnetic susceptibility is likewise the imaginary part and thus the spectral density of the spin fluctuations (the distribution of energy absorbed from the magnetic field) is given by the imaginary part of the suceptibility.

$$A(\tilde{q},\omega) = 2Im\chi(\tilde{q},\omega) \qquad \text{Kubo (1957)}$$

In a transition metal, one may consider a simple two-band model for the electrons in which the d-band is assumed to give rise to the magnetic propoerties and the s-band is assumed to be responsible for the transport properties, although in Rh recent de Haas-Van Alphen measurements show that 80% of the conduction is carried by d-like electrons (Cheng and Higgins 1979). However it is not expected that this will change the character of the calculation of the electron scattering by spin fluctuations significantly. Mills and Lederer (1966) calculated the resistivity of Pd assuming that the experimentally observed resistivity was due to scattering off d-band spin fluctuations. They found the resistivity due to spin fluctuation scattering varied as T^2 at low temperatures in agreement with observation. Regular electron-electron (Baber scattering) scattering is thought to be insufficient to account for the resistivity of Pd at low temperatures.

1.5 Localized Spin Fluctuations

Metals such as Pd and Pt, as discussed in the previous section, are termed nearly magnetic. Consider now the addition of a more nearly magnetic impurtity e.g. Ni into Pd, that is to say an impurity in which the opposite spin d-electron Coulomb repulsion U is larger than the corresponding value in the host.

At impurity sites we find enhanced spin fluctuations occurring in the impurity d-levels. The effect of these localized spin fluctuations, as they are called, upon the susceptibility can be calculated in the following manner.

Consider an impurity replacing a host ion as per the diagram.

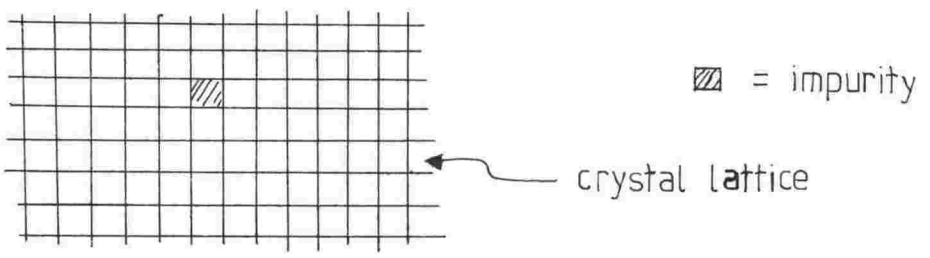

Then $\chi_{alloy} = \chi_{host}(1 - c) + c\chi_i$

where c is the impurity concentration and i refers to the impurity.

Now

$$\chi_i = \frac{\chi_h}{1 - \delta U \chi_h}$$

by analogy with $\chi = \dfrac{\chi_o}{1 - U\chi_o}$

where the intra-atomic exchange (U) at the impurity is δU greater than in the host. (δU is the excess Coulomb repulsion in the impurity over that in the host)

$$\chi_{alloy} = \chi_h(1 - c) + c\frac{\chi_h}{1 - \delta U\chi_h}$$

$$= \chi_h + c\left[\frac{\chi_h}{1 - \delta U\chi_h} - \chi_h\frac{1 - \delta u\chi_h}{1 - \delta u\chi_h}\right]$$

$$\therefore \boxed{\chi_{alloy} = \chi_h + c\frac{\delta U\chi_h^2}{(1 - \delta U\chi_h)}}$$

where $\alpha = (1 - \delta U\chi_h)^{-1}$ is the local enhancement factor.

The frequency and wave-vector dependent alloy susceptibility was calculated by Lederer and Mills (1968) who starting from the Wolff Model obtained the following expression

$$\chi(\tilde{q}', \tilde{q}, \omega) = \chi(\tilde{q}, \omega)\ \delta_{\tilde{q},\tilde{q}'} + c\delta U\ \frac{\chi(\tilde{q}, \omega)\ \chi(\tilde{q}', \omega)}{1 - \delta U\bar{\chi}(\omega)}$$

where $\chi(\tilde{q}, \omega)$ has been generalized to $\chi(\tilde{q}', \tilde{q}, \omega)$ since the impurities have destroyed the translational invariance of the system. $\chi(\tilde{q}, \omega)$ is the enhanced host susceptibility and $\bar{\chi}(\omega)$ is the average of $\chi(\tilde{q}, \omega)$ over wave vector. The local enhancement factor $\alpha = (1 - \delta U\bar{\chi}(o))^{-1}$ provides a measure of how much greater the response to a magnetic disturbance is in the impurity cell when compared to the host response.

The spectral density for the LSF is given by the imaginary part of the impurity susceptibility.

$$A_{LSF}(\tilde{q}, \omega) = 2c\delta U\,\mathrm{Im}\ \frac{\chi^2(\tilde{q}, \omega)}{1 - \delta U\bar{\chi}(\omega)}$$

Using these expressions Lederer and Mills calculated the resistivity due to conduction electrons scattering off enhanced LSF and found a concentration dependent T^2 term which accounted for the then recent resistivity measurements of Schindler and Rice (1967) on Pd(Ni). Schindler and Rice sought to explain the enhanced T^2 term by postulating that the average Coulomb interaction increased as Ni impurities were added to Pd enhancing the d-electron spin fluctuations as a whole. However an average enhancement does not provide an adequate description of a dilute alloy, especially when the wavelength of the spin density fluctuations is short compared to the mean impurity-impurity

separation. The neutron diffraction studies of Low and Holden (1966) show that the extent of the LSF is about 10Å around the impurity. Schindler and Rice's uniform enhancement model incorrectly predicts the variation of the coefficient of the T^2 term with impurity concentration.

Lederer and Mills' LSF model is only valid at low concentrations where interactions between impurities are negligible. However interactions become important as the Ni concentration approaches 2%, above which Pd(Ni) is ferromagnetic, leading to a variation of the coefficient of the T^2 term faster than linear. Whether this occurs and at which concentrations depends upon the degree of exchange enhancement in the host. For instance, although Pd(Ni) is ferromagnetic above 2%, Pt(Ni) does not appear to exhibit inter-impurity interactions even up to Ni concentrations of 10% (Mackliet *et al.* (1970)) e.g. ρ/c is independent of c. The Stoner factor for Pd is about 10 whereas for Pt it is only about 5/3.

Kaiser and Doniach (1970) extended the work of Lederer and Mills to higher temperatures. They obtained the LSF spectral density averaged over wavevector

$$\bar{A}_{LSF}(\omega) = a \frac{\tilde{\omega}}{1 + \tilde{\omega}^2}$$

where a is characteristic of the alloy and independent of ω, and $\tilde{\omega}$ is linear in ω and may be written in terms of a characteristic LSF Temperature T_{sf}

$$\tilde{\omega} = \frac{\omega}{k_B T_{sf}}$$

where T_{sf} is inversely proportional to the local enhancement α.

Thus we see that the LSF spectral density is linear in ω at low energies, peaks at $k_B T_{sf}$ and falls off as ω^{-1} at higher energies. Kaiser and Doniach extended the calculation of LSF resistivity to higher temperatures than those considered by Lederer and Mills the general result they obtained being

$$\rho \simeq \rho_o \beta \int_o^\infty \frac{\omega \bar{A}_{LSF}(\omega)}{(e^{\beta\omega} - 1)(1 - e^{-\beta\omega})} d\omega \qquad \text{eqn. (1.2)}$$

where ω is the energy change on scattering and $\beta = (k_B T)^{-1}$.

Equation (1.2) is the general form of the resistivity due to scattering off Bose-like excitations. For instance if we substitute the Debye energy spectrum for phonons in place of $\bar{A}_{LSF}(\omega)$ we get the familiar Bloch-Gruneisen T^5 law for electron-phonon resistivity.

Inserting $\bar{A}_{LSF}(\omega)$ into equation (1.2) Kaiser and Doniach obtained a universal curve for LSF resistivity as seen in Figure (1.2). At low temperatures we get back the T^2 form as calculated by Lederer and Mills.

$$\tilde{\rho}(T \to 0) = \frac{\pi^2}{3} \left(\frac{T}{T_{SF}}\right)^2$$

where $\tilde{\rho}$ is linear in ρ. At high temperatures we get the linear law which is the general form expected for resistivity due to scattering off Bosons with a temperature-independent energy spectrum since the number of bosons thermally excited is proportional to T at high temperatures.

$$\tilde{\rho}\ (T \to \infty) = \frac{\pi}{2} \frac{T}{T_{SF}} - \frac{1}{2}$$

By fitting experimental resistivity values to the universal curve we get directly the value of T_{sf} for that particular alloy. The shape of the experimental resistivity curve as a function of T should be the same as the universal curve providing T_{sf} is independent of temperature. In fact we find that the host susceptibility decreases slightly with temperature and this has the effect of causing the local enhancement factor α to decrease, for large α, which in turn affects T_{sf}. The effect is greater at higher temperatures and higher α and, in general, we may say that the LSF spectral density decreases in magnitude at higher temperatures i.e. $A_{LSF}(\underset{\sim}{q},\omega)$ is "blurred out". This causes the resistivity to decrease below the linear law at higher temperatures.

Spin fluctuations also affect the specific heat by contributing to the density of excited states in the d-band. Physically the spin fluctuations are an extra excitation which can absorb thermal energy thereby adding extra heat capacity. Alternatively one may say that the effective d-electron mass has been increased enhancing the coefficient of the linear T-term in the electronic specific heat γ. The specific heat enhancement is well known in Pd where the coefficient γ (when spin fluctuations are taken into account) is about twice that in the free electron case (Lederer and Mills 1968a).

Addition of nearly magnetic impurities to the host produces a linear dependence of γ upon impurity concentration c for dilute alloys.

Extending the calculation of the thermal resistivity due to LSF by Schriempf *et al.* (1969), Kaiser (1971) found that as $T \to 0$ W_{LSF} varies linearly with T and as $T \to \infty$ W_{LSF} tends to a constant plus a T^{-2} term although the actual temperature dependence is rather more complex due to the decrease of the local enhancement factor α at high temperatures cf. resistivity.

Kaiser and Doniach applied their extension of the Lederer-Mills LSF model to calculate the resistivities of dilute alloys other than Pd(Ni). Of particular interest is the resistivity of Rh(Fe), the thermopower of which is the topic of this part of the thesis. Now the Kaiser-Doniach model is only valid for those alloys in which the host and impurity are more or less isoelectronic i.e. it is assumed there is little potential scattering of the conduction electrons by the impurity. The neglect of potential scattering has serious consequences for the thermopower of these alloys later on.

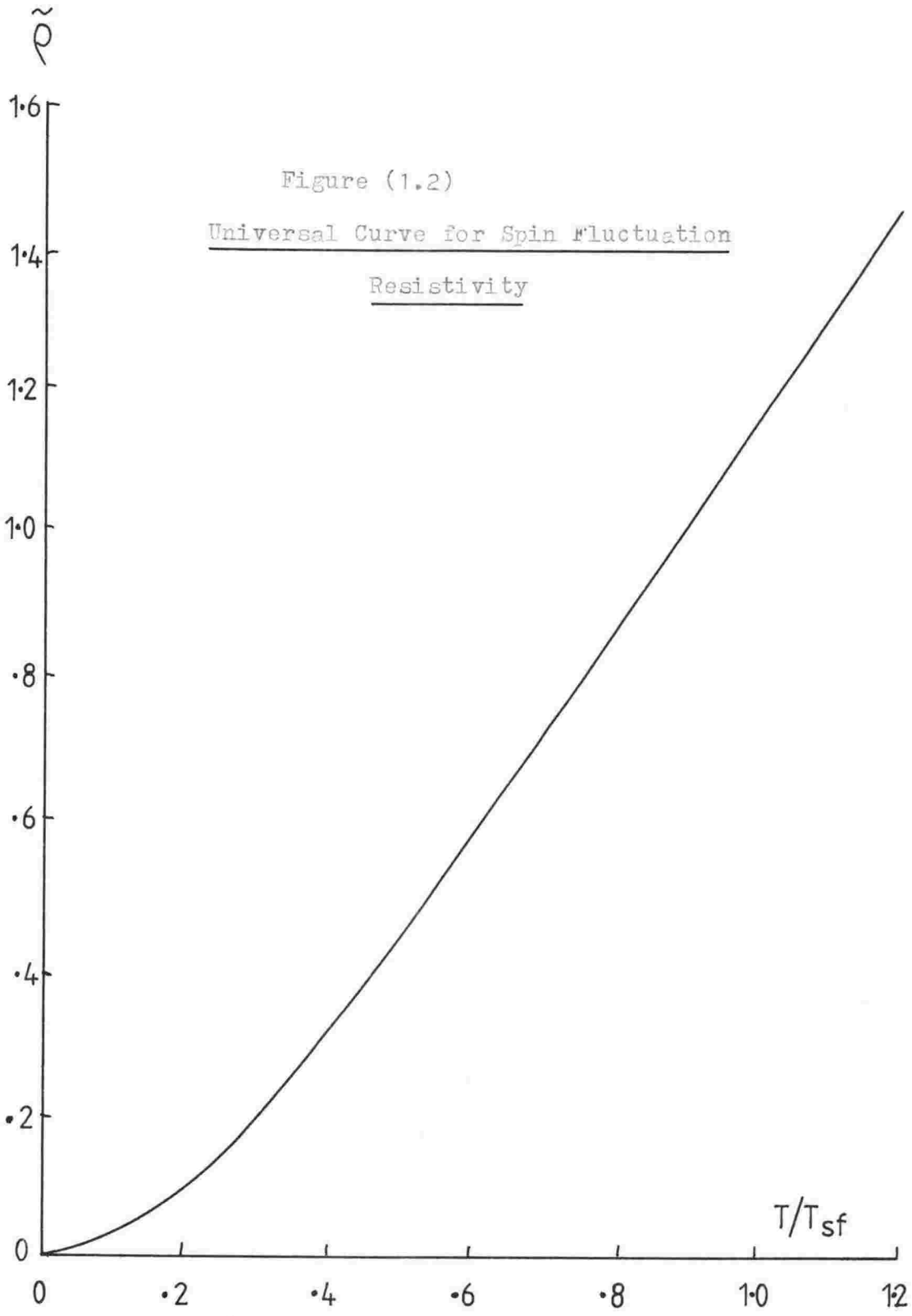

Figure (1.2)

Universal Curve for Spin Fluctuation Resistivity

Chapter Two

THERMOPOWER OF ALLOYS CONTAINING TRANSITION METAL IMPURITIES

2.1 Electron Diffusion and Phonon Drag Thermopower

In a conductor under the influence of an electric field, $\tilde{E}$ and a temperature gradient, ∇T the relationship between these and the electric and thermal current densities, $\tilde{j}$ and $\tilde{u}$, generated as a result, may be written in the following empirical manner.

$$\tilde{j} = L_{11}\tilde{E} + L_{12}\nabla T$$
$$\tilde{u} = L_{21}\tilde{E} + L_{22}\nabla T$$

The coefficients L_{ij} are, for our purposes, just coefficients of proportionality. To be strictly correct the coefficients should be written in the form given by, for instance, Ziman (1964), but as we are merely using our L_{ij}'s as an aid to showing the relationship between various quantities the exact nature of the coefficients is of no importance for the following discussion.

By imposing various conditions upon the conductor the coefficients, or rather combinations of the coefficients, assume well known identities. Putting $\nabla T = 0$ indicates that L_{11} is the electrical conductivity, σ. The thermal conductivity, κ is $-L_{22}$, although this is for conditions of zero electric field rather than zero electric current; however, for $kT \ll E_F$ the difference is negligible. With the thermopower, S is $-L_{12}/L_{11}$, or $-L_{12}/\sigma$. The physical origin of the thermopower can be illustrated in the following manner: in an electrically isolated conductor ($\tilde{j} = 0$) under the influence of a temperature gradient, ∇T the electrons at the "hot" end have, on the average, a higher energy than those at the "cold" end, with the result that the average velocity of the electrons is greater at the hot than the cold end causing a nett diffusion of electrons down to the cold end and creating a surplus of electrons at this end. The electric field, $\tilde{E}$ that is a consequence of this charge imbalance adjusts itself so that the cold electrons are given an energy equivalent to that carried by the hot electrons, and the nett current flow is stopped. The proportionality factor between $\tilde{E}$ and ∇T is the thermopower, S.

Of the many analytical forms of the thermopower the one most commonly encountered is the Mott formula (Mott and Jones 1936).

$$S_d = \frac{\pi^2 k^2 T}{3e}\left[\frac{\partial \ln\sigma(\varepsilon)}{\sigma\varepsilon}\right]_{\varepsilon_F} \qquad \text{eqn. (2.1)}$$

where k is the Boltzmann constant, e the electronic charge, T the absolute temperature and $\sigma(\varepsilon)$ is the electrical conductivity as a function of a hypothetical Fermi level, ε. The logarithmic derivative is evaluated at the actual Fermi level of the metal, ε_F. The Mott formula is only valid in the temperature region where there is a common relaxation time for both thermal and electrical processes, i.e. for $T > \theta_D$ and $T << \theta_D$, electrons being scattered elastically in both regions. (θ_D is the Debye temperature of the metal). Two other assumptions made in the derivation of the Mott formula are that kT is very much smaller than the Fermi energy and that $\sigma(\varepsilon)$ does not vary too rapidly in the neighbourhood of the Fermi energy.

There is a further quantity which will be of interest to us. This is the Thermoelectric ratio, G. Experimentally this is the ratio between electric and thermal currents when $\tilde{E} = 0$. Compare this with the thermopower, which latter is the ratio between $\tilde{E}$ and ∇T for conditions of zero electric current. In terms of the coefficients L_{ij} we can write

$$\begin{aligned} G &= (\tilde{j}/\tilde{u})_{E = 0} \\ &= L_{12}/L_{22} \\ &= S\sigma/\kappa \end{aligned}$$

Now, $\kappa = L\sigma T$ where L is the Lorenz number for the metal, including contributions from inelastic scattering where appropriate (we shall make use of this fact in Chapter Four). In general, L is smaller than L_o, the classical value for the Lorenz number, if there is a substantial amount of small angle inelastic scattering. Substituting for κ we get

$$G = S\sigma/L\sigma T$$

or

$$S = LGT$$

In a formal sense the difference between G and S is that whereas S is the ratio between L_{12} and the <u>electrical</u> conductivity, G is the ratio between L_{12} and the <u>thermal</u> conductivity. This, strictly speaking, includes the thermal conductivity due to the lattice, but in general electronic conduction of heat is much greater than lattice conduction at low temperature i.e. below about 4 K.

We shall now consider the ramifications of the Mott formula. If we write $\sigma(\varepsilon)$ in the following form

$$\sigma(\varepsilon) = \frac{1}{4\pi^3}\int e^2 \tilde{\upsilon}\tilde{\upsilon} \frac{\tau dA}{|\nabla_k \varepsilon|}$$

$$= \frac{e^2}{12\pi^3\hbar} \Lambda A$$

for spherical Fermi surface with isotropic relaxation time τ where the mean free path $\Lambda = \upsilon\tau$ and υ is the electron velocity, we can then write

$$\frac{\partial \ln\sigma(\varepsilon)}{\partial\varepsilon} = \frac{\partial \ln\upsilon^2(\varepsilon)}{\partial\varepsilon} + \frac{\partial \ln\tau(\varepsilon)}{\partial\varepsilon} + \frac{\partial \ln n(\varepsilon)}{\partial\varepsilon}$$

$$= \frac{\partial \ln\Lambda}{\partial\varepsilon} + \frac{\partial \ln A}{\partial\varepsilon} \qquad \text{eqn. (2.2)}$$

where $n(\varepsilon) \sim \int \frac{dA}{|\nabla_k \varepsilon|}$ is the density of states integrated over the Fermi surface, A.

The first term in equation (2.2) is generally positive since the more energetic an electron is the less likely it is to be scattered (this is true in general for impurity scattering, but there are exceptions for electron-phonon scattering) and the longer is its mean free path.

The second term depends upon the geometry of the Fermi surface.

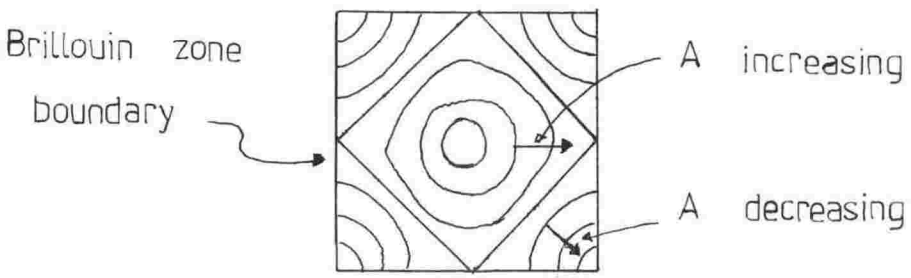

Fig. (2.1) Fermi surfaces and their change in area with increasing energy.

Consider a Fermi surface expanding into a Brillouin zone as in Fig. (2.1). Until it reaches the zone boundary its area increases making $\frac{\partial \ln A}{\partial\varepsilon}$ positive. Thereafter it decreases making $\frac{\partial \ln A}{\partial\varepsilon}$ negative. If it is sufficiently negative it may outweigh the first term $\frac{\partial \ln\Lambda}{\partial\varepsilon}$ and cause the thermopower to change sign e.g. the noble metals.

Low temperature expressions for S_d at very low temperatures for pure metals have been calculated but these vary depending on the structure of the theoretical model chosen to represent the behaviour of the electrons in the metal. The Mott formula cannot be used here because the relaxation times for electrical and thermal processes are different. This is clearly demonstrated in the way the Lorenz number varies from a constant figure L_o as temperature is lowered (see Ziman 1963).

Now for free electrons $n(\varepsilon) \sim \varepsilon^{\frac{1}{2}}$, $v^2 \sim \varepsilon$ hence

$$S_d = \frac{\pi^2 k^2 T}{3e} \left[\frac{\partial \ln n(\varepsilon)}{\partial \varepsilon} + \frac{\partial \ln v^2(\varepsilon)}{\partial \varepsilon} + \frac{\partial \ln \tau(\varepsilon)}{\partial \varepsilon} \right]_{E_F}$$

$$= \frac{\pi^2 k^2 T}{3e\varepsilon_F} \left[\frac{3}{2} + \varepsilon_F \frac{\partial \ln \tau(\varepsilon)}{\partial \varepsilon} \right]$$

For the case of impurity scattering being the dominant relaxation mechanism ($T \ll \theta_D$ in general) one can assume the mfp is independent of the electron energy since electron scattering off "hard sphere" impurities is elastic. Then the relaxation is given by $\tau = \Lambda / v_F \sim \varepsilon^{-\frac{1}{2}}$.

$$\therefore S_d = \frac{\pi^2 k^2 T}{3e\varepsilon_F} \qquad (T \ll \theta_D)$$

At high temperatures elastic electron-phonon scattering occurs and we can write for the relaxation time (Barnard 1972, Wilson 1936)

$$\tau \sim \varepsilon^{3/2}$$

This leads to a commonly quoted result for the diffusion thermopower

$$S_d = \frac{\pi^2 k^2 T}{e\varepsilon_F} \qquad (T > \theta_D)$$

In the foregoing discussion we have assumed the lattice to be in thermal equilibrium. This is not the case since at the "hot" end there will be a higher density of phonons than at the "cold" end giving rise to a flux of phonons. It is this flux of phonons that is responsible for the thermal conductivity of insulators. The interaction of the disturbed phonon system with the electrons gives rise to an additional effect in the thermopower called phonon drag.

To simplify our initial discussion of phonon drag let us assume that the phonons only scatter off the electrons. This is true at low temperatures to a large extent where phonon-phonon scattering is small compared to phonon-electron scattering. In each such scattering event a phonon is absorbed by the electron and the electron gains the corresponding energy and crystal momentum.

In a metal under the influence of a temperature gradient we have a phonon current flowing from the "hot" end to the "cold" end. An electron will be made likely to absorb a phonon travelling from the hot end than from the cold end since there are more of the hot phonons available. Consequently the electrons absorb the phonon momentum and are "dragged" along with the phonons to the cold end.

Electrons pile up at the cold end in addition to those there due to electron diffusion. As in the case of diffusion thermopower an electric field is set up due to the charge surplus which adjusts itself so that the system reaches a steady state. To evaluate this effect we shall use the following argument which is due to MacDonald (1962).

Consider the phonons inside the metal with energy density U(T). The pressure exerted on the electrons by the phonons is

$$P = \frac{1}{3} U(T)$$

The temperature gradient also gives rise to a pressure gradient or nett directed force per unit volume

$$F_x = -\frac{dP}{dx}$$

$$= \frac{1}{3}\frac{dU}{dT} \cdot \frac{dT}{dx}$$

$$= -NeE_x$$

with N electrons per unit volume.

Since $\tilde{E} = S\nabla T$

we get $S_g = \frac{Cg}{3Ne}$ eqn. (2.3)

where $C_g = \frac{dU}{dT}$ is the lattice specific heat.

We have assumed that all the phonon momentum is transferred to the electrons. We would expect this to be true at very low temperatures but in general not all the phonon momentum is transferred to the electrons.

The momentum transfer must be "shared" with other "particles" such as other phonons, impurities etc. So to a first approximation we may modify eqn. (2.3) by a "momentum transfer factor"

$$\frac{P_{p,e}}{P_{p,x} + P_{p,e}}$$

where $P_{p,e}$ and $P_{p,x}$ are the probabilities of an interaction between a phonon and an electron, and a phonon and some other "particle". If relaxation times are appropriate for these probabilities we may write

$$S_g = \frac{C_g}{N\mathbf{e}} \left[\frac{\tau_{p,x}}{\tau_{p,x} + \tau_{p,e}} \right]$$

where $\left[\frac{\tau_{p,x}}{\tau_{p,x} + \tau_{p,e}} \right]$ is a suitable average over the phonon spectrum considering that $\tau_{p,x}$, $\tau_{p,e}$ are usually functions of the phonon frequency.

At sufficiently low temperatures we expect S_g to vary as T^3, remembering that the lattice specific heat varies as T^3 at low temperatures and that $P_{p,e} > P_{p,x}$ in general since most of the phonon momentum is absorbed in phonon-electron collisions.

At high temperatures phonon-phonon collisions become important since the number of phonons excited is proportional to T so the probability of a phonon interacting with another is proportional to T and hence

$$\tau_{p,p} \sim T^{-1}$$

Also at high temperatures $kT > k\theta_D$ phonons can only interact with electrons in a band of width $k\theta_D$ at the Fermi surface. The number of electrons in this band at these temperatures is independent of the temperature and hence $\tau_{p,e}$ is constant. We also have $\tau_{p,x} \to \tau_{p,p}$ and we can write

$$S_g = \frac{C_g}{N_e} \frac{\tau_{p,p}}{\tau_{p,e}} \sim T^{-1}$$

since C_g is constant and $\tau_{p,p} \ll \tau_{p,e}$, $\tau_{p,p} \sim T^{-1}$.

So in general phonon drag thermopower increases as T^3 at low temperatures, and falls off as T^{-1} at high temperatures, exhibiting a peak at about $\theta_D/5$.

In our treatment of phonon drag we have neglected Umklapp processes in the scattering of the phonons. The effect of U-processes is generally to contribute a thermopower component of opposite sign to that caused by normal (N) processes. If U-processes dominate the scattering phonon drag thermopowers of opposite sign can be observed.

Calculations on the diffusion thermopower involving second-order scattering processes by Nielsen and Taylor (1974) have predicted the existence of a hump in the diffusion thermopower at about $\theta_D/5$. These second-order contributions allow us to interpret some experimental results as diffusion effects whereas previously they may have been attributed to phonon drag.

In general the diffusion thermopower and the phonon drag thermopower may simply be added together since it is assumed that the additional momentum given to the electrons from the phonons is independent of that already given to them by the phonons to produce electron diffusion. Napoli and Sherrington (1971) have suggested that an interference term between S_d and S_g exists in the case of alloys, although definitive evidence is yet to appear.

2.2 Enhanced Diffusion Thermopower

a) Pure Metals

The transition metals Pd, Pt and Ni have an order of magnitude increase in thermpower (including S_g) over simple metals due to a high density of states $N(\varepsilon_F)$, giving rise also to a high specific heat and electrical resistivity; in particular a high rate of change of $N(\varepsilon_F)$ with E i.e. $\partial N(\varepsilon)/\partial E$ is large at E_F, where the conduction electrons have the greatest effect upon the electronic properties of the metal.

Now, if we take the Mott Formula for S_d

$$S_d = \frac{\pi^2 k^2 T}{3e} \left[\frac{\partial \ln \sigma(\varepsilon)}{\partial \varepsilon} \right]_{E_F}$$

and we put $\sigma = ne^2\tau/m$ we get

$$S_d = \frac{\pi^2 k^2 T}{3e} \left[\frac{\partial \ln \tau(\varepsilon)}{\partial \varepsilon} \right]_{E_F}$$

Assuming that the relaxation rate $1/\tau$ is proportional to the density of final states $N(\varepsilon)$ we get

$$S_d = - \frac{\pi^2 k^2 T}{3e} \left[\frac{\partial \ln N(\varepsilon)}{\partial \varepsilon} \right]_{E_F}$$

Thus we have a ready explanation for the large thermopowers of Pd, Pt and Ni.

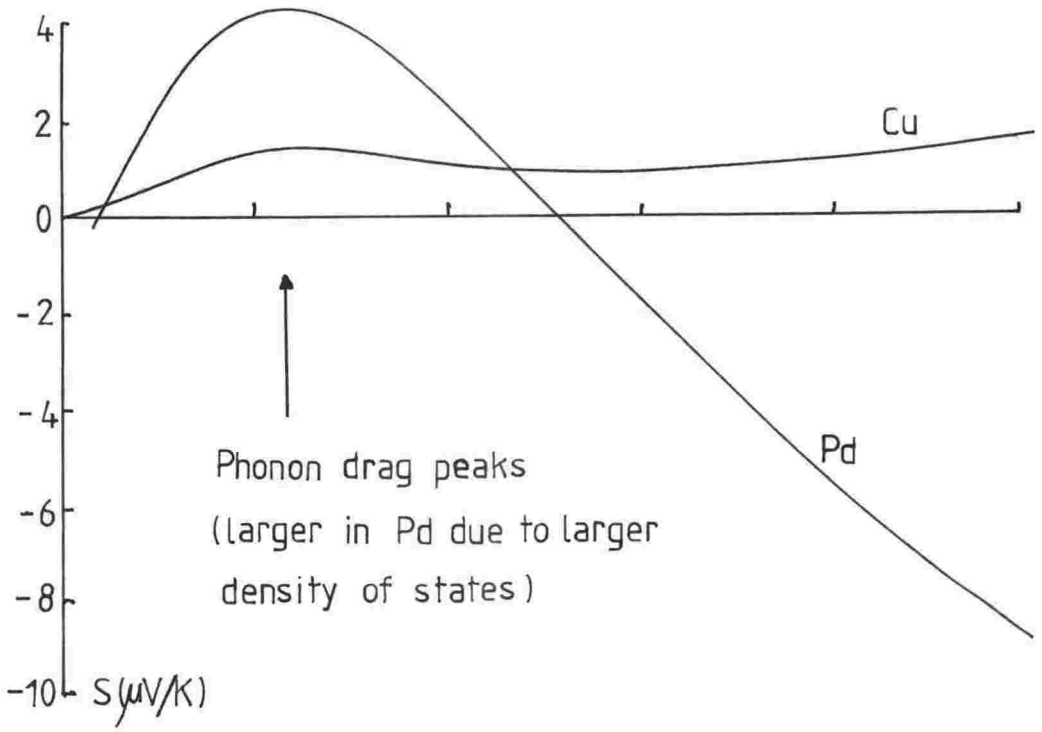

Figure (2.2). Thermopower of Transition Metal with thermopower of Noble Metal for comparison.

For ferromagnetic metals below the Curie temperature T_c, i.e. Co, Ni and Fe, the situation is complicated by the existence of a split density of states due to the spin up and spin down electrons being displaced above and below the Fermi level by mechanisms similar to those responsible for the splitting of virtual bound states in local moment alloys as outlined in Chapter One.

However it is not enough for the density of states merely to be split to give rise to an enhanced thermopower. If the density of states was symmetric about E_F no enhanced thermopower would result since $\partial N(\varepsilon)/\partial \varepsilon$ would be zero. Now, if the relaxation rate for spin up electrons was different

from that for spin down electrons we could have circumstances favourable for enhanced thermopowers. In general some source of elastic scattering is required to produce this state of affairs, since elastic scattering is usually energy-dependent. For example, for free electrons the relaxation time for scattering off "hard spheres" goes as $E^{-\frac{1}{2}}$ and thus, since the spin up and spin down electrons are separated by the exchange energy, the relaxation time (and hence the relaxation rate) is different for both. Essentially this means that more electrons are scattered one way across the Fermi level than the other. This, combined with the symmetric, but large, split density of states, gives rise to an enhanced thermopower, since, as we have shown just previously, the relaxation rate is also proportional to the density of final states.

b) Dilute Alloys with Transition Metal Impurities

The behaviour of transition metal impurities in simple and transition metal hosts has already been outlined in Chapter one. The effect of VBS's and LSF's upon the resistivities of such alloys has been discussed; the effects upon the thermopower will now follow.

i) Simple metal hosts

As an example let us consider the Al(3d) system. We have seen how the residual resistivity reaches a maximum when the VBS due to the 3d impurities is located at the Fermi level (see Figure (2.3)). The residual resistivity is governed by $N(\varepsilon)$; the thermopower by $\partial N(\varepsilon)/\partial \varepsilon$. Hence we would expect to find a minimum thermopower when the VBS was at the Fermi level. This, broadly, is the observed behaviour. From the following diagram we can see that the thermopower does indeed appear to be the energy derivative of the resistivity plot. This is, of course, an oversimplification; in fact LSF effects narrow the VBS and produce an even more enhanced thermopower above that expected from a simple application of the Friedel-Anderson model. Zlatic and Rivier (1974) calculated the effects of the interaction of LSF's with VBS. They came to the general conclusion that elastic as well as inelastic scattering is necessary to produce an enhanced diffusion thermopower of the "giant" type. The results of their calculations are plotted as crosses in Figure (2.3).

Figure (2.3)

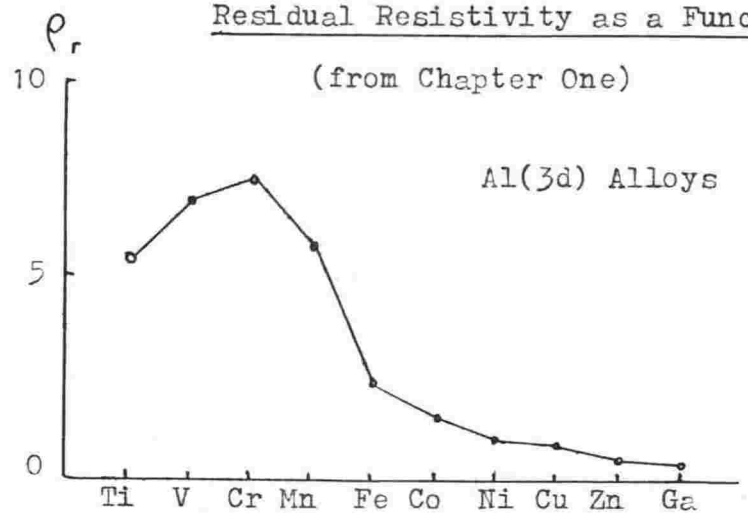

Residual Resistivity as a Function of Z

(from Chapter One)

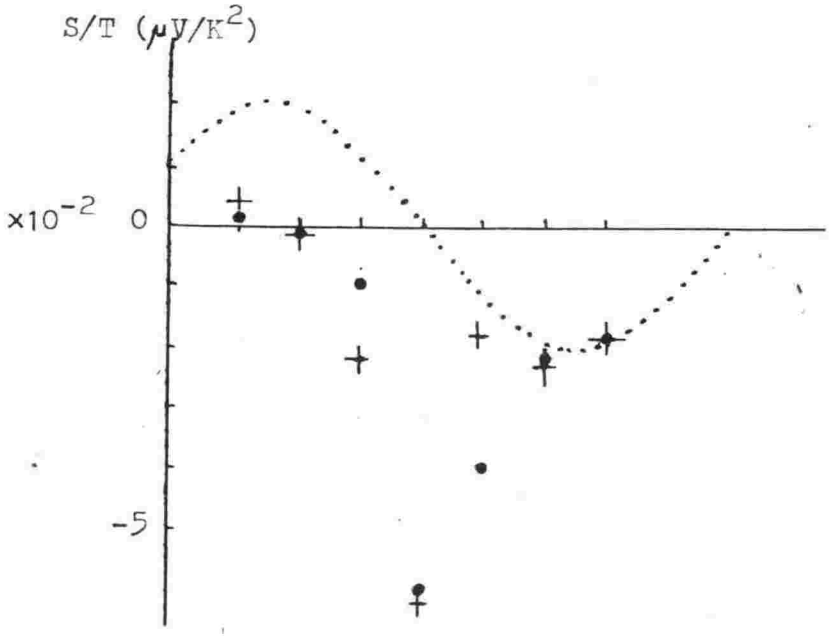

Zero Temperature Slope S/T of the Thermopower as a Function of Z (Zlatic and Rivier 1974)

● experimental values

\+ calculated values

..... due to a VBS alone

ii) Transition-Metal Hosts

a) Kondo Alloys

A Kondo alloy is, strictly speaking, any dilute alloy in which exist impurity spins of fixed magnitude. Traditionally they have been associated with magnetic (e.g. Fe) impurities in transition-metal hosts e.g. Cu(Fe), Au(Fe) etc. Here the host and impurity are not isoelectronic so there exists a substantial amount of potential scattering due to the impurities. The "giant" thermopowers observed in these alloys were first explained by Kondo (1965) following the success of his model in explaining the resistance minimum. In addition to the exchange interaction coupling host and impurity electron spins there must be added to the scattering some spin-independent interaction in the form of potential scattering. The model fails to account for the observed thermopowers if this potential scattering is neglected.

Suhl and Wong (1967), using a more complete treatment than did Kondo, predicted that the thermopower should show a peak at the Kondo temperature T_K. Kondo's original treatment, due to the neglect of some important higher-order terms, was not really adequate in explaining the observed thermopowers although it did provide some understanding of the giant thermopowers.

Guenault and MacDonald (1961) discussed the probable causes of the giant thermopowers in Kondo alloys and came to the conclusion that simultaneous elastic potential scattering of the conduction electrons was required in addition to the inelastic exchange scattering already present. The situation is somewhat similar to that in ferromagnetic metals and alloys.

b) LSF Alloys (Coles alloys)

A "Coles" alloy is one in which the host and impurity are more or less isoelectronic e.g. Pd(Ni), Rh(Fe) etc.

Fischer (1974), deciding that mixing between conduction electrons and impurity d-electrons was too difficult to include into a calculation of thermopower, simplified matters by assuming that a single band of electrons could describe the conduction and magnetic properties in these alloys. Then, limiting his treatment to hosts with no exchange enhancement, thus excluding Pd and Pt, he included the effect of potential scattering in his LSF model and predicted that the thermopower should show a peak, the nature of which

in part depended upon the amount of potential scattering. For Rh(Fe) a large negative peak at about 4K is predicted.

The two band LSF model of Lederer and Mills, and Kaiser and Doniach, specifically excludes potential scattering thus rendering itself unable to explain the giant thermopowers.

In general, we can say that in order to be able to account for giant diffusion thermopowers potential scattering as well as inelastic exchange scattering must be included in any theory.

2.3 Spin Fluctation Drag Thermopower

It is possible that a further effect in the thermopower of nearly magnetic alloys could occur (Kaiser 1976).

In the treatment of diffusion thermopower due to LSF the LSF's were considered to be in thermal equilibrium. This is not the case. Just as for the case of phonons the presence of a thermal gradient will produce disequilibrium in the LSF distribution since more LSF are excited at higher temperatures. Consequently there will be a bias of spin fluctuation wave vectors in the direction of the thermal gradient. This bias will tend to be transferred to the conduction electrons when they scatter off the spin fluctuations giving rise to a drag component in the thermopower. Any disequilibrium of excitations would be expected to produce a drag effect in the thermopower. Phonon and magnon drag thermopower are already well known (Blatt *et al.* 1967).

Adopting a model similar to that used to determine a qualitative expression for phonon drag thermopower we shall do likewise here.

In the presence of a thermal gradient there will also be a gradient in the spin fluctuation energy density U(T). This energy density gradient will lead to a spin fluctuation drag thermopower component. At very low temperatures, where we suppose that only spin fluctuation-electron collisions are dominant, the spin fluctuation drag thermopower is given by

$$S_{sf} \sim \frac{1}{3Ne} \frac{\partial u}{\partial T} \qquad \text{eqn. (2.4)}$$

where N is the conduction electron density, e the electronic charge and $\frac{\partial u}{\partial T}$ the constant volume specific heat C_{sf} of the spin fluctuations.

The expected characteristics of spin fluctuation drag thermopower are as follows:

1) S_{sf} ,in the low temperature limit, varies as C_{sf} and is therefore linear in temperature (see Chapter One). This linear T dependence is analogous to the T^3 dependence for phonon drag and the $T^{3/2}$ dependence for magnon drag (Blatt *et al.*).

2) The magnitude of S_{sf} ,like C_{sf} ,in the very low concentration limit should be proportional to the number of spin fluctuations i.e. proportional to the impurity concentration c, and relatively independent of the presence of other scattering.

3) The sign of S_{sf} is negative since e is negative and normal electron scattering by spin fluctuations "drags" electrons down the temperature gradient as for phonon drag. Umklapp processes can, however, drag electrons up the gradient giving rise to a positive contribution. If U-processes dominate the scattering a positive S_{sf} would result.

Equation (2.4) is essentially a free electron gas model and assumes that all the spin fluctuation momentum is shared equally among the conduction electrons. For a metal with a complex band structure this may not necessarily be the case.

4) At temperatures above T_{sf} the thermopower will be greatly reduced since the spin fluctuation spectrum becomes blurred out and the effect of spin fluctuations on the physical properties is reduced. The decrease of resistivity below the linear T law is an example. In addition, if spin fluctuation interactions other than collisions with conduction electrons become important, not all the spin fluctuation momentum will be transferred to the conduction electrons.

In general S_{sf} is expected to exhibit a peak at about T_{sf} somewhat analogous to the phonon drag peak at about $\frac{\theta D}{5}$, where θD is the Debye temperature.

5) Since independent sources of thermopower are additive we may simply add S_{sf} onto the already present diffusion and phonon drag components to give a total thermopower

$$S = S_d + S_g + S_{sf}$$

For dilute alloys we may assume that S_d and S_g are the same as in the host. Hence the thermopower due to LSF is the difference between the alloy and host thermopowers. This is not true if the impurities added dominate the scattering. Then the host thermopower S_d is washed out as we shall show in Chapter Four. If S_d is small this is of little consequence if S_{sf} is large.

Chapter Three

EXPERIMENTAL DETAILS

3.1 Resistivity of Wire Samples

Most of the Rh(Fe) samples used in this study were prepared by Engelhard Industries Ltd. and kindly supplied to us by R. Rusby (National Physical Laboratory, U.K.). One additional sample (number 6 in Table 4.1) was prepared by Johnson-Matthey Ltd. and supplied by G.K. White (CSIRO, Australia).

The resistivities of these Rh(Fe) wire samples were measured in a cryostat designed by Dr H.J. Trodahl of Victoria University. As this cryostat is not specific to this study its functioning will be only briefly outlined.

Two samples were measured simultaneously by winding several cms of each wire around a copper rod with a layer of cigarette paper soaked in GE7031 varnish for adhesion. The purpose of the cigarette paper is, of course, to provide electrical insulation while at the same time providing reasonable thermal contact between the wires and copper by dint of its thinness. Reference to Figure (3.1) should clarify constructional details.

Standard four-terminal resistance measurements were made on the samples with the sample current being common to both. Thin, enamelled copper wires were used to provide contact with the samples. The wires were attached with non-superconducting Bi-Cd solder. The current was supplied by a voltage source in series with a large resistance (about 10,000 ohms) and the samples. The current was monitored with a voltmeter measuring the potential drop across a standard resistance in series with the current circuit. The potential drops across the samples were each measured with a Keithley model 148 nanovoltmeter with its output fed into a Hewlett-Packard model 7100B chart recorder. The large voltage proportional to the residual resistivity of the samples was nulled out within the NVM so that the temperature-dependent component of the resistivity could be more accurately measured.

The l/A ratios of the samples were determined by an indirect method. Rather than measuring the diameters of the wires directly and converting to cross-sectional area in the usual manner, it was decided, for better accuracy, to determine l/A by weighing a measured length. Measuring the diameters

directly introduces an uncertainty of greater than 10% into 1/A on account of the thin diameters involved (nominally 0.13 and 0.05 mm). Briefly, the method involves determining the length of the sample between the potential probes, cutting the wire at these points and subsequently weighing the resulting piece. The cross-sectional area of the wire is calculated from the volume and length assuming that the mass-density of the sample is the same as that of pure Rh. With the small concentrations of Fe involved (less than 1 at .%) this seemed a reasonable assumption. The diameters of all of the wires were checked for uniformity as the method could give erroneous results if the diameters varied widely. All diameters were found to be uniform over the lengths of interest within the uncertainty limits of the travelling microscope employed for the purpose, about 10% for these diameters. Changes in cross-section of a random nature of up to 10% were calculated to cause an error of about 1% in 1/A. The overall accuracy due to this method is about 1% in 1/A.

Uncertainties due to non-linearities in both the NVM and the chart recorder should each be about 1% of full scale deflection, if the manufacturers are to be believed. If it were possible to keep to the same part of the scale throughout the measurement the resulting accuracy would, theoretically, be considerably less. However the overall accuracy is limited by the accuracy to which the chart record can be read. We estimate the overall uncertainty in the magnitude of the resistivity to be less than 3%.

With the sample currents employed, up to 50 mA, Joule-heating effects were found to be negligible. The effect of stray thermal voltages (due to the temperature difference between the measurement leads at the top and bottom of the cryostat) was determined by performing the measurement with the sample current reversed. No measurable difference was discerned.

Sample temperature was determined by means of agermanium resistance thermometer attached to the cryostat base. Providing that any heat flows into or from the sample do not measurably raise or lower the sample temperature above or below that of the cryostat base the assumption that the sample and thermometer are at the same temperature is probably justified. This state of affairs is facilitated by thermally attaching all leads going to the sample (and thermometer) to the cryostat base and by keeping the gas pressure within the cryostat as low as practicable to minimise heat flows through the gas. A "conduction shield" connected to the cryostat base was employed to enclose the inner workings of the cryostat so that the sample

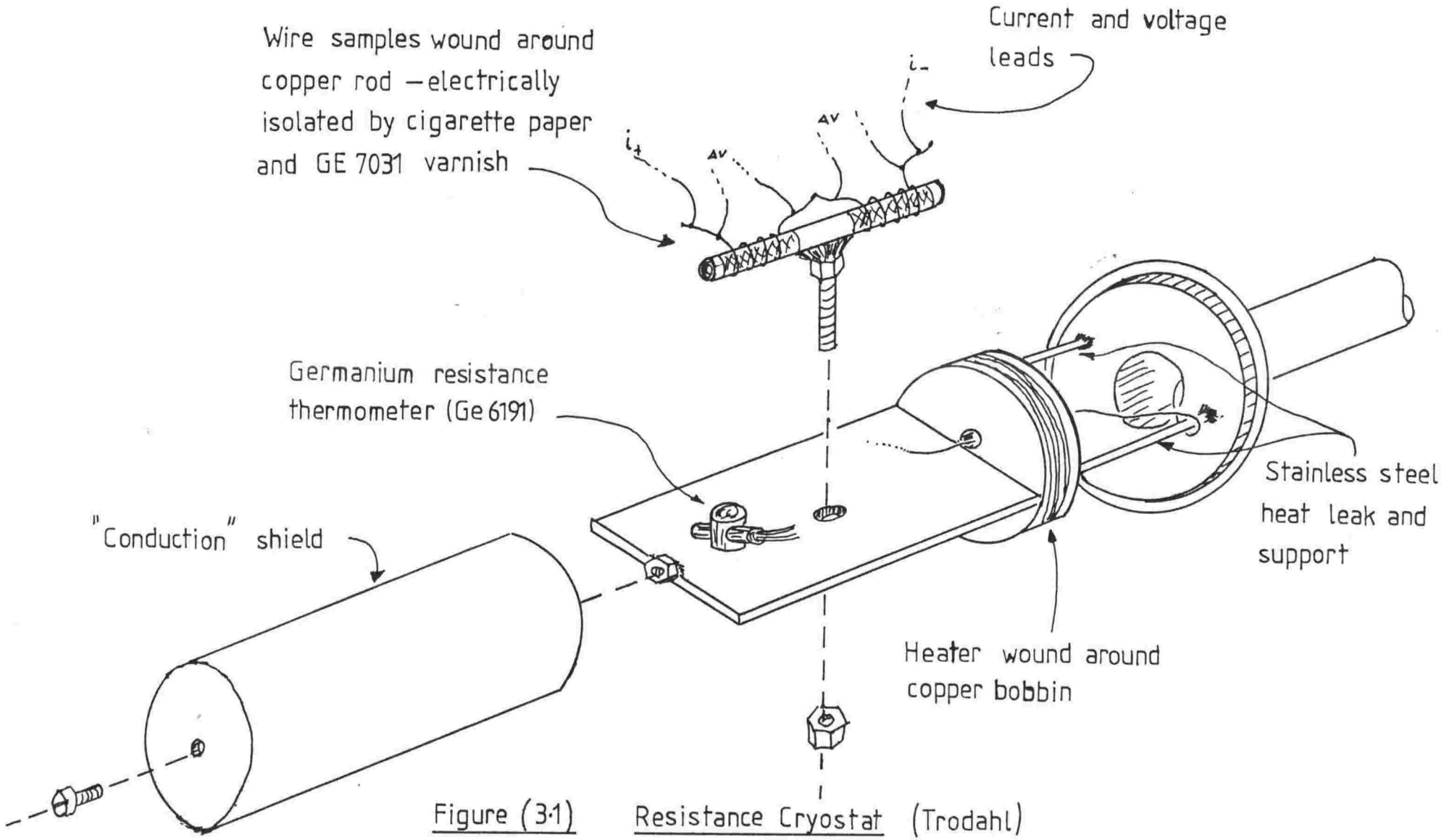

Figure (3·1) Resistance Cryostat (Trodahl)

"sees" a large surface at the same temperature as itself rather than a large surface (the outer can) at a constant liquid helium bath temperature. We estimate that the sample temperature is reliably known to better than 0.05K over the low temperature range of interest.

The sample temperature was maintained above the bath temperature by means of a nichrome wire resistance heater wound around a copper bobbin attached to the cryostat base.

3.2 Sample Treatment

In order to observe the effect of changing dislocation scattering on the resistivity and thermopower two wire samples were rolled flat between hard-nickel rollers to increase the residual resistivity, and one was annealed in a high vacuum for 15 minutes at 450 C to reduce its initially large residual resistivity. Another sample was stretched in an attempt to increase its residual resistivity although its thermopower was not measured.

Since calculation of l/A for the rolled samples by direct measurement of the cross-sectional area was precluded because of the irregular shape it was determined in the same fashion as for the wires. However the uncertainty in l/A is not important for the method of analysis outlined in Chapter Four.

The consequences of these treatments will be discussed in Chapter Four.

3.3 Thermopower of Wire Samples

In Chapter Two the absolute thermopower S of a material was defined by $\tilde{E} = S\nabla T$ where $\tilde{E}$ is the electric field created in the material by the action of electrons under a temperature gradient ∇T. If we consider a length of conductor with a small temperature difference across the ends we find there will exist a potential difference across the ends. Experimentally, then, the thermopower is $S(T) = \frac{\Delta V}{\Delta T}$ evaluated at the average sample temperature $T = To + \frac{\Delta T}{2}$.

In order to evaluate S(T) we must measure ΔV, ΔT and T. Now, since we have no practical means of measuring a potential difference without drawing some current from the circuit we cannot directly measure ΔV due to the sample. The reason for this is as follows: suppose we have two wires connected in a close circuit under the influence of a temperature difference as in the following diagram:

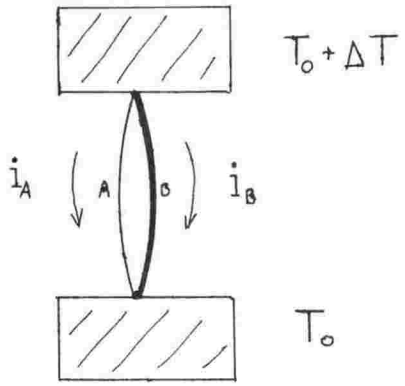

unless A and B are different materials (or different states of the same material e.g. one under strain) the two currents i_A and i_B are equal and no nett current will flow around the circuit. Hence to observe a thermoelectric current A must be different from B, or as it turns out, the absolute thermopower of A and B must be different.

In practice we use the following thermocouple circuit to measure the thermopower of a sample, A.

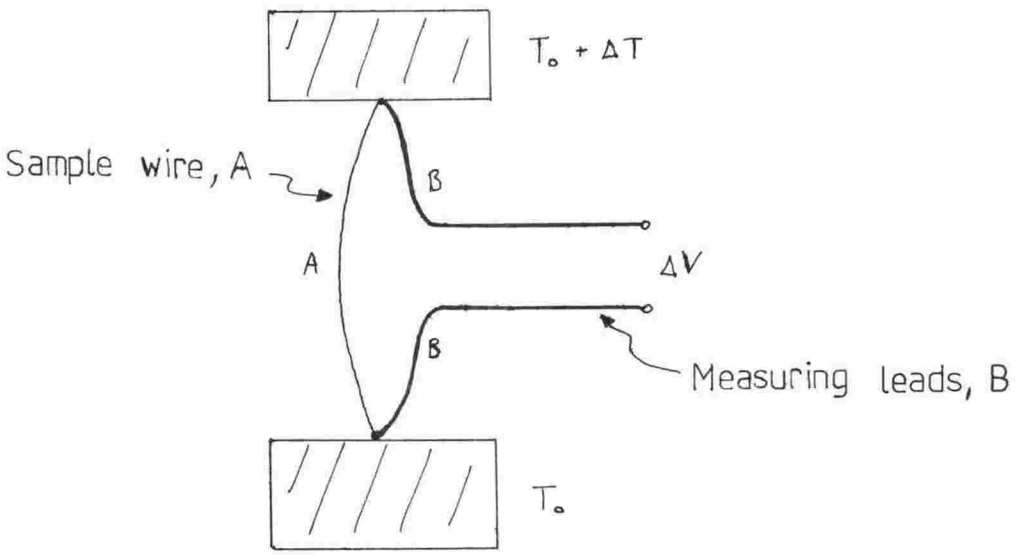

The thermopower of the thermocouple is $S_{total} = \frac{\Delta V}{\Delta T}$ with ΔV, ΔT being defined as in the diagram.

Integrating the experimental formula we may write

$$\Delta V = \int_{To}^{To + \Delta T} S_{total} dT$$

Now ΔV is due to contributions from both A and B. To determine S_{tot} in terms of S_A and S_B we sum the contributions to ΔV around the circuit.

$$\Delta V = \int_{Ti}^{To} S_B dT + \int_{To}^{To + \Delta T} S_A dT + \int_{To + \Delta T}^{Ti} S_B dT$$

$$= \int_{To}^{To + \Delta T} (S_A - S_B) dT$$

Hence $S_{total} = S_A - S_B$, the difference between the absolute thermopowers.

Now we can measure S_{tot}. Provided we know S_B we can evaluate the sample thermopower S_A. This brings us to the problem of how to evaluate S_B, the reference thermopower. If we can only measure the difference between thermopowers how do we initially determine an absolute reference thermopower? Luckily, as it turns out, there is another thermoelectric property of conductors known as the Thomson heat which is related to the absolute thermopower in the following manner. In a conductor under the influence of a temperature difference through which an electric current also flows we find that, in addition to the Joule heating, there is an evolution or absorption of heat throughout the conductor depending upon the relative directions of the current I and the temperature difference ΔT, which is directly proportional to the product $I\Delta T$ and dependent in magnitude upon the absolute temperature of the conductor.

The rate of heat production in the conductor may be written

$$\dot{Q} = I^2R - \mu I \Delta T$$

where R is the resistance of the conductor and μ is the proportionality factor called the Thomson heat of the conductor. The relation between μ and S is

$$\mu = T\frac{dS}{dT}$$

first derived by William Thomson in the 19th century from thermodynamic principles. Integrating,

$$S(T) - S(O) = \int_{o}^{T} \frac{\mu(T')}{T'} dT'$$

It can be argued from an application of the 3rd Law of Thermodynamics that the thermopower must be zero at T = OK. Hence,

$$S(T) = \int_{o}^{T} \frac{\mu(T')}{T'} dT'$$

Thomson heat measurements have been made on lead (Pb) by Christian *et al.* (1958) and, more recently, by Roberts (1977). The thermopower calculated from these Thomson heat data are presented on the following graph for temperatures up to 20K. The outstanding feature on this graph is that below 7.2K the thermopower is identically zero.

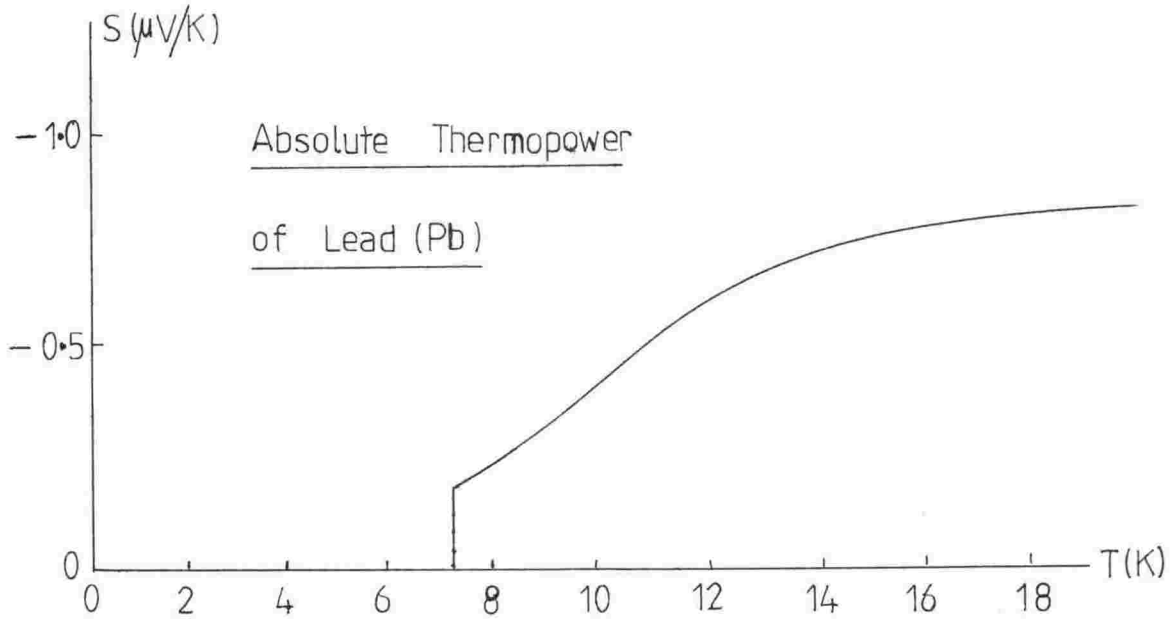

A simple argument involving another thermoelectric coefficient, known as the Peltier heat, and the 2nd Law of Thermodynamics tells us that below its transition temperature a superconductor will have zero thermopower, under normal conditons, Pb being a well-known superconductor.

Up to about 300K Pb has been chosen as an absolute reference standard for thermopower since pure Pb wires can be easily made and annealed thus keeping variations in thermopower from sample-to-sample to a minimum. There is the added bonus that the thermopower of Pb is zero below 7.2K so that the

reference thermopower is known exactly below this temperature.

3.4 Thermopower Cryostat for the Measurement of Low Temperature Thermopower of Wire and Thin Film Samples.

There are two basic techniques for measuring thermopower: the integral method and the differential method.

In the integral method one junction of the thermocouple is held at a constant, known temperature while the other junction is raised in temperature and the total emf across the thermocouple is measured over the temperature range of interest. To obtain the thermopower from the data the emf vs. temperature curve is differentiated.

In the differential method the thermopower is obtained directly by raising both junctions to the required temperature T and then further raising one junction by a small temperature ΔT, and measuring the small emf ΔV created. The thermopower at the average sample temperature $T + \frac{\Delta T}{2}$ is then simply $\frac{\Delta V}{\Delta T}$.

The differential method has all the advantages of measuring a small voltage difference ΔV directly whereas the integral method inherently measures ΔV as the difference between two relatively large voltages. Zero drifts in voltage (that is, the spurious voltages that almost always exist in the absence of an applied ΔT) are not easily accounted for in the integral method whereas in the differential method the time interval when measuring ΔV is generally so small that drifts in voltage have relatively little effect upon the accuracy in determining ΔV.

Liquid helium is universally used as the refrigerant at these low temperatures. We can cover the temperature range from 4.2K down to about 1.35K by controlling the vapour pressure of the liquid helium. Liquid helium has a boiling point of 4.2K at atmospheric pressure; reducing the vapour pressure by pumping on the vapour reduces the boiling point to a practical minimum of around 1K. (See White (1959) for tables of vapour pressure vs. temperature).

From 4.2K upwards we use an electrical heater thermally attached to the sample to raise it to a suitable temperature above the bath temperature of 4.2K. The temperature difference ΔT is maintained across the sample by means of another heater attached to the end of the sample distant from the main heater used to maintain the temperature of the sample above the bath temperature.

i) General Construction

The interior layout of the low-temperature end of the cryostat should be evident from the ensuing diagrams; the following brief description should clarify any further important details.

The cryostat was designed with a view to making thermopower measurements upon evaporated metal thin-film samples deposited on glass substrates. The manufacture of these thin-film samples will be described, together with the measurements, in the second part of this thesis. The heart of the cryostat consists of a frame constructed from copper within which is accommodated the sample together with all the ancillaries, such as the sample heater and the differential heater etc.

Connecting the frame to the stainless-steel flange, which is at the helium bath temperature, is a length of stainless-steel rod which serves as a heat leak to the bath. The main sample heater is connected to the frame at the top of this rod, the application of electrical current to which serves to maintain the entire frame assembly at a certain temperature above the bath temperature. The heater consists of several turns of 44g enamelled manganin wire wound around a copper bobbin and attached between the rod and the frame. This manganin wire has a resistance of on the order of an ohm per cm. The differential heater at the far end of the sample was a similar affair.

Completely surrounding the frame assembly, although not air-tightly, is an inner can constructed from copper foil. The purpose of this is to act as a "radiation shield", or more correctly a "conduction shield". The presence of exchange gas in the cryostat provides the means by which heat may flow from various parts of the frame assembly to other parts, and also to the outer can which is at bath temperature. This means that, when the sample has been heated several degrees above bath temperature, heat flows could be sufficient to create considerable temperature differences of an undesirable nature. An example will serve to illustrate the point. Suppose the thermometers attached to the sample were not in very good thermal contact with the samples. Heat flowing from the sample, at temperature T, say, across the imperfect connection between the thermometer and the sample, thence through the thermometer and finally to the outer can via the exchange gas, will create a temperature difference between the sample and the thermometer. This is of vital importance since we wish to know the temperature of the sample at the point of contact between the thermometer and sample. The

inner can is thermally connected to the frame assembly by soldering to a flange with Wood's Metal, a low melting-point solder. Thus the sample should "see" a large surface at the same temperature as itself rather than a surface at the bath temperature. The only temperature differences then should be those created by the differential heater; at least they should be considerably smaller than they would be without the inner can.

The outer can is made of brass and is bolted to the flange at the end of the stainless steel tube, through which wires pass and gas is pumped into or out of the cryostat. Six 6BA steel bolts and an O-ring made from Pb wire plus a smear of Apiezon-N grease serve to provide a vacuum-tight seal.

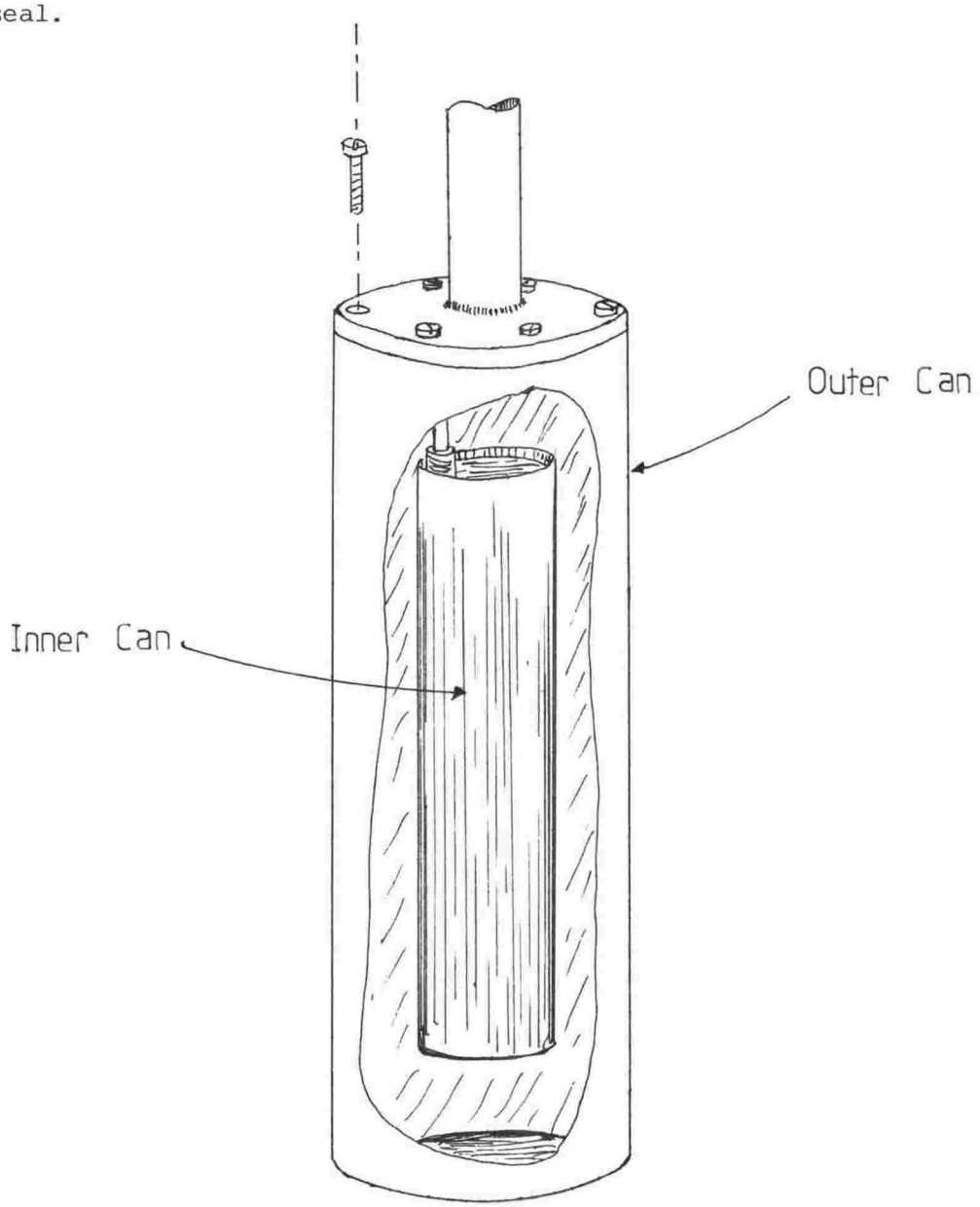

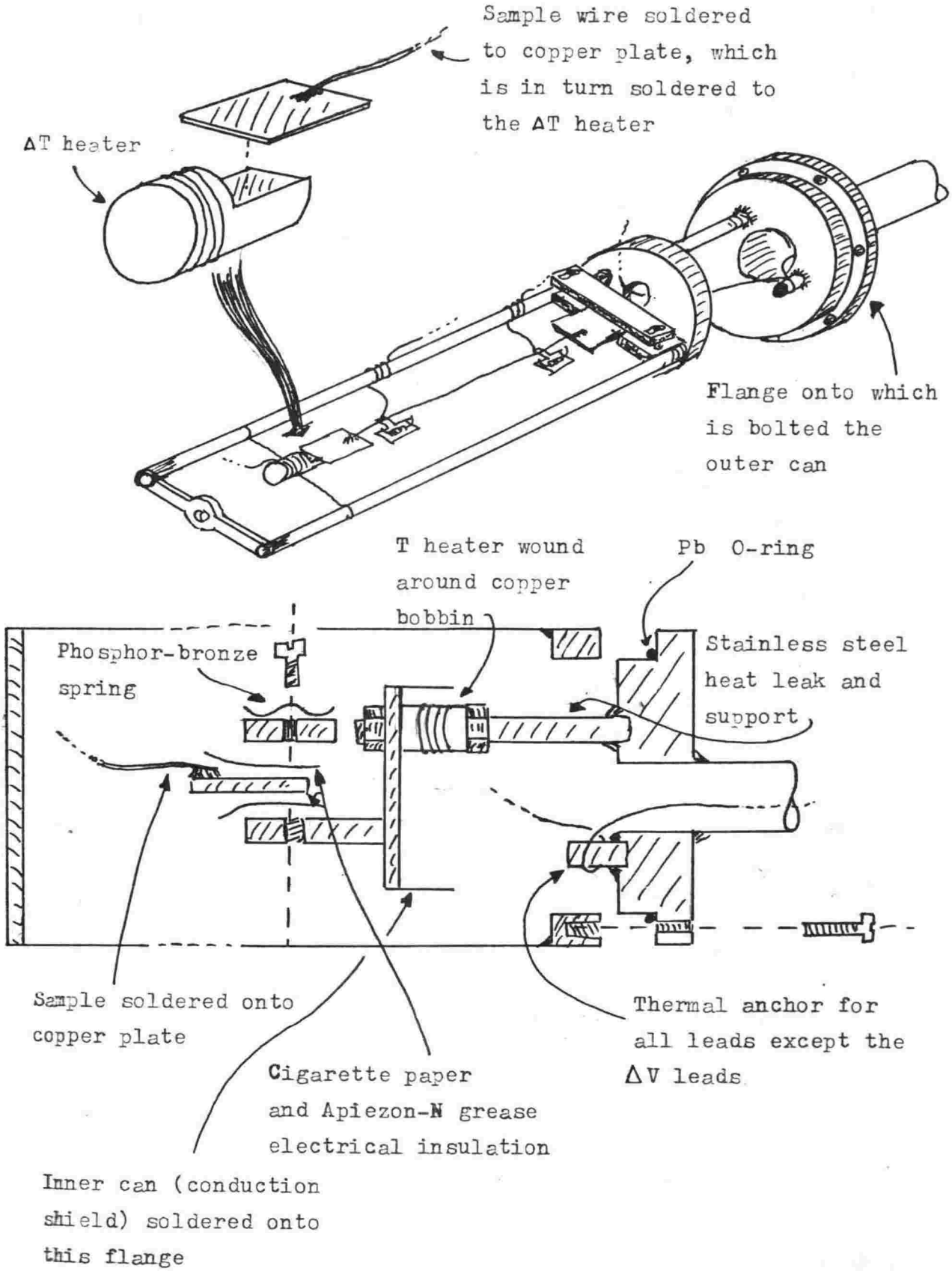

Thermopower Cryostat

ii) Measurement of the Sample Temperature Difference, ΔT.

The temperature difference across the sample was measured with carbon resistance thermometers attached to the same points as were the manganin reference leads used in the measurement of the potential difference, ΔV. A well-known property of carbon is that, at low temperatures, the electrical resistance is a very strong function of temperature, going as $R \sim \exp \frac{1}{T}$, similar to germanium, which is used, suitably doped, in commercial thermometers. The one major disadvantage of using carbon as a thermometer material lies with changes in the resistance upon thermal cycling between room and liquid helium temperatures, the resistance usually increasing slightly after each "run". In practice we found that the resistance increased by several ohms at 4.2K after one thermal cycle and that it would remain constant for several subsequent runs, after which it would increase markedly once more, usually rendering the thermometer useless unless calibrated again. The one big advantage of carbon resistance thermometers is that they can easily and cheaply be made to suit the purpose at hand. Our thermometers were made from 33 ohm "Ohmite Little Devil" resistors ground flat on one side and attached to "T"-shaped plates of copper with cigarette paper and GE7031 varnish.

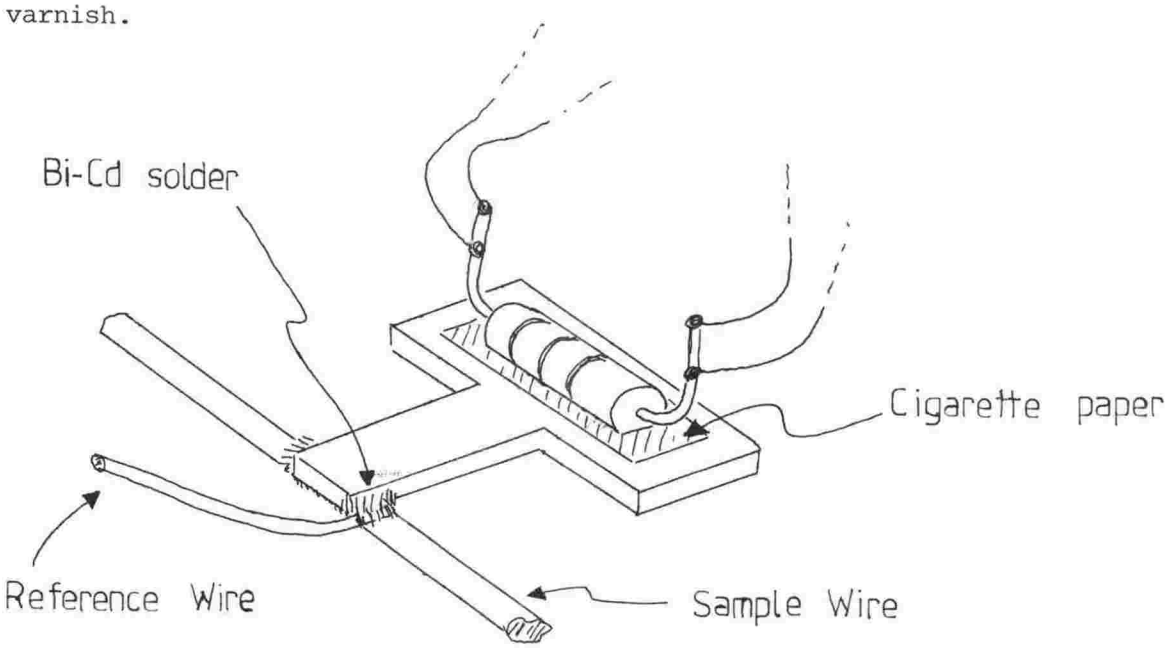

The thermometers thus constructed were placed in a "calibration cryostat" and their resistance vs. temperature characteristic determined up to 100K, the limit of calibration for the standard commercial germanium thermometer used as a "primary" standard.

After calibration the thermometers were installed in the experimental cryostat. Manganin wires were used to make electrical connection to each thermometer as these possess a high electrical resistance, and hence a high thermal resistance, per unit length, thus impeding any heat flows into or out of the thermometers via the leads. We wish the thermal resistance between thermometer and sample to be as small as possible and between thermometer and the rest of the universe as large as possible so that the thermometers are thermally "anchored" to the sample. The resistances of the two thermometers were determined by a standard 4-terminal technique, the same current flowing through each resistor. The potential drop across each resistor was sampled alternately, without and with a temperature difference applied. The temperature difference was essentially then just the difference in absolute temperatures at each thermometer, albeit determined in a more sophisticated fashion than by merely subtracting absolute temperatures, which latter was found to give rather large uncertainties unless temperature differences on the order of degrees were employed, since the temperature difference is the small difference between two large quantities. Although the absolute temperatures may be found to, say 0.05 K, if a temperature difference of 0.2K is needed for resolution (e.g. in the thermopower of Pb) this results in an uncertainty of 50% in ΔT!

To take advantage of the sensitivity of carbon resistance thermometers a means of measuring the voltage across the resistors down to 10 μV was required. This was achieved by feeding the voltage into the same nanovoltmeter (Keithley 148) used to measure the voltage across the sample. The output of the nanovoltmeter was then fed into a digital voltmeter so that the voltage could be accurately read to 10 μV. A system of peg switches and rotary switch was employed to switch the single nanovoltmeter between the sample and the two thermometers.

Now, determining ΔT as the direct difference between the absolute temperatures at each thermometer leads to the absolute uncertainty in ΔT being the sum of the absolute uncertainties in the two temperatures, an undesirable aspect of determining ΔT directly. While errors in plotting the R vs. T data for the resistance thermometers do not unduly affect the determination of T to any great extent (at least not for our purposes where an uncertainty in T of 0.05K has very little effect upon the final thermopower data points as plotted up on a graph), such an uncertainty has an enormous effect upon ΔT, as mentioned previously. Clearly, some means of reducing the effect of uncertainties in the R vs. T thermometer data was required. As the resistance of the thermometers was of necessity only

determined at intervals of about 0.25 to 0.5K uncertainty in interpolation between these calibration points leads to an uncertainty in finding the absolute temperature between these points. If the data could be made to fit a straight line characteristic interpolation would then become more accurate. This was achieved by first taking the natural logarithm of the raw R vs. T data and plotting a graph of lnR vs. $\frac{1}{T}$. The slope of the tangent to this curve at various points along the curve was next plotted as a function of $\frac{1}{T}$. The resultant characteristic is more or less a straight line over substantial portions of temperature range. The theory behind this method is as follows: since $R \sim \exp(\frac{1}{T})$, at least over small ranges of temperature, we then have $\ln R \sim \frac{1}{T}$, and furthermore, $d(\ln R)/d(\frac{1}{T}) \sim a$, where a is a constant, or at least a slowly varying function of T. Thus it can be seen that at each operation we reduce the temperature-dependence of the curve i.e. we "flatten" it out.

A graph of $d(\ln R)/d(\frac{1}{T})$ vs. $\frac{1}{T}$ was drawn for each thermometer and the temperature change for each thermometer upon the application of a temperature difference to the sample is given as follows:

$$\delta T = \frac{\Delta \ln R}{\alpha_{average}} \, T^2_{average}$$

where $\alpha_{average}$ is the average value of $d(\ln R)/d(\frac{1}{T})$ between the initial and final temperatures, for each thermometer. ΔT is then just the difference in the temperature changes δT at each end. It can easily be shown that the % uncertainty in ΔT is proportional to the % uncertainty in T, whereas in the determination of ΔT by the direct difference method the absolute uncertainty in ΔT was proportional to the absolute uncertainty in T. The uncertainty has thus been reduced considerably.

Graphs of R vs. T, lnR vs. $\frac{1}{T}$ and $d(\ln R)/d(\frac{1}{T})$ may be seen on the following pages.

iii) Measurement of the Sample Potential Difference, ΔV.

The emf produced by the sample under the influence of a temperature difference ΔT was measured by placing the sample in one arm of a thermocouple circuit. As the reference arm of the thermocouple manganin alloy wires were chosen. Although the use of a material such as Pb would have been preferable from the point of view of its thermopower being accurately known, and also that it has zero thermopower below 7.2K, for practical reasons it was not done so; Pb wires tend to be fairly fragile and the relatively high thermal conductance compared with the manganin which was available to us were factors

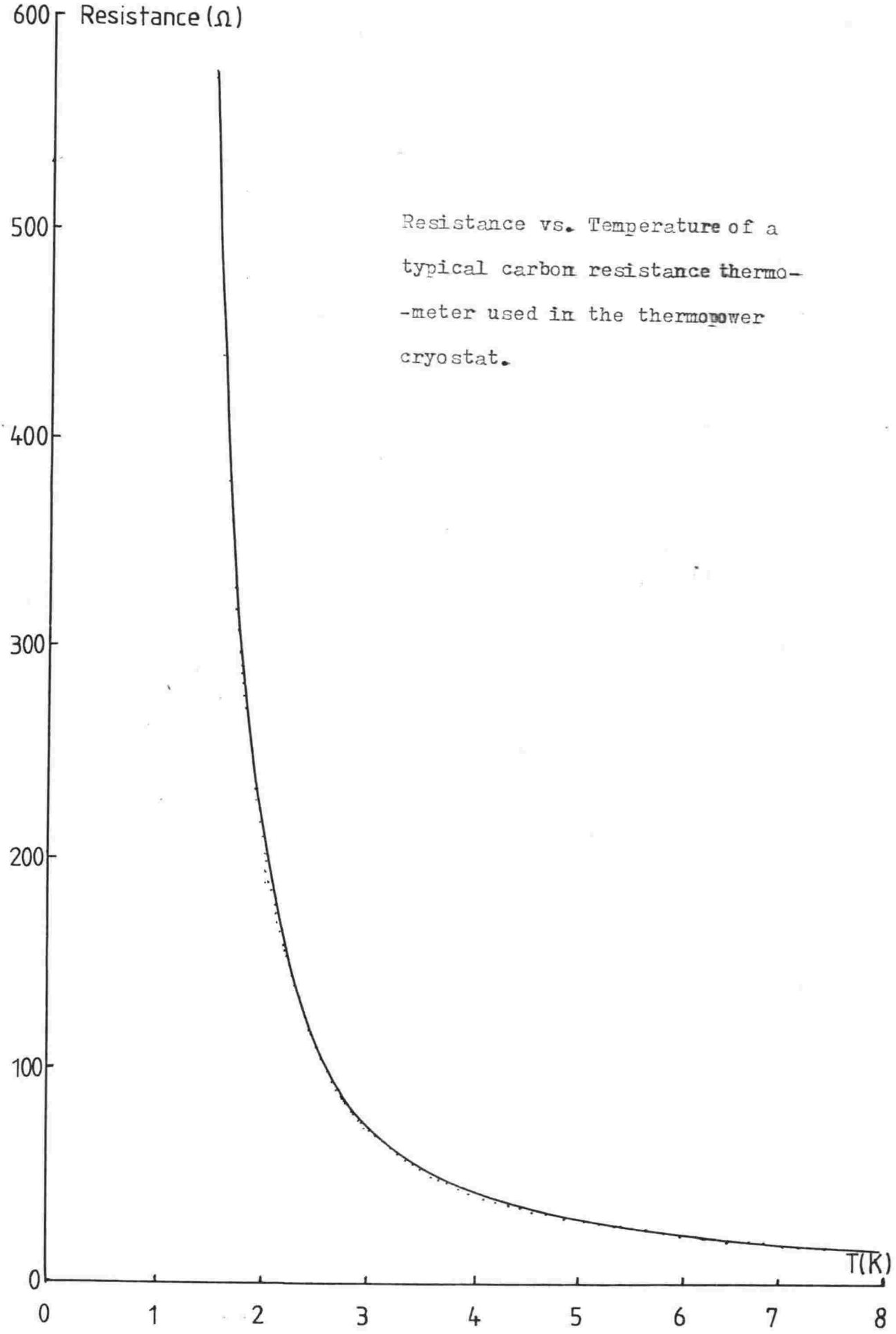

Resistance vs. Temperature of a typical carbon resistance thermo--meter used in the thermopower cryostat.

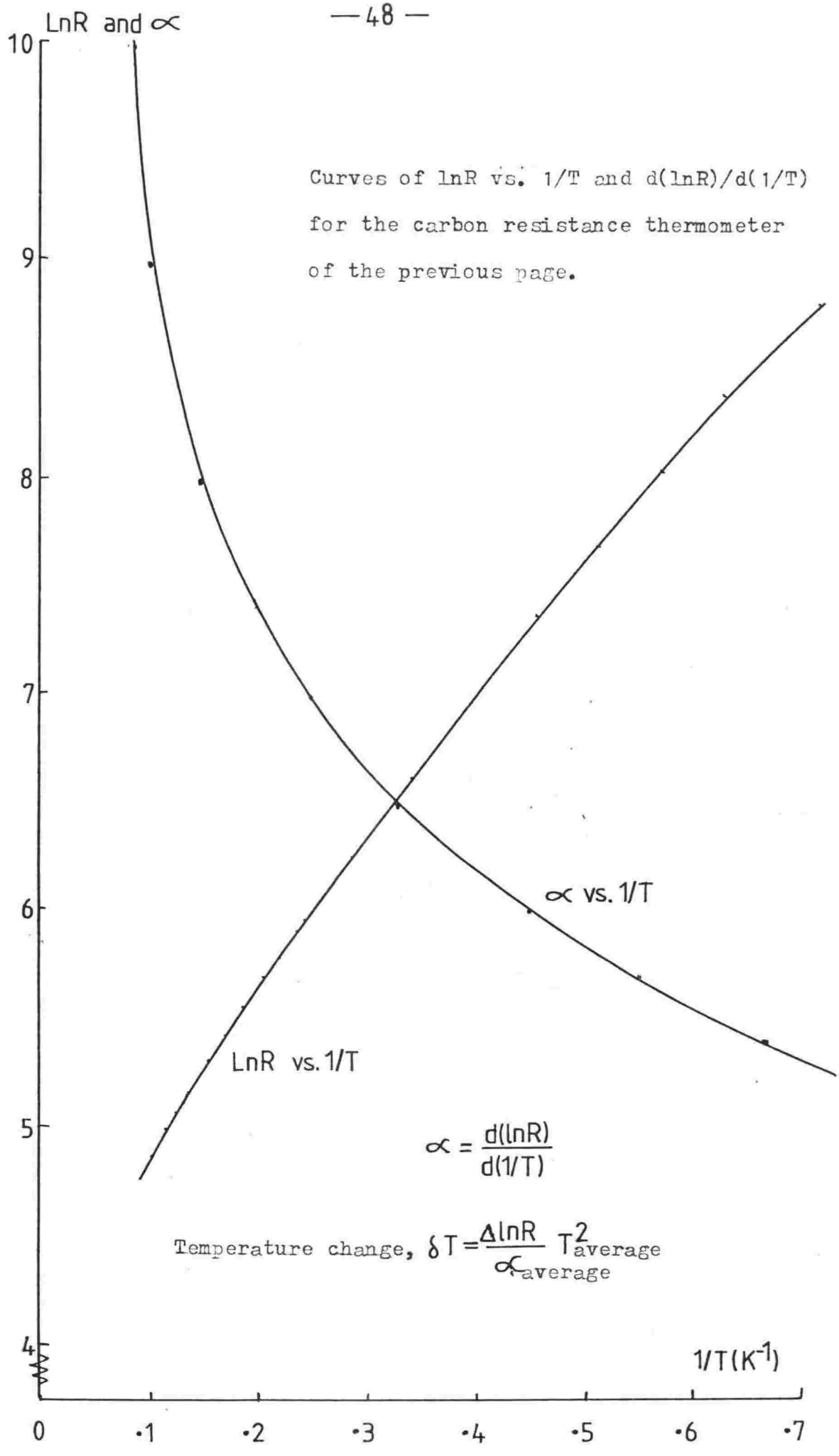

Curves of lnR vs. 1/T and d(lnR)/d(1/T) for the carbon resistance thermometer of the previous page.

$$\propto = \frac{d(\ln R)}{d(1/T)}$$

Temperature change, $\delta T = \frac{\Delta \ln R}{\propto_{average}} T^2_{average}$

which helped decide against Pb in favour of manganin. As no low temperature thermopower data for manganin were available at the time of performing the measurements we determined the thermopower by calibrating against a Pb wire connected in place of the sample proper. Manganin was found to have a small, positive and linear thermopower, up to 11K. That the thermopower was small was a boon to us since uncertainties in the reference (manganin) thermopower thus have only a slight effect upon the total measured thermopower. This comes about because most of the uncertainty in determining thermopower by our method creeps in via the ΔT measurement, and so the uncertainty in thermopower tends to be a constant percentage of the thermopower rather than a constant absolute value. Thus the smaller thermopower look "more accurate".

Inhomogeneities in the thermopower of manganin along its entire length were checked by rubbing a piece of dry ice (solid CO_2; $T \simeq 200K$) along the wire and measuring the emf's produced across the ends. The maximum emf's produced were $\pm$ 2 μV, indicating a maximum local change in the thermopower of about $\pm$ 0.02 $\mu V/K$.

The manganin reference leads were thermally anchored to the frame by winding the leads around the frame members and securing in place with GE7031 varnish. It should be pointed out that the manganin leads had been enamel-coated to provide electrical insulation.

The reference leads were soldered to the sample using Bi-Cd solder, which is superconducting only below the temperature range of access to us. A non-superconducting solder is necessary to prevent shorting out of the sample below the solder's transition temperature. The procedure for attaching both the reference leads and the thermometers onto thin film samples will be outlined in Part Two of this thesis.

The manganin reference leads were brought up the cryostat tube through polythene tubing, direct contact between the walls and wires being avoided this way. The reference leads were then connected to a peg switch made from brass. A switch was necessary since our only nanovoltmeter (Keithley model 148) had to do duty measuring both ΔV and the voltage from the ΔT thermometers (see the wiring diagram for details). Because, at the peg switch, we have a junction between two dissimilar metals viz. manganin and copper, it was necessary to ensure that an isothermal environment was created here to prevent spurious thermo-emf's occurring. This was achieved quite satisfactorily by covering the switch area with wads of cotton wool. In spite of this precaution it was found that long term spurious voltages were present together

with the ΔV signal. These were relatively constant in time and could be followed on the chart recorder connected to the output of the nanovoltmeter (Hewlett-Packard model 7100B). These voltages are probably a result of the temperature difference between the top of the cryostat and the bottom (temperature difference of about 300K) acting upon inhomogeneities in the manganin leads. While the maximum local change in manganin thermopower was only about 0.02 $\mu V/K$ these local changes could, for instance, all occur in only one of the reference leads, giving possibly a substantial difference between the thermopower of one reference lead and the other. The spurious voltages were on the order of microvolts.

It should be mentioned that extreme care needs to be taken with earthing of the ΔV circuit. In an early experimental set-up the sample was connected directly to the copper frame, which was in turn connected to the rest of the cryostat, and earthed at the top. Measurement of the thermopower of Pb this way led to the transition step being an order of magnitude larger than it actually is! The conclusion reached as a result of this state of affairs was that unfavourable earth loops had been formed somewhere in the ΔV circuit. Having the entire ΔV circuit above ground eliminated this effect. The only earth connection was between the nanovoltmeter input leads and the cryostat case to electrically shield the manganin reference leads from stray electrical disturbances.

iv) Operating Procedure and Test Checks

Ther thermopower was measured with a bath temperature of 4.2K and also with a bath temperature of about 1.4K. The sample was heated to various temperatures above the bath temperature and the thermopower measured. Overlap of the thermopower data points in each temperature range was evidence that the system was at least not malfunctioning. The dependence, or rather lack of it, of thermopower upon ΔT was likewise deemed a favourable sign. One factor which does affect the magnitude of the thermopower is the pressure of helium gas inside the cryostat. Too much or too little exchange gas could, under certain circumstances, lead to the thermopower being incorrectly measured. In practice it was found that the presence of too much exchange gas was the main problem. At the start of each run the thermopower at 4.2K was measured as a function of gas pressure. A graph of S vs. -p was then plotted and the plateau region (see below) was taken to be the correct operating point. That the thermopower of Pb when measured in this pressure region agrees with published data is good evidence that the procedure was valid.

Of course the gas pressure as measured at the room temperature end of the cryostat is not necessarily related to the pressure at the low temperature end in an obvious manner, so some quantity proportional to the pressure at the bottom was needed. The quantity chosen was the effective thermal resistance between the two thermometers. This is more or less the ratio between the measured ΔT and the heat input to the ΔT heater, I^2R, where I and R are the heater current and resistance respectively. Of course this is not the thermal resistance of the gas in parallel with the sample since, for large gas pressures (around 0.1 atmosphere and above) the thermometers appear to become "detached", in a thermal sense, from the sample. As the gas pressure decreases the thermometers become more thermally "attached" to the sample and the measured thermopower reaches its correct value. The curve of S vs. W, where W is the effective thermal resistance between the thermometers, has the following shape:

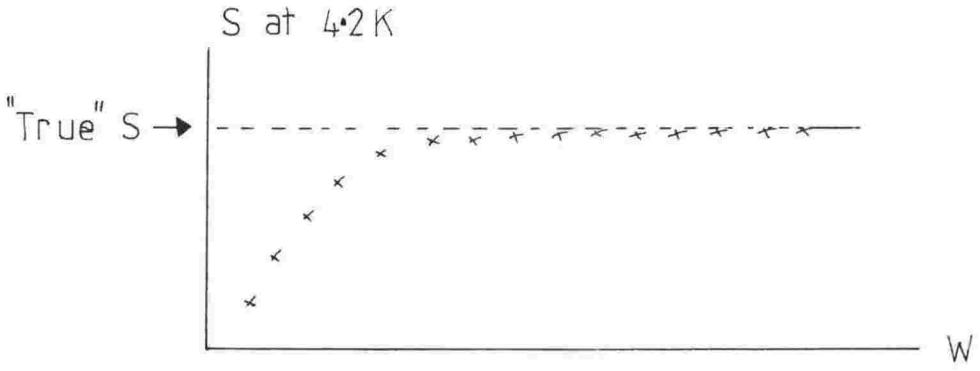

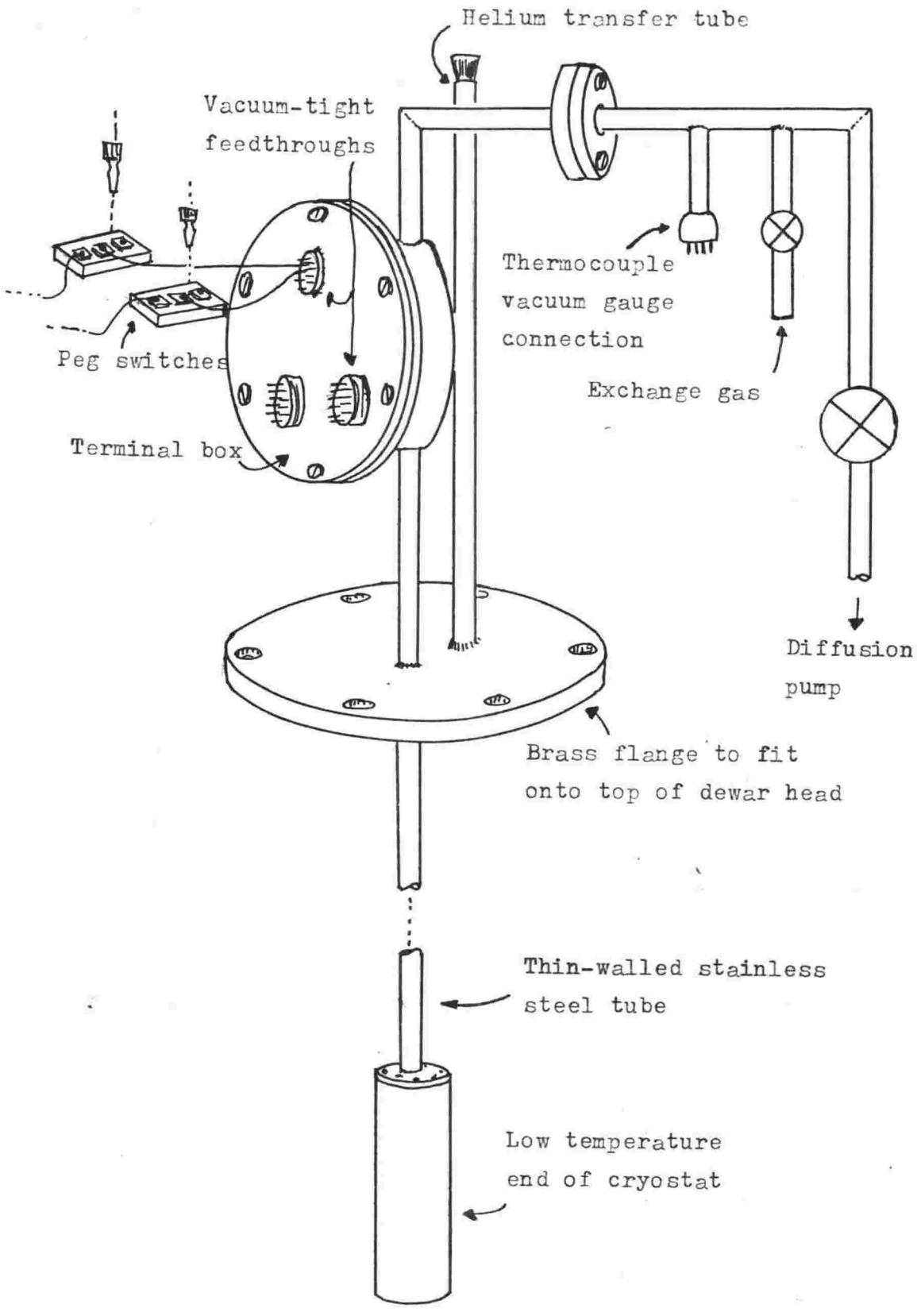

Room Temperature End of Thermopower Cryostat

Wiring Diagram for Thermopower Cryostat

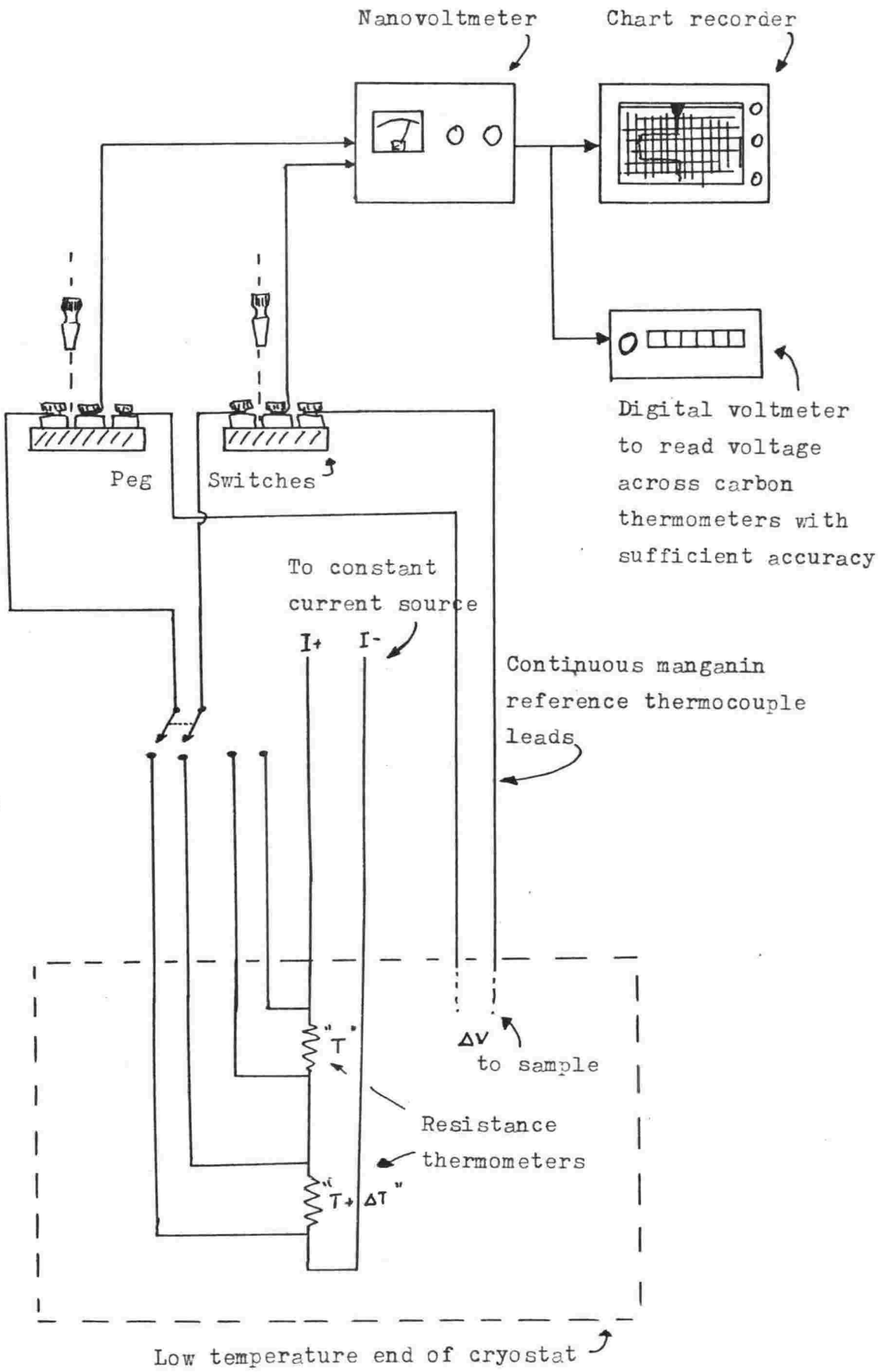

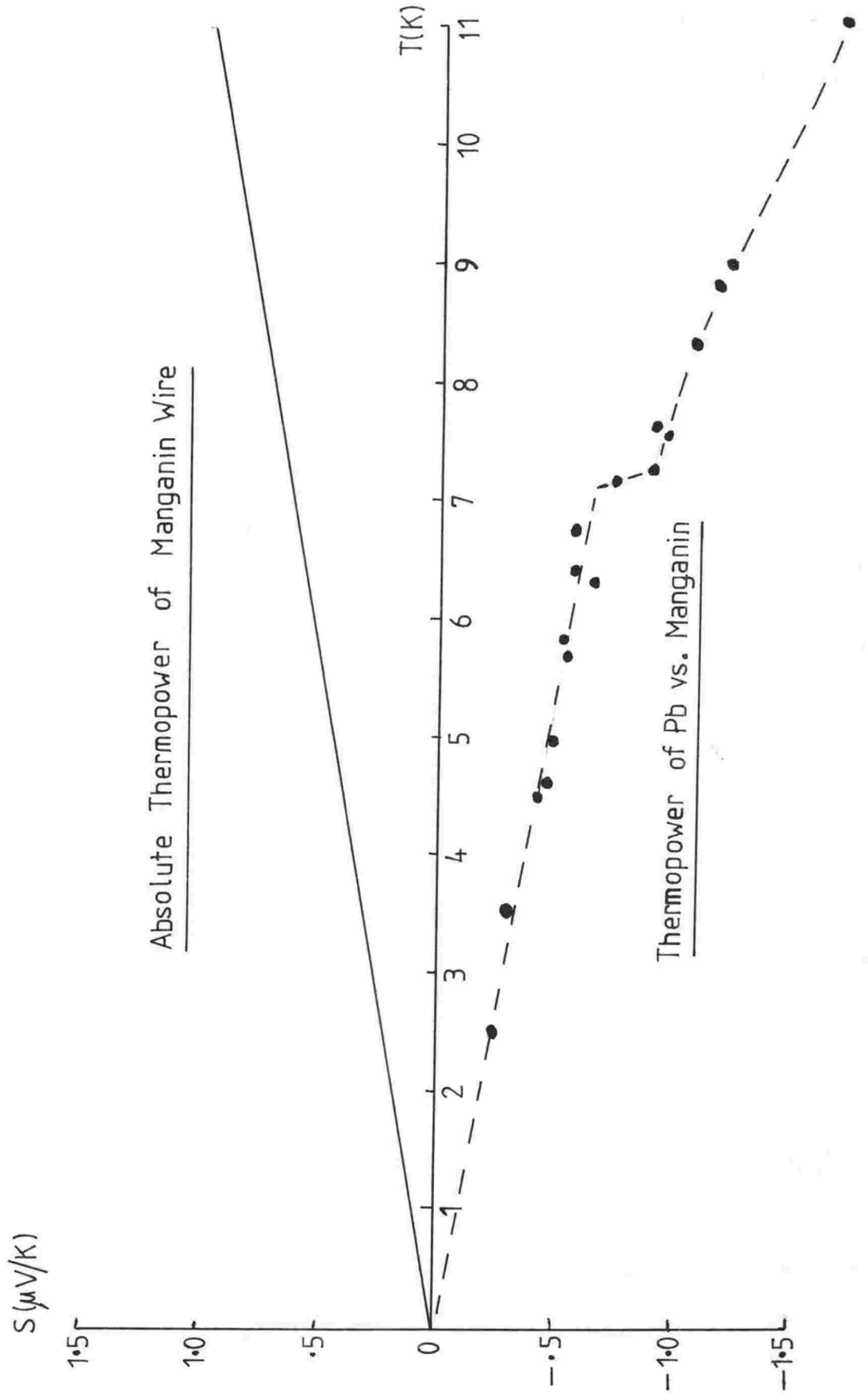
S (μV/K)
1·5
1·0
·5
0
-·5
-1·0
-1·5
1
2
3
4
5
6
7
8
9
10
11
T(K)
Absolute Thermopower of Manganin Wire
Thermopower of Pb vs. Manganin

Chapter Four

ANALYSIS OF DATA - GENERALIZED NORDHEIM-GORTER RELATION

4.1 The Nordheim-Gorter Rule

In a conductor in which the scattering mechanisms are independent of each other and the charge carriers are a single, homogeneous group e.g. s-electrons etc. the Nordheim-Gorter Rule is used to predict how the thermopower changes from the value S_i characteristic of the added impurities e.g. Fe in Au (Fe), to the value S_h characteristic of the host (due to dislocations etc.). If the above conditions are satisfied we can replace the sample with two scattering mechanisms by two hypothetical samples each with only one mechanism operating.

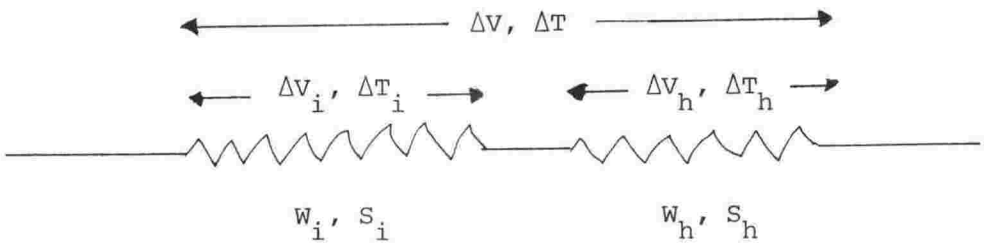

W_i and W_h are the thermal resistances due to the added impurity and host respectively, and W is the total thermal resistance. Throughout this discussion "impurities" will refer to the added magnetic atoms e.g. Ni, Fe etc. while "host" will refer to all other sources of electron scattering. When applying the Nordheim-Gorter Rule all the relevant quantities are evaluated at the same temperature. The temperature gradient across the sample is divided up according to the values of W_i and W_h. The total thermopower is combined of the individual thermopowers due to each source as follows:

$$S_{total} = \frac{\Delta V}{\Delta T}$$

$$= \frac{\Delta V_i}{\Delta T_i} + \frac{\Delta V_h}{\Delta T_h}$$

$$= S_i \frac{W_i}{W} + S_h \frac{W_h}{W}$$

If the scattering is elastic, the thermal resistances may be replaced by the corresponding electrical resistances (resistivities for convenience since the form factor 1/A is common to both impurity and host)

$$S_{total} = S_i \frac{\Delta\rho}{\rho} + S_h \frac{\rho_h}{\rho} \qquad \text{Equation (4.1)}$$

where $\Delta\rho$ is the electrical resistivity due to the impurity, ρ_h is that due to the host and ρ is the total electrical resistivity,

$$\rho = \Delta\rho + \rho_h$$

Strictly speaking we should use the Lorenz ratios appropriate for each type of scattering e.g. phonon, LSF etc. when converting from thermal to electrical resistivities, but providing the scattering is predominantly elastic, our sweeping assumption of the one, common Lorenz ratio should not introduce an appreciable discrepancy. In practice this means that the residual resistivity must dominate the scattering, a condition usually met in experiment.

Re-writing Equation (4.1), we obtain the Nordheim-Gorter Relation;

$$S_{total} = S_i \frac{(\rho - \rho_h)}{\rho} + S_h \frac{\rho_h}{\rho}$$

$$= S_i + (S_h - S_i) \frac{\rho_h}{\rho}$$

The total thermopower is now seen to be dependent, providing the host characteristics do not alter as impurities are added to the alloy, only upon the total resistivity. Thus by plotting a graph of S_{total} vs. $1/\rho$, which should be a straight line, we can determine the characteristic thermopower of the impurity in that particular host i.e. what the thermopower would be if the impurities dominated the scattering. The impurities need not dominate the scattering in order for us to be able to determine what it is.

The major drawback (from our point of view) of the Nordheim-Gorter Rule as it stands is that the host resistivity must remain absolutely constant upon the addition of impurities, a condition not always met in practice. To enable us to cope with an experimental situation in which the host has a varying resistivity from sample to sample, the Nordheim-Gorter Rule must undergo a slight modification.

4.2 Generalized Nordheim-Gorter Relation

The primary concern of this study is to elucidate the behaviour of the thermopower of two LSF alloy systems; Rh(Fe) and Pt(Ni). In particular we wish to determine whether the observed "giant" thermopower peak seen in Rh(Fe) at low temperatures is due to electron diffusion or LSF drag. Our results and a discussion on previously published Rh(Fe) data will follow in sections (4.4) and (4.3).

If the host resistivity was constant we could apply the Nordheim-Gorter Rule as it stands and decide between the two effects; however, in our samples, it is not and, besides, we deliberately alter the residual resistivity of some samples by rolling and annealing the wires to change the scattering to see the effect upon the thermopower. If the observed peak is a diffusion effect the change in the balance of scattering between host and impurity should affect its magnitude and position; if it is a drag effect the change in scattering should have little or no effect.

The following treatment is a slight modification of the method of Kaiser *et al.* (1980) who developed a modified form of the Nordheim-Gorter Relation to distinguish between diffusion and drag effects in Pd(Ni). Where Kaiser *et al.* used thermal resistivities in their method we shall use electrical resistivities. For the temperatures of interest to us, and since the residual resistivities dominate for both impurity and host scattering in all our alloys, the method should give perfectly valid results.

Assuming that drag thermopower (including LSF drag) are negligible, or at least the same in the host and alloys, we can re-arrange the Nordheim-Gorter Relation and write,

$$S = S_h + (S_i - S_h) \frac{\Delta\rho}{\rho}$$

The total impurity resistivity $\Delta\rho$ is usually difficult to estimate, since the impurity residual resistivity is not easy to separate out from the host residual resistivity, but its temperature-dependent component $\Delta\rho_s$ can be estimated since the host resistivity is essentially constant (at least for Rh) up to the peak temperature, 3K for Rh(Fe). We therefore take

$$\Delta\rho_s = \rho - \rho_r$$

where ρ_r is the residual resistivity of the alloy, in our case actually the resistivity at the lowest temperature of measurements, 1.3K, although the difference is not important for our purpose.

Now, the temperature-dependent part of the impurity resistivity should, at least in the dilute limit, be proportional to the residual resistivity of the same. This is fairly reasonable since both the temperature-dependent part $\Delta\rho_S$ and the temperature-independent part (the residual impurity resistivity) $\Delta\rho_r$ should both be proportional to the impurity concentration, and therefore proportional to each other. We can write

$$\Delta\rho_r = a\Delta\rho_S$$

where a is constant at some particular temperature. $\Delta\rho$ then becomes

$$\Delta\rho = (1 + a)\Delta\rho_S$$

and the Nordheim-Gorter Relation becomes

$$S = S_h + (S_i - S_h)(1 + a)\Delta\rho_S / \rho$$

If the peak is due to a diffusion mechanism a plot of S vs. $\Delta\rho_S / \rho$ should be a straight line (provided inter-impurity interactions are neglected - or that inter-impurity interactions do not affect S_i, at higher concentrations of impurity). The constant a need not be evaluated unless S_i is required to be evaluated, in which case a can be estimated from a perusal of the residual resistivities of all the alloys.

The method is also independent of the geometrical parameters used to determine the resistivities, unlike the traditional Nordheim-Gorter Relation where the resistivities must be used (or at best the resistance ratio between room temperature and low temperature). In practice we can get away with using resistances, thus eliminating one source of uncertainty - that due to determining 1/A.

4.3 Review of Some Published Data on the Resistivity and Thermopower of Pd(Ni), Ir(Fe) and Rh(Fe).

a) Resistivity

In order to separate out the effects of LSF upon the resistivity of these alloy systems we shall assume that Matthiessen's Rule (independent

scattering probabilities for different scattering mechanisms) is valid and state

$$\Delta\rho(T) = \rho_{alloy}(T) - \rho_{host}(T) \qquad \text{Equation (4.2)}$$

where $\Delta\rho(T)$ can be separated into two components

$$\Delta\rho(T) = \Delta\rho_{s}(T) + \Delta\rho_{r}.$$

$\Delta\rho_{s}(T)$ is the resistivity due to LSF and $\Delta\rho_{r}$ is the residual resistivity due to non-magnetic scattering off the added impurities (potential scattering). For sufficiently dilute alloys we assume that the addition of impurities does not significantly change the electron-phonon resistivity and thus we may apply equation (4.2).

For alloys with LSF at impurity sites (such as these are taken to be) we expect to see both the T^2 and the linear T law in the impurity resistivity. Fitting the experimental data to the universal LSF resistivity curve should give us directly the value of T_{sf} for that particular alloy.

For Pd(Ni) alloys Purwins *et al.* (1972) deduced a value of $T_{sf} \sim 23K$ by extrapolating to zero Rh concentration the resistivity of Pd(RhNi) alloys.

By fitting the data of Sarachik (1968) on Ir(Fe) to the universal curve Kaiser and Doniach (1970) obtained $T_{sf} \sim 28K$.

The resistivity of Rh(Fe) was first measured at low temperatures by Coles (1964) who found that it decreased with decreasing temperature, in contrast to the opposite behaviour for Kondo alloys. The resistivity was linear in temperature down to very low temperatures indicating that if LSF are responsible for the temperature-dependence the T_{sf} for Rh(Fe) is very low.

By fitting their resistivity measurements upon Rh(Fe) to the universal curve Graebner *et al.* (1975) deduced a $T_{sf} \sim 2K$ for low concentrations of Fe. Since T_{sf} is inversely proportional to the local enhancement factor for the alloy the low value of T_{sf} indicates a very large local enhancement for Rh(Fe), provided that LSF are responsible for the resistivity. Hence at higher temperatures, where the LSF spectral density becomes blurred out, this effect being significant for large α, we should see the resistivity decrease below the linear law. A decrease is experimentally observed in the resistivity results of Coles, and Graebner *et al.*

It is interesting to note that Graebner *et al.* attribute the observation that the total resistivity does not appear to be linear in Fe concentration to the possible presence of inter-impurity interactions. They also attribute the dependence of the value of T_{sf} upon Fe concentration to these interactions. We shall show later on in this chapter that the dependence of ρ/c upon c is due primarily to the residual resistivity not being proportional to the nominal Fe concentration rather than being completely due to inter-impurity interactions. Their nominal values of Fe concentration also do not represent the actual Fe concentration and so ρ/c has no meaning under these circumstances. Our analysis of the thermpower of Rh(Fe) seems to indicate that inter-impurity interactions do not affect the thermopower, at least not in such a fashion as to cause deviations from the kind of behaviour to be expected if interactions were not present at all. To put it another way; there is no evidence of inter-impurity interactions in the thermopower data. This is a rather odd turn of events since Rusby (1974) concluded that the "interaction-free" limit for the resistivity of Rh(Fe) lies below 0.1% Fe, evidence for inter-impurity interactions being found in the observation that ρ/c was not independent of c. It might reasonably be expected that, since thermopower is essentially a second-order scattering process, any interactions affecting the resistivity (a first-order process) would manifest themselves in quite definite deviations from interaction-free behaviour.

Rusby fitted his Rh(Fe) resistivity data to the alternative LSF model of Rivier and Zlatic (1972). Rivier and Zlatic term Rh(Fe) a "Coles" alloy, after Coles (1964) who first discovered the resistivity behaviour of Rh(Fe). Rivier and Zlatic proposed a single-band LSF model in which a single, homogeneous band of electrons is assumed to be responsible for both conduction and magnetic properties. They say that a single band is probably a good representation of the electronic states in Rh (Kasuya 1956; also Cheng and Higgins 1979). The value of T_{sf} from this model is about 15K for Rh(Fe). That it is different from that obtained from the Kaiser-Doniach model is not too surprising since T_{sf} from the latter is that temperature where the resistivity changes from T^2 to linear in temperature whereas in the former T_{sf} occurs between the linear and the logarithmic region. Rivier and Zlatic explain the decrease in resistivity below the linear law as a transition to scattering by a well-defined local moment hence the appearance of a logarithmic term which they say is indicative of a target with an internal structure. The decrease below the linear law in the Kaiser-Doniach approach is attributed to the blurring out of the LSF spectrum.

Fischer (1974) also calculated the resistivity of LSF alloys using a single-band model with variable potential scattering. Fischer's approach is a generalization of Rivier and Zlatic's model and the spin fluctuation temperature T_{sf} is more or less the same as in the Rivier and Zlatic approach.

b) Thermopower

"Giant" thermopowers have been observed at low temperatures in Pd(Ni), Ir(Fe) and Rh(Fe) alloys. The variation of thermopower peak magnitude with impurity concentration was taken to be evidence of an effect other than due to electron diffusion by Kaiser (1976) especially since, at the concentrations involved, the impurities could reasonably have been expected to dominate the scattering and the thermopower thus be independent of impurity concentration, barring interaction effects. To explain the peaks Kaiser proposed the LSF drag theory already outlined in a previous chapter.

In Pd(Ni) alloys the pure Pd used to make the alloys had a very low residual resistivity ($\simeq$ 0.01 $\mu\Omega$.cm) so if it were assumed that this was also the resistivity due to all extraneous scattering other than Ni in the alloys, i.e. the host resistivity, then the Nordheim-Gorter Rule predicts that the thermopower should be concentration-independent at the concentrations employed in the alloys (up to 1.67%). The large increase in the thermopower peaks could then be explained in terms of an effect other than due to electron diffusion i.e. LSF drag (Foiles and Schindler 1968, Schindler and Coles 1968).

The situation with Ir(Fe) alloys is similar: at Fe concentrations of 1.0 at.% the Fe might be expected to dominate the scattering (Touger and Sarachik 1975).

Further evidence for the existence of LSF drag in Pd(Ni) and Ir(Fe) was found in the observation that the impurity thermopower (after subtracting off the host thermopower) was linear in temperature at low temperatures, the peaks occurred at about T_{sf} and the increase in peak magnitude with impurity concentration was roughly in accordance with LSF drag predictions, non-linearity with concentration being ascribed to inter-impurity interactions at higher concentrations.

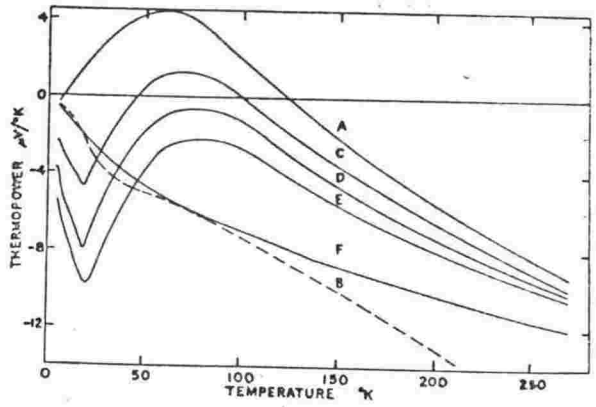

Fig. 1. Thermoelectric power as a function of temperature. Curve A is the pure Pd data of Fletcher and Greig [5] and Taylor and Coles [6]; Curve B is the unannealed pure Ni data of Blatt et al. [7]; Curves C, D, E and F are the data for Pd Ni alloys with the at. % of Ni being as follows: C 0.5; D 1.0; E 1.66; and F 6.16.

Figure (4.1) Thermopower of Pd(Ni) alloys

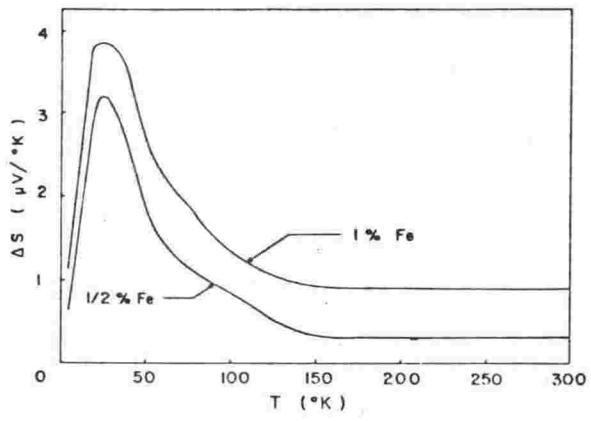

FIG. 2. Impurity contribution $\Delta S = S - S_0$ as a function of temperature, where S is the thermoelectric power of Ir containing 0.5 and 1 at.% Fe and S_0 is the thermoelectric power of pure Ir.

Figure (4.2) Thermopower of Ir(Fe) alloys

Recourse to Figure (4.3) and Figure (4.4) will show that the residual resistivities for Pd(Ni) and Ir(Fe) used in these measurements suggest a large amount of extraneous scattering. The residual resistivities of the Pd(Ni) samples of Schindler and Coles (1968) extrapolate at zero Ni concentration to about 0.23 $\mu\Omega$.cm, and not to the very low value of their pure Pd samples.

Converting the measured resistivities of the Pd(Ni) samples used in the thermopower measurements into thermal resistivities, since Lorenz ratio data was available from other work on Pd(Ni) (Schriempf *et al.* 1969, Kaiser 1971), Kaiser *et al.* (1980) used their modified Nordheim-Gorter Relation (using thermal rather than the less-appropriate electrical resistivities) to attempt to distinguish between diffusion and drag explanations for the observed thermopower peaks. However, due to the uncertainty in estimating the value of the coefficients of the temperature-dependent part of the resistivity, the data did not, by themselves, clearly distinguish between diffusion and drag explanations.

The most conclusive proof of the diffusion origin of the peaks in Pd(Ni) was provided by Kaiser *et al.* when they considered how the peaks in Pd(NiPt) decreased in magnitude upon the addition of increasing amounts of Pt (Caldwell and Greig 1978). Converting the resistivity data of Greig and Rowlands (1974) (on the same samples as used in the thermopower measurements) into thermal resistivities, and plotting up the data according to their modified Nordheim-Gorter Relation, Kaiser *et al.* found excellent agreement with the diffusion prediction for the peaks. That the reduction of the peaks upon addition of Pt was not due to a change of the LSF spectrum (causing a decrease in Drag thermopower) was evident from the observation by Greig and Rowlands that the coefficient of the spin fluctuation resistivity remained unchanged, indicating that the LSF spectrum was unaffected by the added Pt.

Although the available thermopower and resistivity data on Ir(Fe) gave good agreement with a diffusion explanation for the thermopower peaks, the possibility of inter-impurity interactions reducing a drag component in the thermopower at higher Fe concentrations could not be discounted and thus, for the present data, the mechanism responsible for the thermopower of Ir(Fe) is still undecided. To clarify this state of affairs unequivocably a method similar to that employed in the case of Pd(NiPt) must be used. Essentially a sample of constant impurity concentration (to eliminate changes in thermopower due to changes in possible inter-impurity interactions) must be operated upon in some fashion as to change the balance of scattering from impurity to some other scattering mechanism i.e. introduce extra scattering.

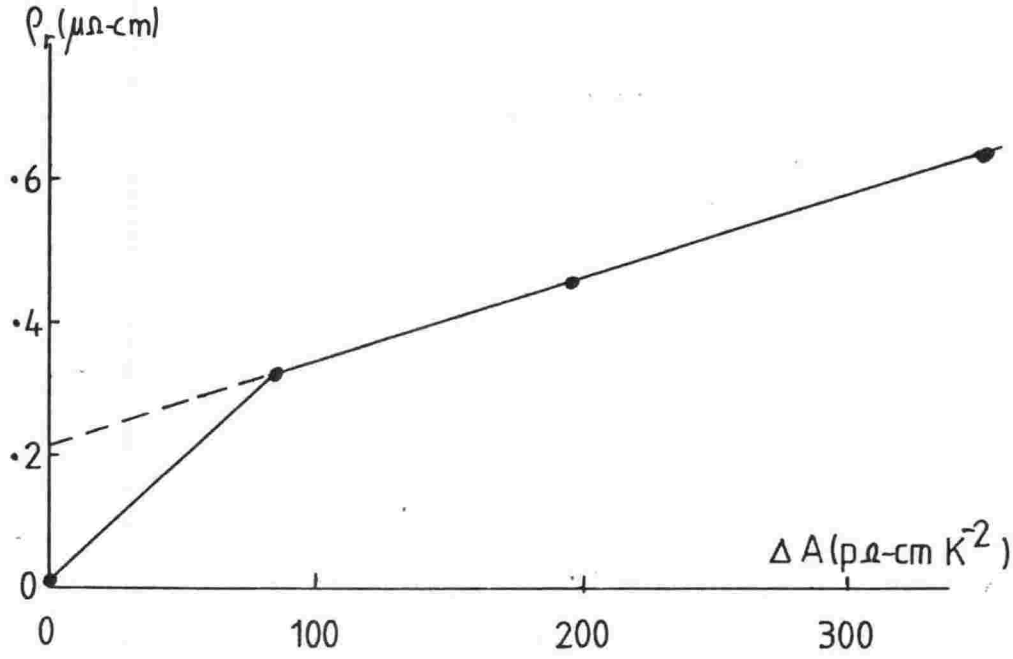

Figure (4.3)

Residual resistivities of Pd(Ni) alloys (Schindler and Coles 1968) vs. ΔA, the increase in the co-efficient of the T^2 electrical resistivity comp-onent, which is proportional to Ni concentration. (After Kaiser et al. 1980)

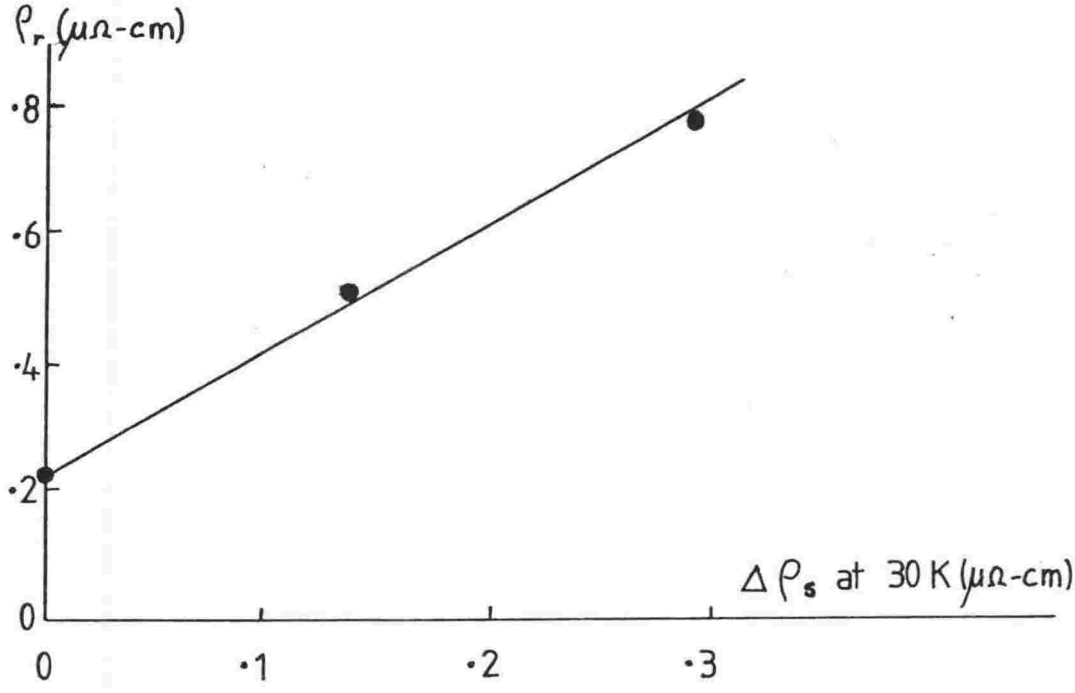

Figure (4.4)

Residual resistivities of Ir(Fe) alloys (Sarachik 1968). (Also after Kaiser et al.)

The thermopower of Rh(Fe) alloys has, up until the present, been a source of some confusion, both in the interpretation of the mechanism responsible for the observed "giant" thermopower at low temperatures, in the actual thermopower measurements themselves, i.e. the location of the peak, and in the concentration-dependence of the peak magnitudes.

Coles (1964) measured the thermopower of a 0.5 at.% Fe Rh(Fe) alloy and found the magnitude to increase as temperature was lowered. His data suggest a giant negative peak below 1.5K. The later thermopower measurements of Nagasawa (1968) on a 0.72 at.% Fe Rh(Fe) alloy suggest similar behaviour. There is some doubt as to the reliability of Nagasawa's results: the sudden increase in thermopower as temperature is lowered just below about 7K suggests some contamination due to Pb (T_c of 7.2K) somewhere in the measurement system at low temperature. Sharp features in the thermopower would not be expected if the thermopower was due to LSF.

The thermopower data on ostensibly pure Rh (actually containing traces of Fe) by Huntley (1971) showed a broad, negative peak at about 3K, presumably attributable to the Fe (Figure (4.5)).

Graebner *et al.* (1975) measured the pseudothermopower L_oGT of various Rh(Fe) samples, which measurements indicate a negative peak at about 3K whose magnitude decreased with increasing impurity concentration (Figure (4.6)). Graebner *et al.* ascribe this decrease to inter-impurity interactions, since these manifest themselves in the resistivity data, on the same samples, in the form of a dependence of $\Delta\rho/c$ upon c. Now, we have already stated that a significant portion of the dependence of ρ/c upon c is due to errors in the values of c, but taking account of this there remains a true dependence of ρ/c upon c, especially in the temperature dependent part of the resistivity $\Delta\rho$. We shall show shortly that the decrease of peak magnitude with increasing impurity concentration can largely be explained by the modified Nordheim-Gorter Relation as a diffusion mechanism weighted by extraneous scattering, although inter-impurity interactions may well have some effect.

An interesting feature of the thermoelectric data of Graebner *et al.* is that the one comparison between S and L_oGT indicates that S is about double L_oGT. Neglecting lattice conduction of heat, which at these temperatures should be much less than that carried by the electrons, the thermopower S is equal to LGT, as outlined earlier. Now, including contributions from inelastic scattering, one finds that the Lorenz number for the alloy is less than the classical value L_o. (See, for example, Kaiser (1971) where the Lorenz number for spin fluctuation scattering in Pd(Ni) alloys was found

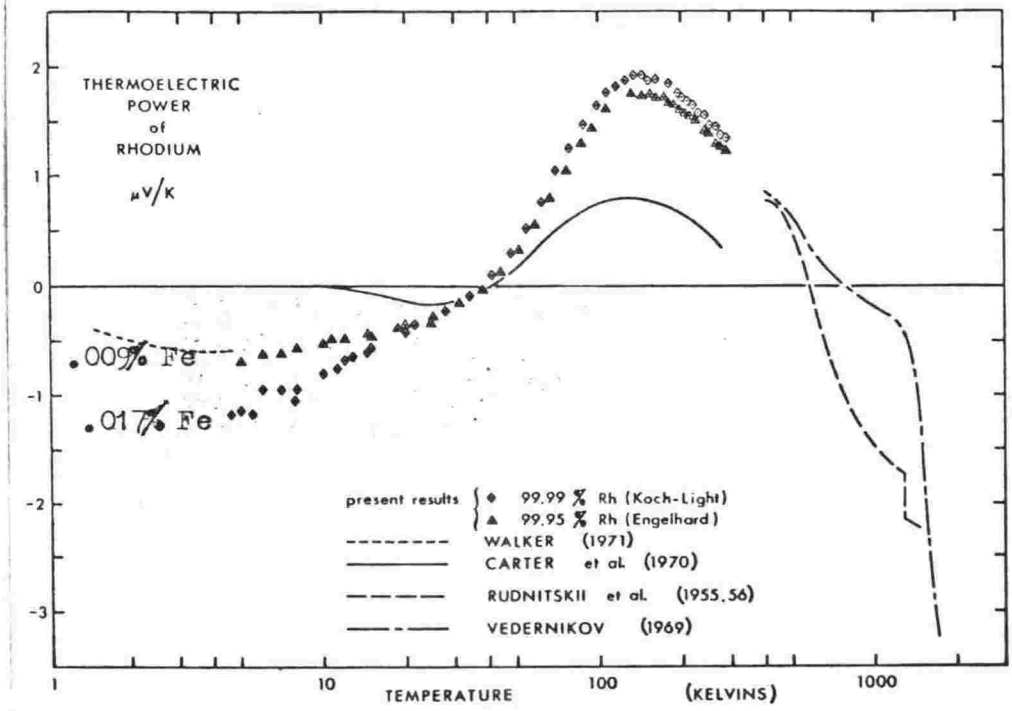

FIG. 1. Variation of thermoelectric power with temperature for pure rhodium.

Huntley (1971) Figure (4.5)

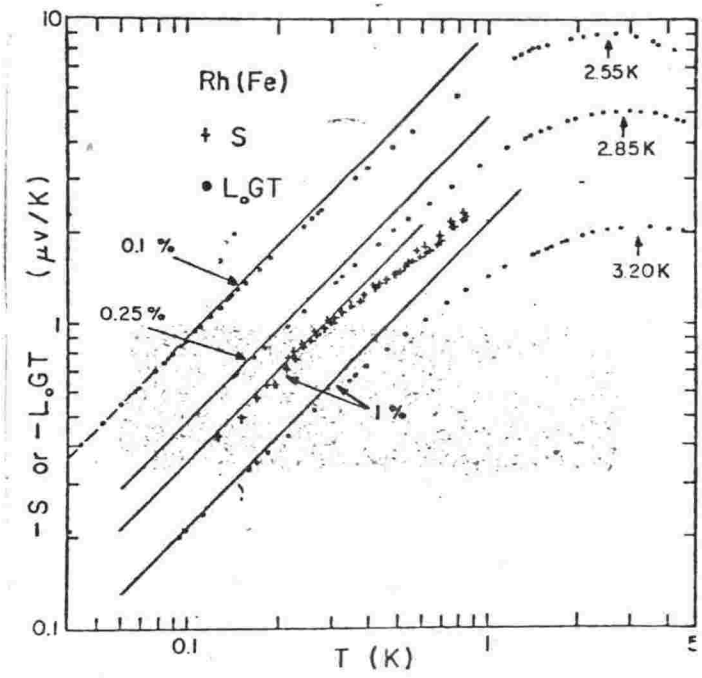

Fig. 4. Thermoelectric data vs. T. The straight lines indicate linear temperature dependence.

Graebner et al. (1975) Figure (4.6)

to be about 0.45 L_o). It is thus rather surprising to find S actually larger than L_oGT - the discrepancy should be in the opposite direction. If the lattice actually conducted as much heat as the electrons in this particular alloy then we would have a situation where S would be about twice L_oGT. However this would require lattice conduction to be about two orders of magnitude higher than in dilute Pd alloys (Fletcher and Greig 1967, Schroeder and Uher 1977). Even in a 5% Pd-Ru alloy with a residual resistivity more than twenty times larger than the alloy of Graebner *et al.*, Schroeder and Uher found S to be only about 14% larger than L_oGT. We can assume that this is not the reason for the discrepancy. Anticipating our results, we shall assume that Graebner *et al.*'s L_oGT data is more nearly equal to S than their actual measurement of S, and shall speculate no further as to the possible reasons for the discrepancy.

4.4 Results on Rh(Fe) Wire Samples

We measured the thermopower (and resistivity) of several Rh(Fe) wire samples in order to clear up the previously mentioned problems concerning the thermopower of Rh(Fe):

1) The temperature of the peak has not been certain.
2) The concentration-dependence of the magnitude of the peaks is apparently opposite to that observed in similar alloys.
3) The mechanism responsible for the peaks could be either a diffusion effect or a spin fluctuation drag effect.

Our measurements on alloys of different concentration and purity should clarify 1) and 2), while measurements on alloys before and after annealing, and rolling of the wires between hard-nickel rollers to alter the residual resistivity, should clarify 3) unequivocably.

Most of the samples used in this study were prepared by Engelhard Industries Ltd. and kindly supplied to us by R. Rusby (National Physical Laboratory, U.K.). One additional sample (number 6 in Table 4.1) was prepared by Johnson-Matthey Ltd. and supplied by G.K. White (C.S.I.R.O., Australia).

Our measurements on the resistivity of our samples may be seen on Figure (4.7). Although most of these wires had already had their resistivity measured by Rusby (1974) it was decided to measure the resistivities as a check. It can be seen that our measurements do not extend to low enough temperatures to be able to see the change to a T^2 dependence predicted (and

Sample no.	ρ_r (μΩ-cm)	c (at. %)	c deduced by Rusby	Treatment
1	0.066	0.004	0.004	
1'	0.093	0.004?		Stretched
2	0.104	0.07	0.06	
2'	0.720	0.18		Rolled
3	0.215	0.33	0.35	
4	0.223	0.41		
4'	0.798	0.50		Rolled
5	0.400	0.56	0.58	
6	1.392	0.52		
6'	0.844	0.68		Annealed
Standard	0.322	0.50	0.50 (Rusby's standard also)	

Table 4.1

Rh(Fe) samples used in this study, with their resistivities ρ_r @ 1.3 K and effective conc--entrations c (deduced from the magnitude of their temperature-dependent resistivities). Primed sample numbers indicate the original sample has undergone the treatment specified. The deduced effective concentrations of Rusby are also given where appropriate.

Figure (4.7(a))

Total Resistivity of Rh(Fe) Samples

-numbers identify the samples as in Table (4.1)

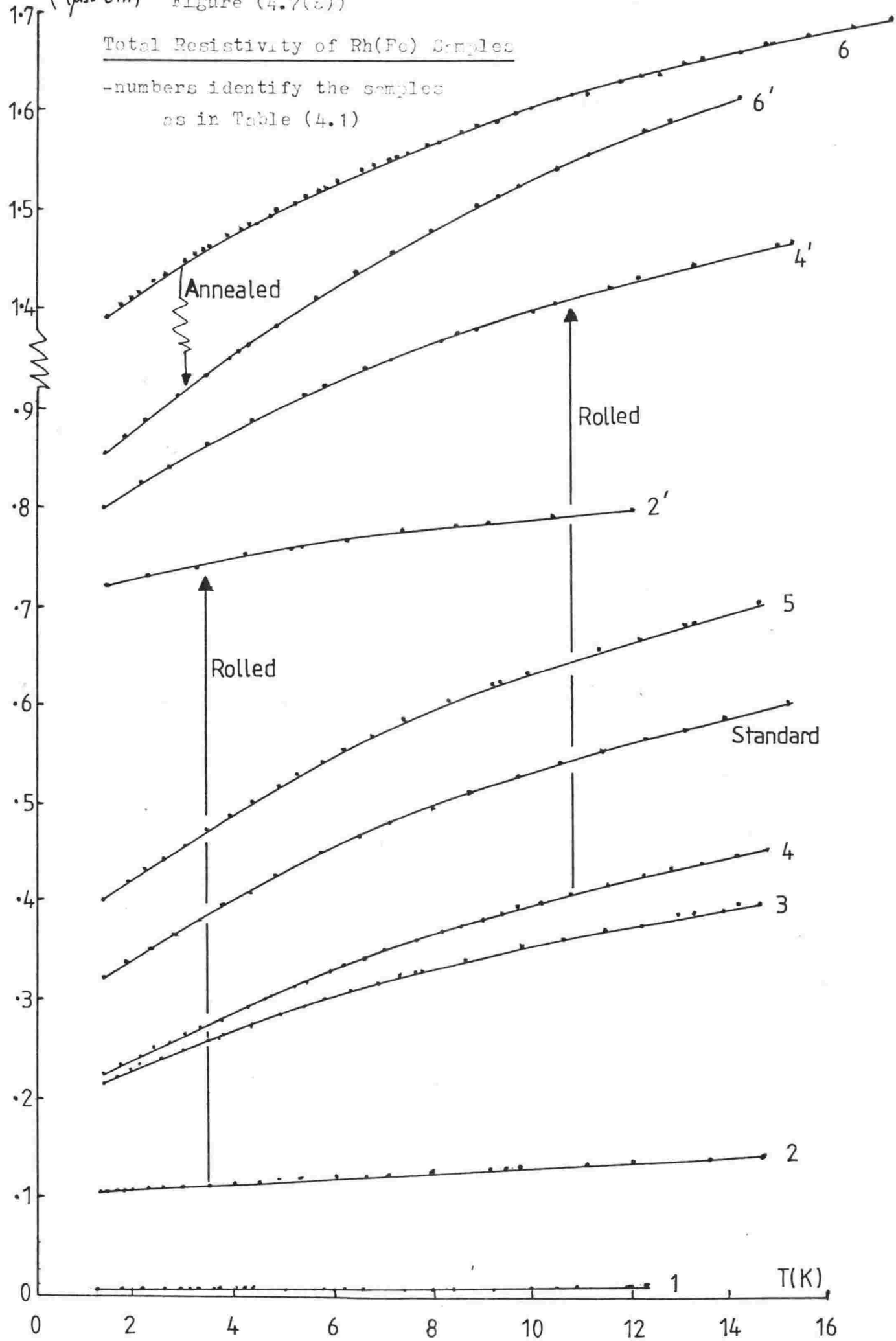

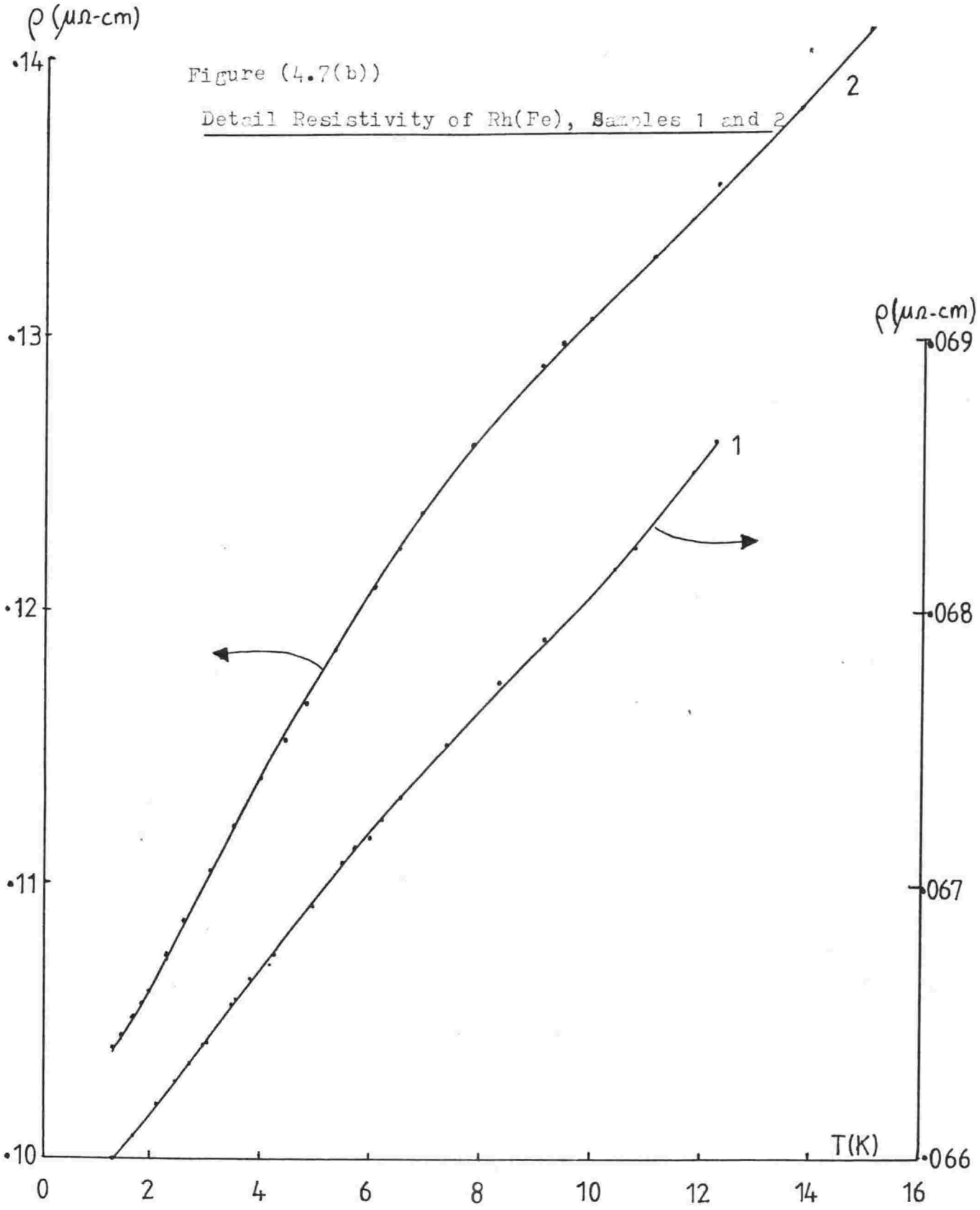

Figure (4.7(b))

Detail Resistivity of Rh(Fe), Samples 1 and 2

seen by Graebner *et al.* and Rusby). So we are unable to deduce the T_{sf} from our measurements and we will rely upon that deduced by Graebner *et al.* i.e. about 2K.

While the modified N-G relation does not require the absolute impurity concentration it was decided to deduce the concentrations, or rather the relative concentrations, as a further "handle". Rusby found that the Fe concentrations differed from their nominal values, determined from the actual amounts of Fe used in making the alloys. It appears that not all the Fe is dissolved in some instances. Following Rusby's method of comparing the temperature-dependence of the resistivity with that of a standard sample whose concentration is assumed to be known, we deduced the concentrations relative to a standard Rh(Fe) alloy whose "absolute" concentration was assumed to be its nominal value of 0.5 at.%Fe. The results of this method can be seen in Table (4.1) together with Rusby's concentrations for the same samples where applicable, and the residual resistivities. Note that even though the Fe concentrations are proportional to $\Delta\rho_s$, the impurity temperature-dependent resistivity between 1.3K (our lowest measurement temperature) and 3K (the temperature of the thermopower peaks), the quantity $\Delta\rho_s/\rho$ used in the modified N-G relation is independent of 1/A while using c/ρ introduces a further uncertainty in the form of 1/A which is necessary to deduce the concentration c. However, it was thought that knowledge of the actual Fe concentrations would be useful if it became necessary to comment upon any possible inter-impurity interactions if they were found to be manifest in the thermopower.

Rusby's method involved plotting the resistivity of the unknown sample at a particular temperature vs. the resistivity of the standard sample at the concentrations of the unknown and standard samples. Our plots for typical samples can be seen in Figure (4.8).

The most interesting case is sample 2, whose deduced concentration is considerably less than the nominal concentration of 0.5%. Electron microprobe analysis of this sample showed concentrated pockets of undissolved Fe, so results for this sample should be treated with some caution. Most of the Fe was contained in "holes" in the Rh host of about 0.5μ in diameter while the remaining Fe was evenly distributed elsewhere throughout the host. Obviously the effect of rolling this sample is to partially re-melt the metal and re-distribute it in some measure thereby changing conditions, in particular the concentration which shows that more Fe has gone into solution (sample 2'). This effect can also be seen in the other treated samples.

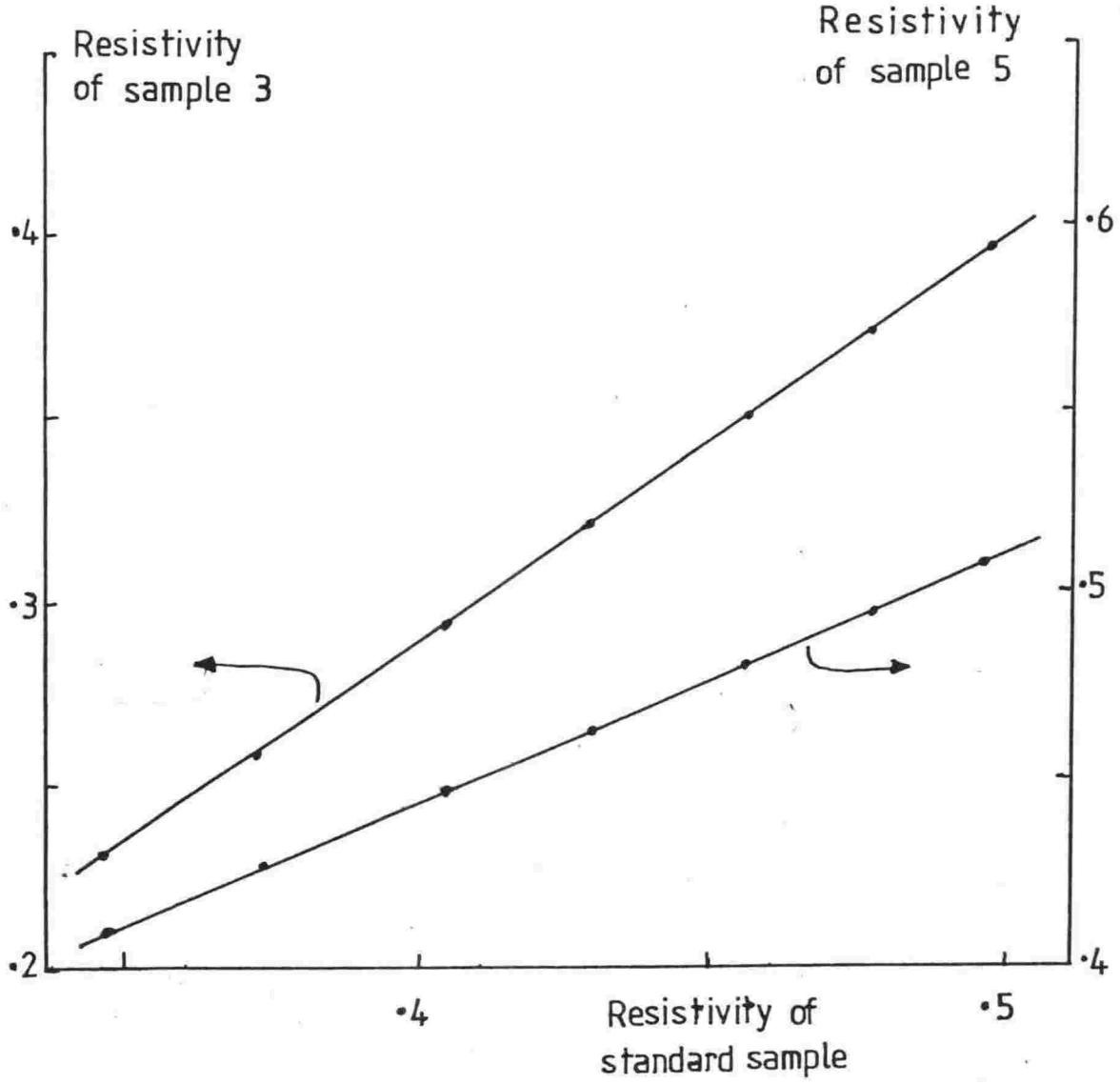

Figure (4.8)

Resistivity plots for two Rh(Fe) samples (nos. 3 and 5) from the slopes of which the ratios of the concen-trations were determined, using the assumed concentra-tion of the standard sample, plotted on the abscissa.

Another not less interesting phenomenon is the anomaly observed in the resistivity of one of the lowest concentration samples, sample 1'. Why stretching should have such an effect is at present still a mystery (Figure (4.9)).

The deduced concentrations of our "Rusby" samples agree with those deduced by Rusby to within a few percent, and with the nominal concentration of the Johnson-Matthey one.

Turning now to measurements upon the thermopower of our Rh(Fe) alloy wires, our results are plotted up in Figures (4.10) and (4.11). It is clear from our data that the negative thermopower peak occurs at about 3K i.e. approximately T_{sf}, in agreement with Huntley (1971) and the pseudothermopower data of Graebner *et al.* (1975). It is also clear that the peak magnitudes are not unique functions of Fe concentrations but depend strongly upon the amount of other scattering present in the alloy. This argues against the drag explanation for the thermopower.

Figure (4.12) shows our thermopower and resistivity data plotted up according to the modified Nordheim-Gorter Relation of Section (4.2). The thermopower used is that at the peak i.e. at about 3K. Figure (4.12) shows that our data are in good agreement with the modified Nordheim-Gorter Relation, except for sample 2 in which, it will be recalled, there is a substantial amount of Fe which does not appear to have been dissolved. Especially, and in fact more importantly, the thermopower changes upon rolling and annealing are in accordance with the predictions of the modified Nordheim-Gorter Relation. It would have been more convincing had the effective Fe concentrations not altered upon rolling and annealing, as then any changes in thermopower due to changes in any inter-impurity interactions could have been absolutely ruled out. However, the relative changes, except for sample 2, are small and so it is reasonable to assume that such interactions would not be expected to produce changes on the order of those seen. In any event, interactions would be unlikely to produce thermopower changes which, by chance, just happen to agree with the predictions of the diffusion explanation.

The pseudothermopower data of Graebner *et al.* are also in reasonable agreement with the modified Nordheim-Gorter Relation. It is fairly clear that the decrease of L_oGT with concentration found by Graebner *et al.* is a result of increasing extraneous scattering in their more concentrated alloys, evidence for this assertion being found in the excessive increase of residual

resistivity in these alloys (Figure (4.13) rather than inter-impurity interactions, although these may account for the deviation from the rest of the data points of their most concentrated alloy, nominally 1 at.%Fe Figure (4.12) shows that essentially all the Rh(Fe) peak sizes are consistent with a large diffusion thermopower S_i which is reduced in any alloy according to the balance of Fe impurity and other scattering.

Now, in addition to reducing the peak size, an increase in host resistivity would be expected to alter its shape. From the following figure it can be seen that whereas the impurity resistivity increases with temperature, the host resistivity is essentially constant up to about 10K. Hence at higher temperature $\Delta\rho$ becomes a greater proportion of ρ and so, as

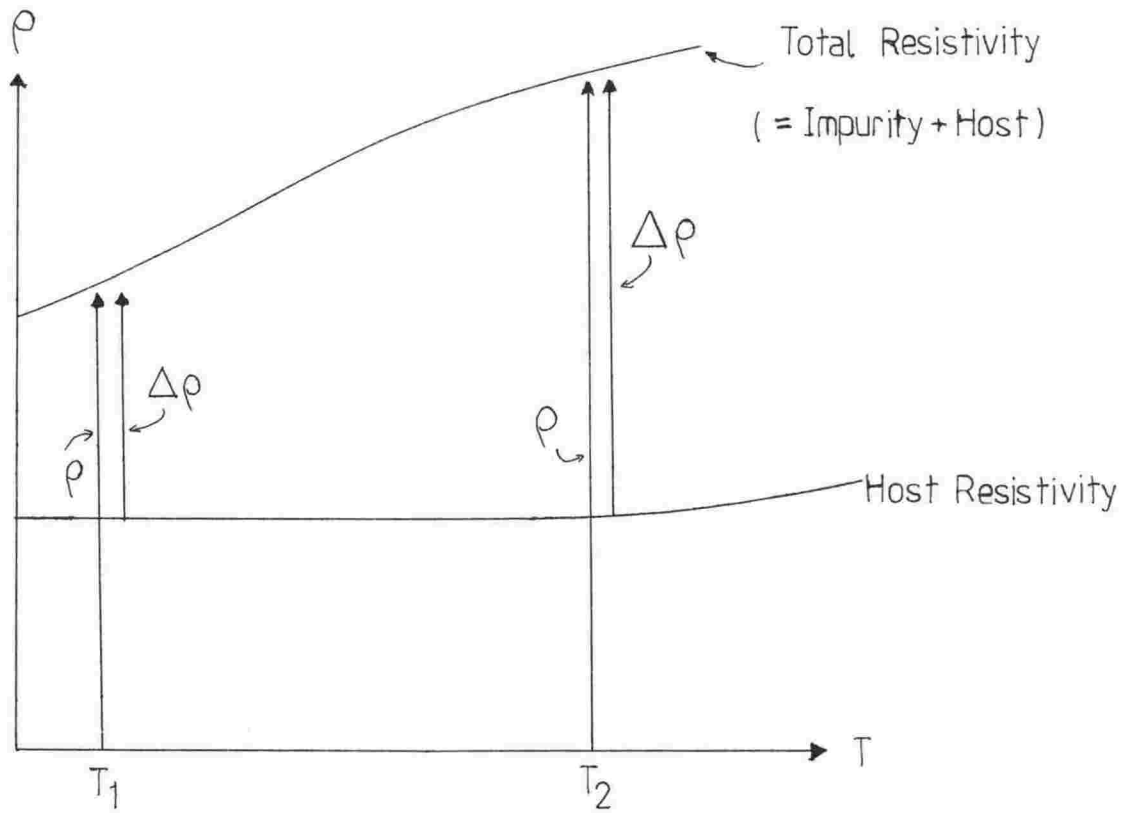

a consequence, the thermopower is reduced less. This means that in alloys where the host resistivity is large compared with the impurity resistivity i.e. for the smaller thermopower peaks, these smaller peaks would be broadened and shifted to a slightly higher temperature. That this effect is visible in the data of Figures (4.10) and (4.11) provides additional support for the diffusion model.

Having thus established that the peaks are a diffusion effect, we can use the modified Nordheim-Gorter Relation to estimate the characteristic thermopower S_i of Fe in Rh. Whereas in the conventional Nordheim-Gorter

Relation the characteristic thermopower is just the intercept on the thermopower axis, with the modified form the characteristic thermopower is determined from the slope of S vs. $\Delta\rho_s/\rho$. Hence the "constant", a, must be determined at each temperature i.e. ρ_r must be divided up into an impurity component $\Delta\rho_r$ and a host component ρ_{rh}. The broken line in Figure (4.13) shows one plausible division, but clearly there is some uncertainty involved. If we assume S_h to be small (as indicated by the intercept in Figure (4.12), we can then calculate S_i from the measured data. The resulting S_i is plotted as a broken curve in Figure (4.10), this being the mean result using the thermopowers of samples 2, 3, 4 and 5 with the largest thermopowers for the greatest accuracy. Now while the peak magnitude is uncertain due to the uncertainty in the estimation of the constant a from Figure (4.13), the shape and location of the peak are much less dependent upon the value of a. We estimate the characteristic thermopower of Fe impurities in Rh to have a peak magnitude of between -9 and -15 μV/K with a mean of -11 μV/K at a peak temperature of (2.7 ± 0.3) K.

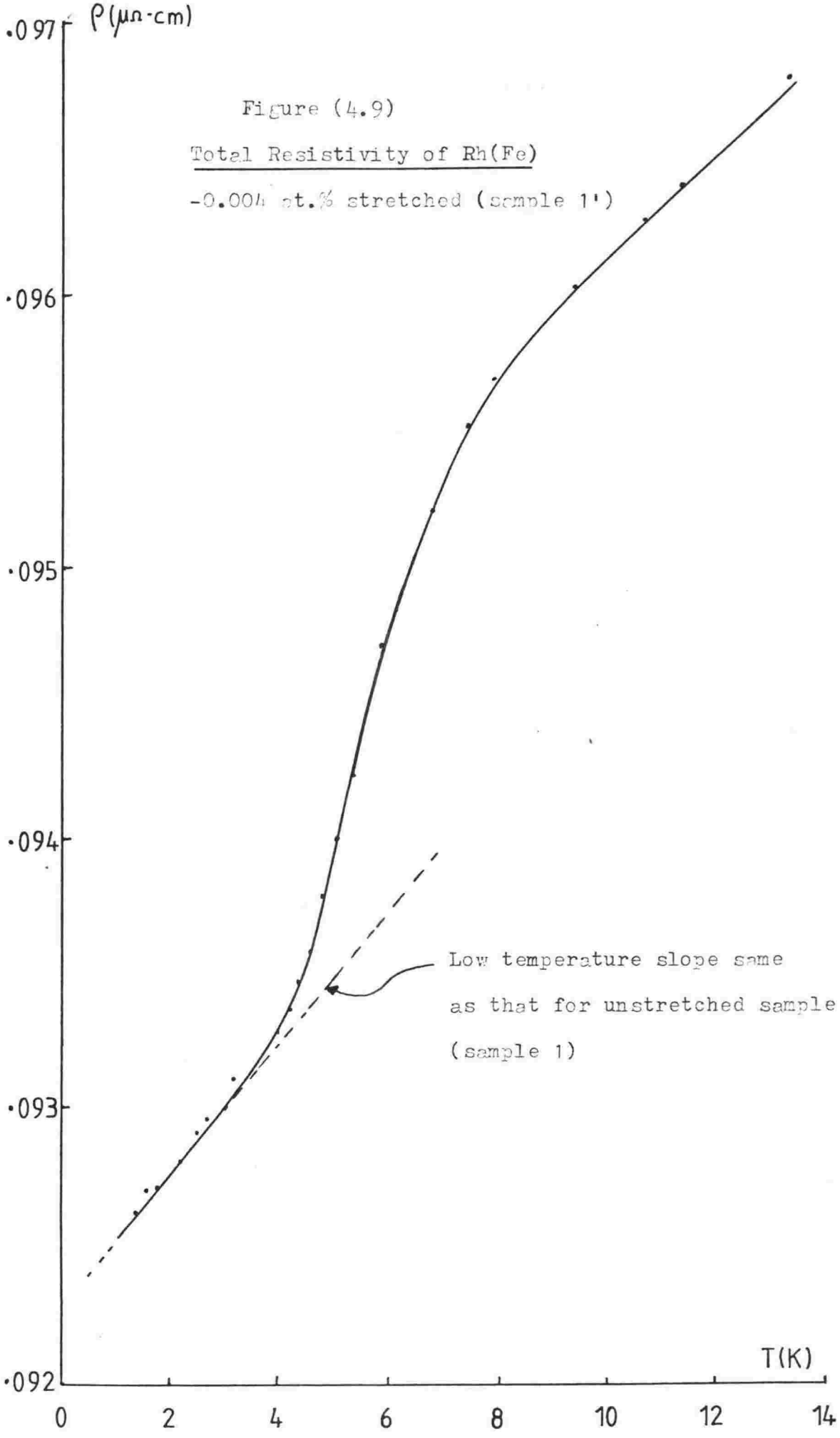

Figure (4.9)

Total Resistivity of Rh(Fe)

-0.004 at.% stretched (sample 1')

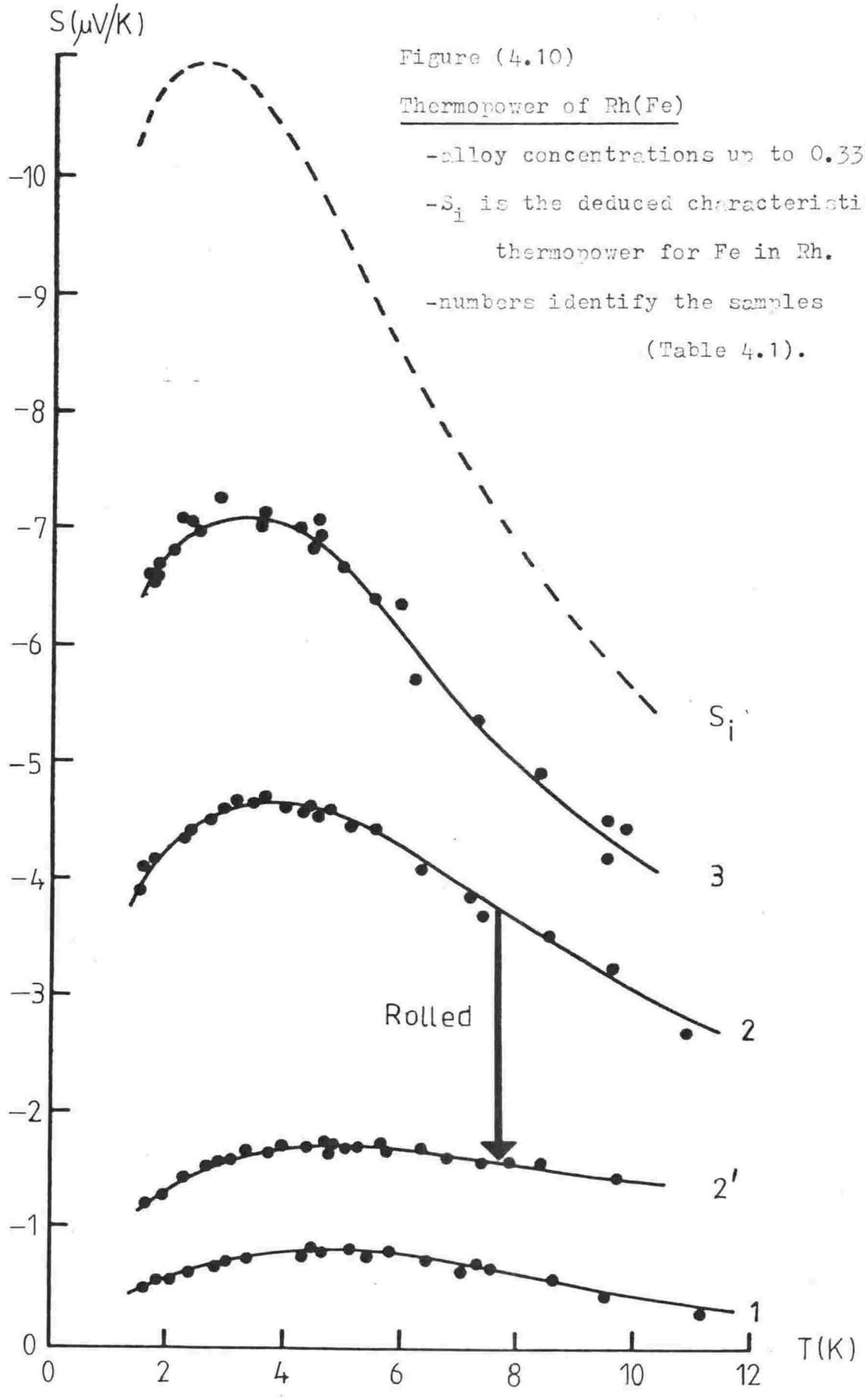

Figure (4.10)

Thermopower of Rh(Fe)

-alloy concentrations up to 0.33%.

-S_i is the deduced characteristic thermopower for Fe in Rh.

-numbers identify the samples (Table 4.1).

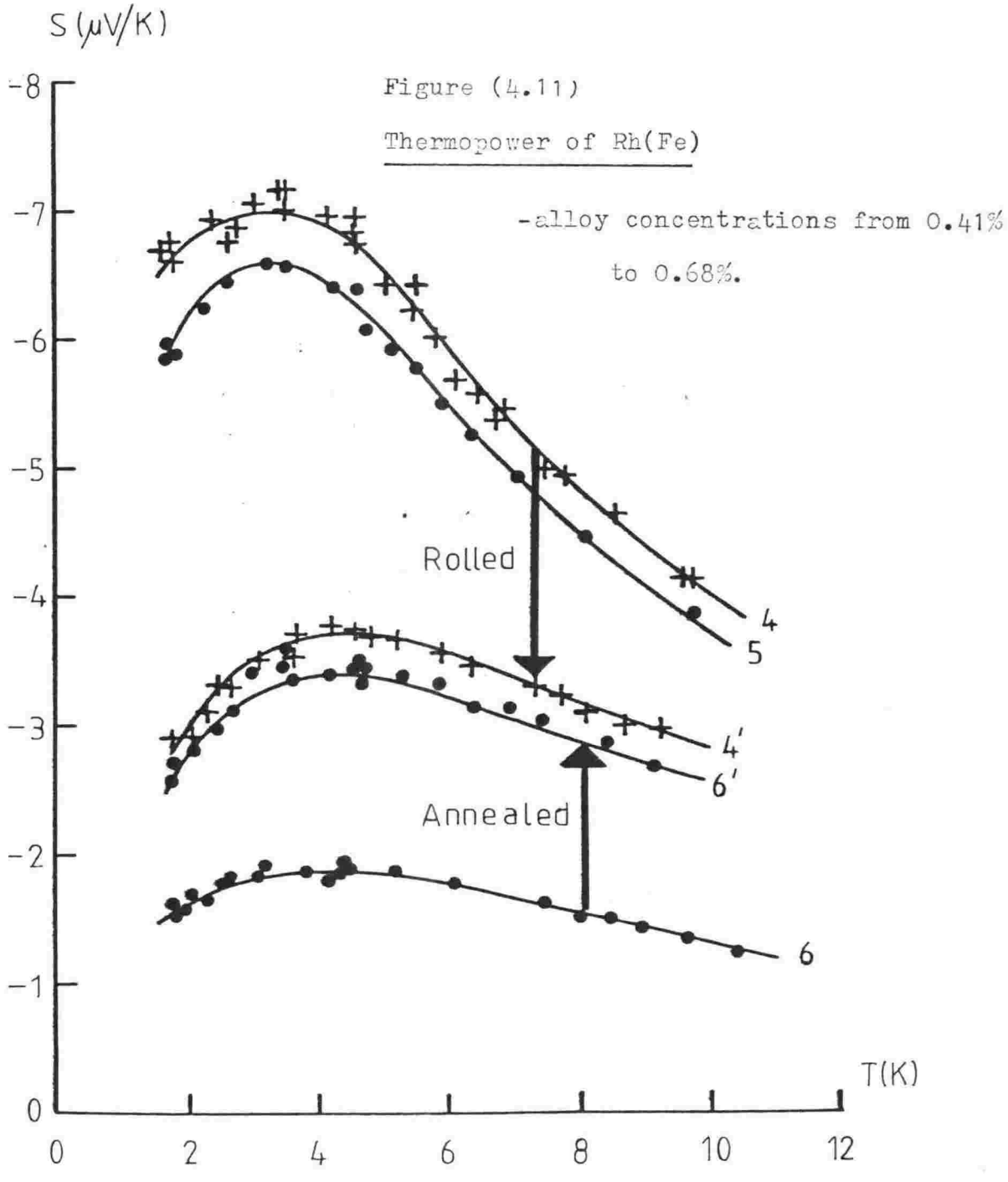

Figure (4.11)

Thermopower of Rh(Fe)

-alloy concentrations from 0.41% to 0.68%.

Figure (4.12)

Modified Nordheim-Gorter Plot for Rh(Fe)

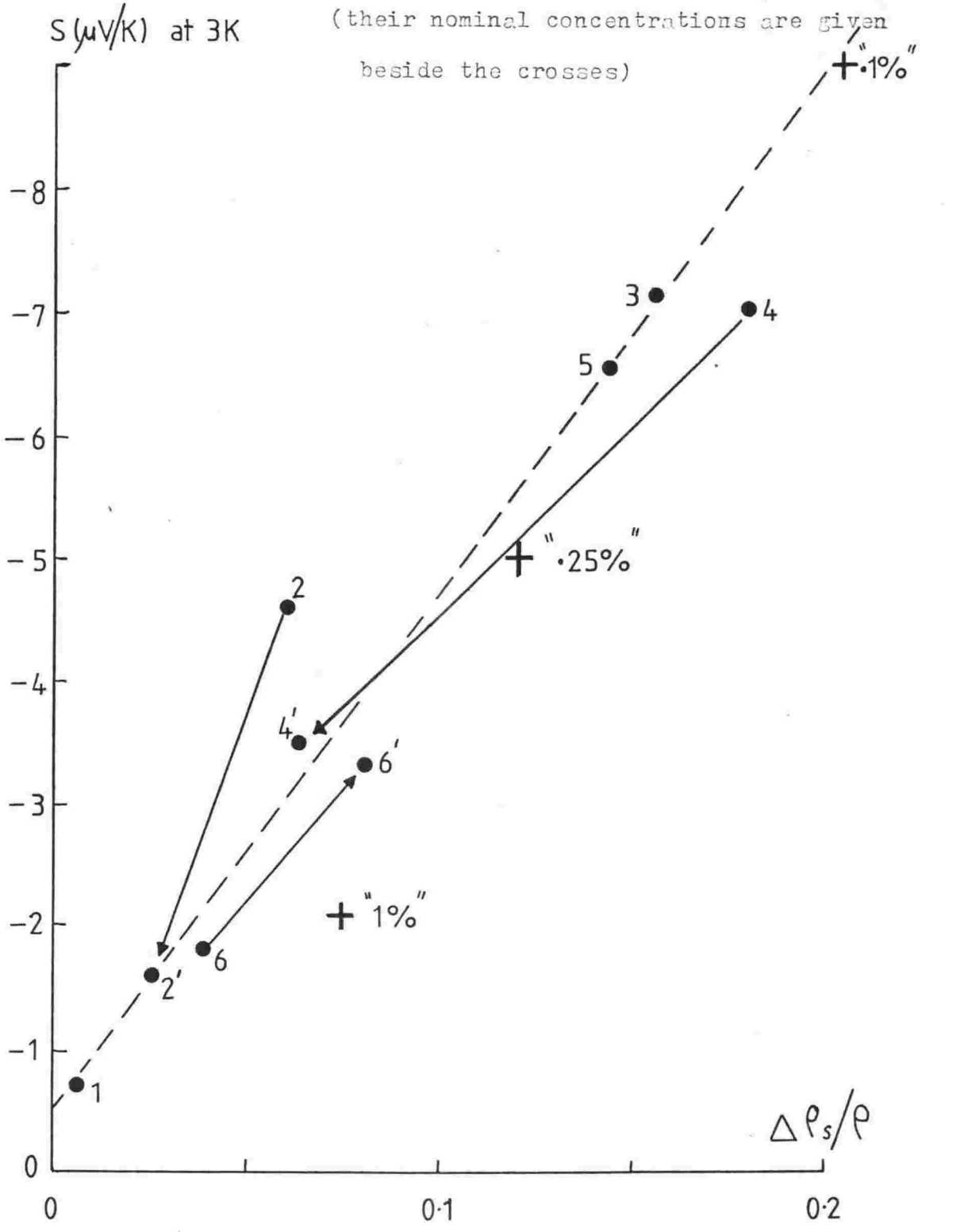

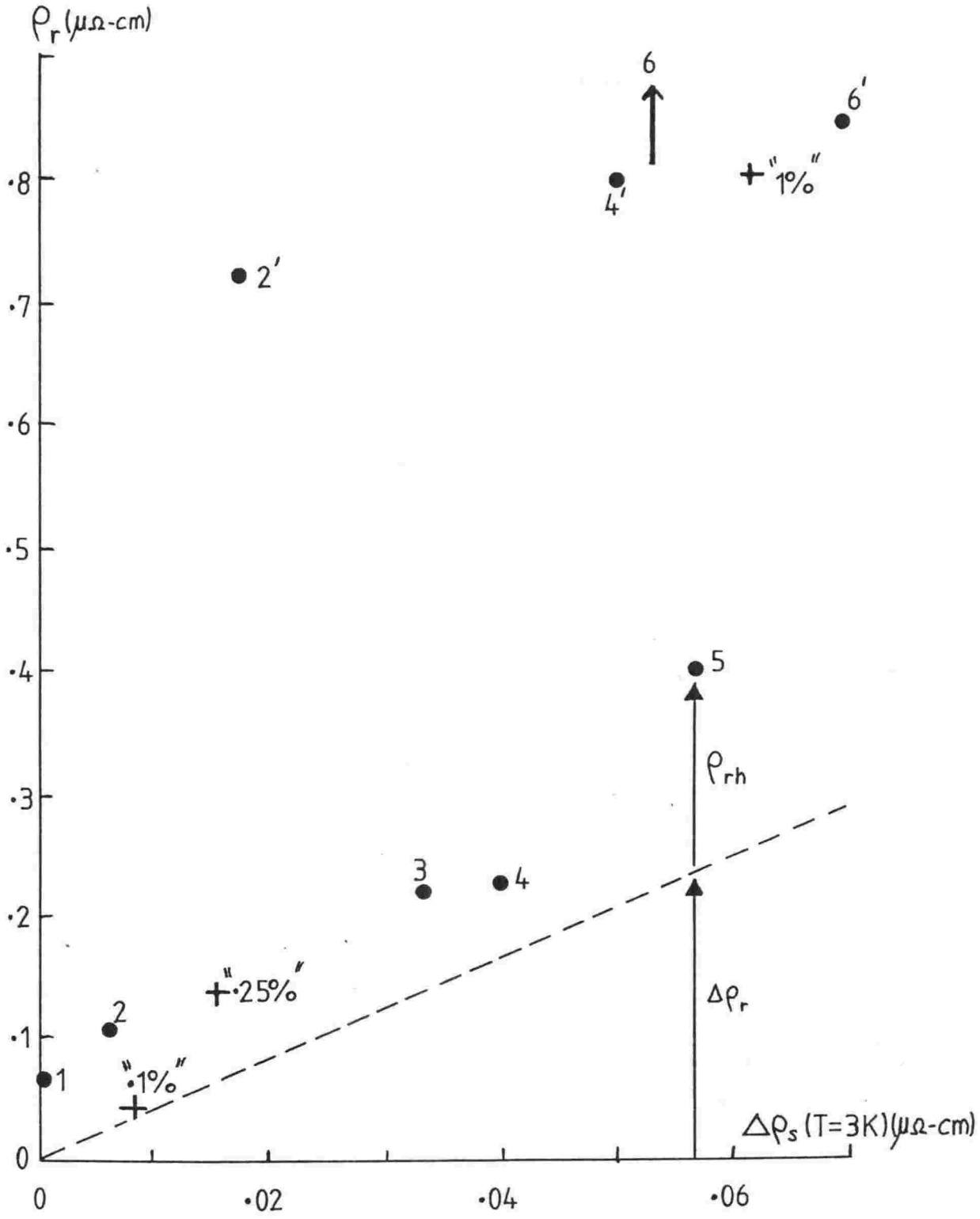

Figure (4.13)

Residual resistivities (actually the resistivity at 1.3 K) of our Rh(Fe) alloys and those of Graebner et al. The broken line shows a possible division of the resistivity into impurity ($\Delta\rho_r$) and host (ρ_{rh}) components.

PART II

THERMOPOWER AND RESISTIVITY OF Pt(Ni)

Introduction

Dilute Pt(Ni) should be an alloy of the LSF type. Pt has similar electronic properties to Pd, being immediately below it in the periodic table. Therefore it is not unreasonable to expect similar behaviour in both Pt(Ni) and Pd(Ni) the only difference being in a scaling of effects in temperature and magnitude. The resistivity, thermopower and magnetic susceptibility of Pd(Ni) have already been well studied (see Part I of this thesis).

In this part of the thesis we will attempt to measure the resistivity and thermopower of Pt(Ni), just as we have done in Part I with Rh(Fe) for the same reasons viz. to elucidate thermopower effects and try to distinguish between diffusion and drag effects if present.

The resistivity of Pt(Ni) alloys has been measured up to 4K (Mackliet *et al.* 1970). They found the impurity resistivity to vary as T^2 linearly with impurity concentration, as would be expected if Pt(Ni) was an LSF alloy. No deviation from T^2 was found indicating that T_{sf} was higher than 4K. We will estimate T_{sf} for Pt(Ni) using measured values of host enhancement and impurity susceptibility and then measure the resistivities of wire and thin film samples to determine T_{sf} experimentally.

1. Spin Fluctuation Temperature of Pt(Ni)

Recourse to Appendix I will show that the localized spin fluctuation temperature, T_{sf} ,of dilute Pt(Ni) is on the order of 1000K. This is much higher than that of Pd(Ni) alloys and as a result any effects due to the localized spin fluctuations, LSF, would be expected to extend to higher temperatures viz. thermopower peaks and the T^2 part of the impurity resistivity. Whether we actually do see these depends upon other factors such as possible inter-impurity interactions, the "blurring out" of the LSF spectrum, etc. It may not be easy to separate out the impurity behaviour from other effects.

Now, since we have T_{sf}^{-1} proportional to both $\frac{1}{\chi}\frac{d\chi}{dc}$ and α_o where $\frac{1}{\chi}\frac{d\chi}{dc}$ is a measure of local enhancement and α_o is a measure of host enhancement, we can see that the greater the host is to magnetic instability, the less effect the impurity needs to have i.e. the smaller the T_{sf} the greater is the host to magnetic instability. Hence, Ni is not as magnetic in Pt as it is in Pd and so any effects in the resistivity and thermopower are expected to be of a smaller magnitude with a higher T_{sf}, which latter we have already shown. Furthermore, whereas Pd(Ni) becomes ferromagnetic at about 2 at .% Ni concentration, Pt(Ni) would be expected to tolerate a much higher concentration of Ni. This does indeed appear to be the case as Pt(Ni) with concentrations of up to 9.4 at .% Ni do not display any of the usual signs of inter-impurity interactions e.g. $\frac{\rho}{c}$ dependent upon c, as would be the case if the alloy were about to go ferromagnetic.

2. Resistivity of Pt(Ni) Wire Samples

Pure Pt, Pt(Ni) 2 at.% and Pt(Ni) 5 at .% wires of 0.45 mm diameter were supplied by Professor Peter Schroeder of Michigan State University. The resistivity of these wires was measured at liquid helium temperatures in a cryostat designed by Dr Joe Trodahl of V.U.W.; the same cryostat used in the measurement of the resistivity of Rh(Fe) wires in Part I. The only difference in the measurement of the Pt(Ni) wires was in the mounting of the wires. Because only short lengths were available, rather than winding several cms around a bobbin, the wires were mounted as shown in the following diagram:

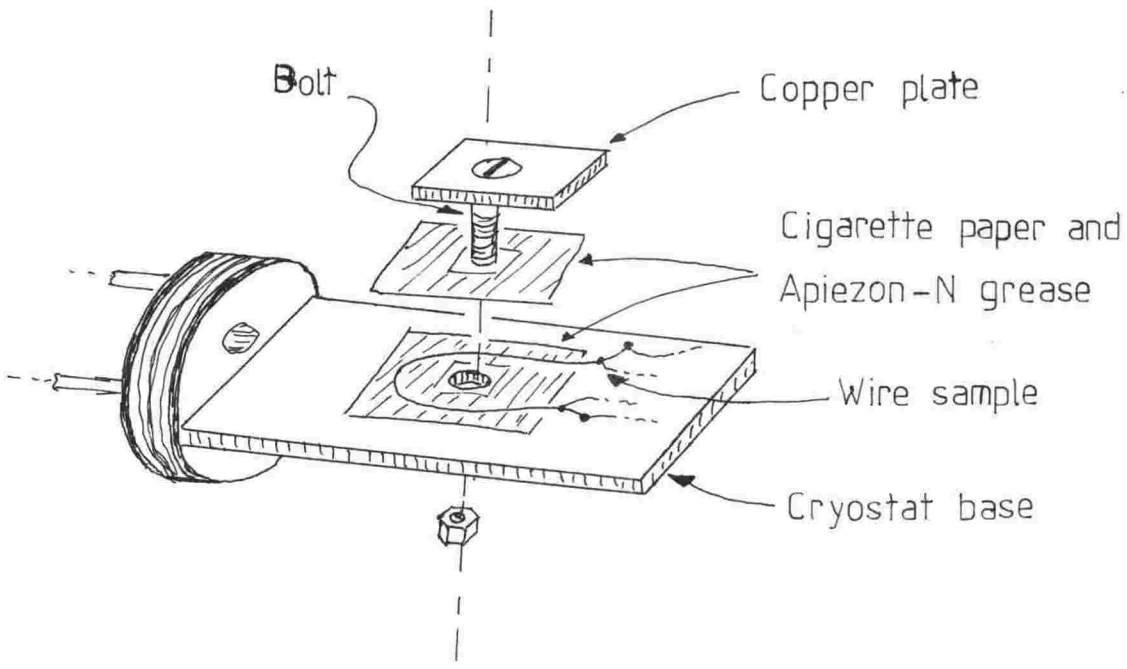

The pure Pt wire was annealed in O_2 at 1200C for 6 hours to oxidize any Fe impurities that might have been present. The 2% and 5% wires had already been annealed at MSU in a high vacuum for 2 and 6 hours respectively and allowed to slow cool.

From the results which may be seen on Graph (2.1) it is clear that both samples contained some impurity in addition to Ni. Subsequent analysis by atomic absorption and XRF indicated that there was 0.23 at.% Fe in the 2% sample and 0.44 at.% Fe in the 5% one. No trace of Mn was found in either. Co was not looked for. The magnitude of the "knee" in the 5% sample is about what could be expected for that amount of Fe contamination (Loram *et al.* 1972). The magnitude of the knee in the 2% sample is most puzzling. The residual resistivity is also several times what could be expected of 2% Ni and 0.23% Fe. No satisfactory explanation has so far been forthcoming to explain this unprecedented behaviour, for it is entirely absent in the 5% sample. The residual resistivity here is consistent with that expected for 5% Ni (Mackliet *et al.* 1970).

The resistivity of pure Pt can be fitted to an $AT^2 + BT^5$ law at low temperatures below 15K. Above 15K the resistivity tends towards the linear phonon contribution.

3. Thin Film Samples of Pt(Ni) - Resistivity and Thermopower

In order to study Pt(Ni) samples which were free of Fe contamination and also to have some control over characteristics such as residual resistivity (for the purpose of applying the Nordheim-Gorter rule) it was decided to manufacture samples of Pt(Ni) by thermal evaporation of Pt and Ni onto glass substrates.

To measure the resistivity and thermopower of these evaporated thin films it was necessary to construct cryostats to accommodate glass substrates. The construction of the thermopower cryostat has already been described in a previous chapter so it will not be repeated here. The only practical difference between measuring the thermopower of wires and that of films is in the mounting of the carbon resistance thermometers onto the sample. The copper plates, upon which are glued the thermometers, are placed directly on the film, as shown below, and held in place by phosphur-bronze spring clips. No grease or varnish was used between film and plate. This latter observation is critical as the ΔV leads were soldered directly to the plates (rather than attached to the film itself). As the electrical and thermal resistance of the

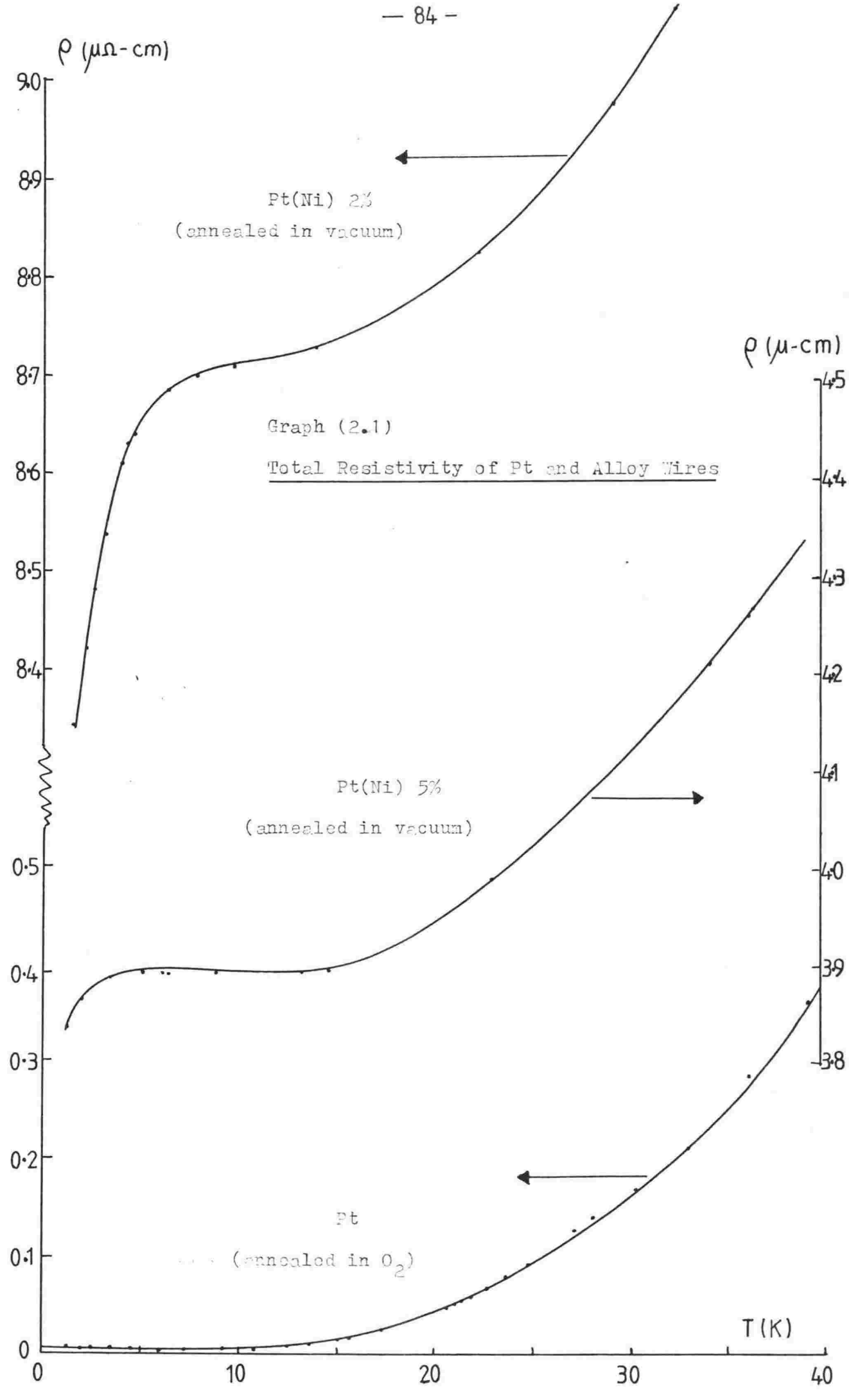

Graph (2.1)

Total Resistivity of Pt and Alloy Wires

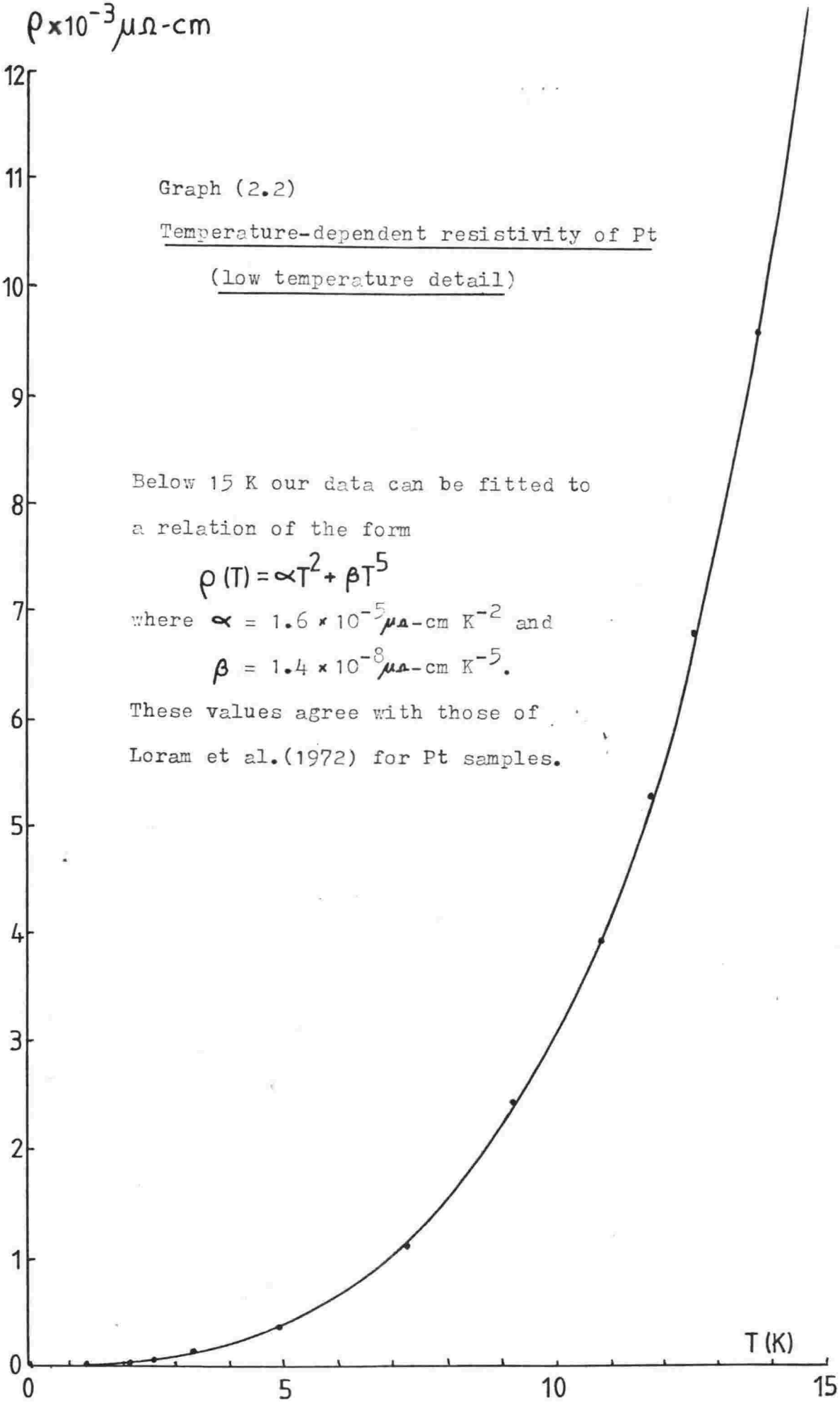

Graph (2.2)

Temperature-dependent resistivity of Pt

(low temperature detail)

Below 15 K our data can be fitted to a relation of the form

$$\rho(T) = \alpha T^2 + \beta T^5$$

where $\alpha = 1.6 \times 10^{-5}$ μΩ-cm K^{-2} and

$\beta = 1.4 \times 10^{-8}$ μΩ-cm K^{-5}.

These values agree with those of Loram et al.(1972) for Pt samples.

copper plates is very much less than that of that portion of the film it short circuits attaching the leads thus introduces negligible error into the thermopower measurement. (No ΔT drops across the plate $\therefore$ no ΔV contribution from the copper-electrically the same as attaching the leads directly and much more convenient).

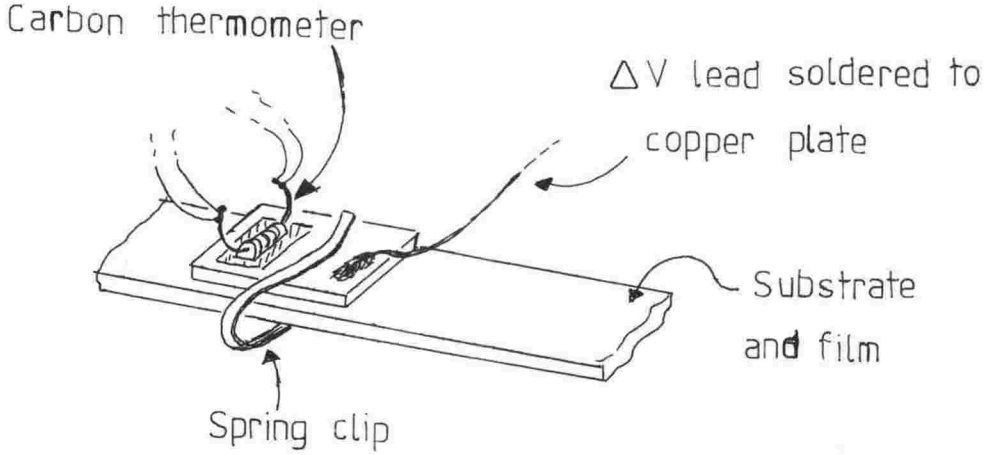

Method of attaching thermometers to the film

The resistivity cryostat was designed to accommodate two substrates simultaneously. A standard 4-terminal measurement technique was employed as previously. Current and voltage probes consisted of adjustable phosphor-bronze strips cemented into a perspex block. "Dimples" were punched into the ends to provide contact with the film. Differential expansion between the glass substrates and the perspex, which has a considerable contraction between room temperature and 4K, was prevented by screwing down the probe assembly to the cryostat base, the screws being located near the ΔV probes thus preventing the probes from coming closer together as the temperature is lowered and introducing a relatively unknown systematic uncertainty into the resistivity via the l/A ratio. This was found to work satisfactorily between room temperature and liquid N_2 temperature and was hence assumed to also work down to liquid He temperature. This is a reasonable assumption since most of the contraction will have already taken place between room temperature and liquid N_2 temperature. Perspex was used because of ease of construction. In any case, all calculated contractions were found to introduce small errors in comparison with the uncertainty in the measurement of the film thickness, which could only be determined to about 10%.

A GE6191 germanium resistance thermometer was employed to measure the sample temperature between 1.5 and 100K. This was fitted snugly into a hole in the copper base of the cryostat with Apiezon-N grease. The leads were thermally anchored to the base with GE7031 varnish. The sample temperature (and that of the base) was maintained by means of a nichrome heater wound around the base.

The essential difference between the measurement of the resistivity of wires and that of thin films is in the attachment of the current and potential leads. In the former soldering directly to a length of wire sample was used; in the latter the probes made contact by pressure. Soldering was tried (Wood's metal) but this caused the film to lift off at the point of solder contact. The thing to watch out for is to make sure that the potential probes make contact with the film at points where there is an even distribution of equipotentials otherwise the resistance and the resistivity will not be related only via l/A.

The other assumption was that the film was at the same temperature as that measured by the thermometer. Provided that the sample current is sufficiently low not to cause excessive Joule heating (1mA was found to be the maximum that could be used), and that the heat from the cryostat base has no path through the substrate, this is a reasonable assumption. This is ensured by keeping the gas pressure as low as possible in the cryostat and with the use of a "radiation shield". The substrate is fixed to the base with Apiezon-N grease.

Resistivity Cryostat for Thin Film Samples

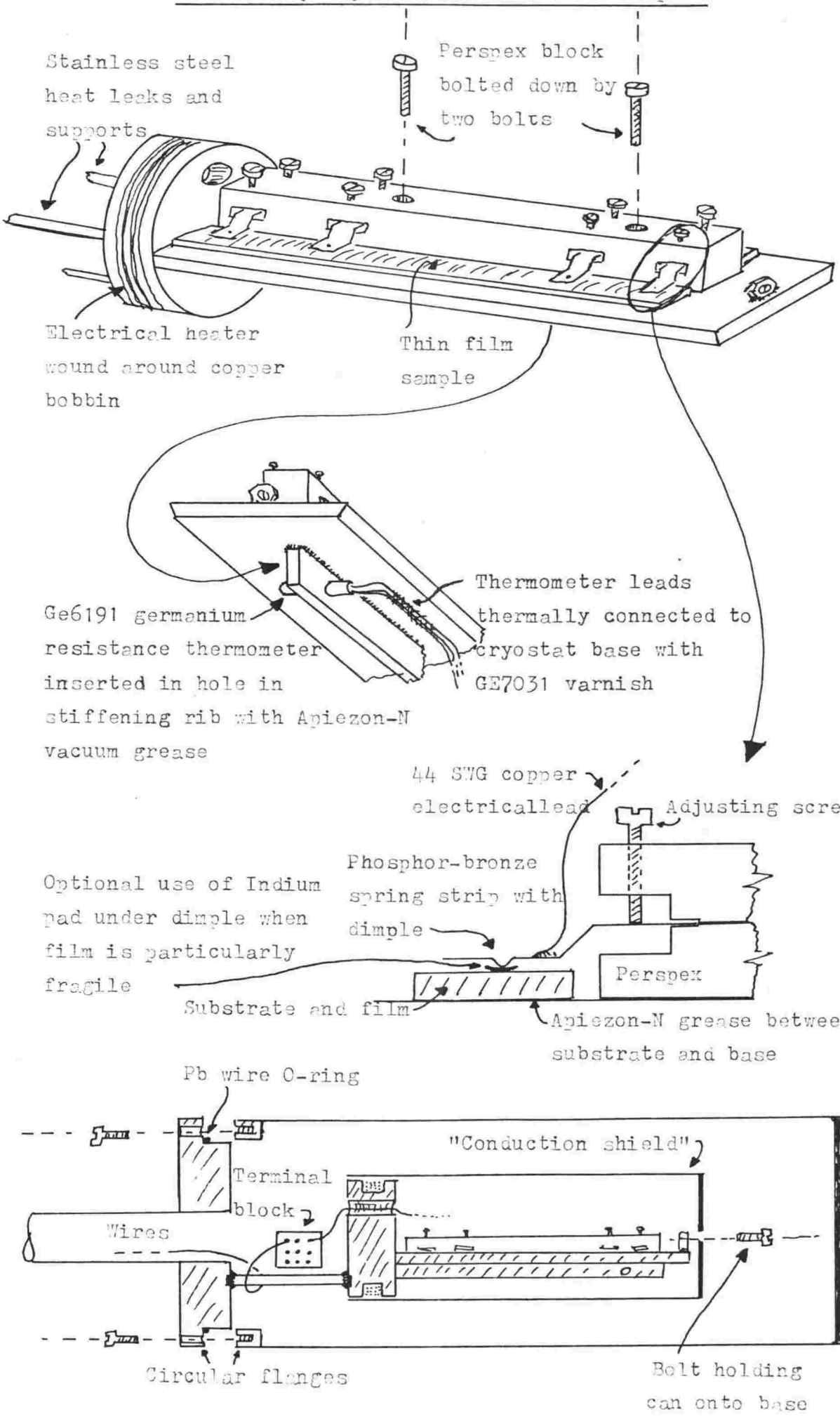

4. Manufacture of Thin Films by the Thermal Evaporation Method

The Pt(Ni) alloy films used in this study were made by the thermal evaporation of Pt and Ni simultaneously in a dual electron gun ultra high vacuum system by Varian Associates. Pt and Ni were deposited simultaneously onto cleaned glass substrates made from cut down microscope slides. The slides were cut to a length of 60 mm and a width of 7.5 mm. The slides were about 1.5 mm thick.

The evaporation system interior was designed largely by Mr Peter Gilberd and exact details will not be given here. Rather an outline of the procedure employed and the principles involved should suffice to tell the story.

The heart of the system consists of two electron guns which generate a beam of electrons which by means of magnetic focussing is caused to impinge upon a chunk of the metal to be evaporated sitting in a hearth. The kinetic energy of the electrons is converted into heat and the metal is heated until it begins to evaporate. The rate of evaporation is controlled by controlling the beam current and the deposited film thickness is monitored by means of an oscillating quartz crystal microbalance. ("Sloan 1000 Evaporation Control Units"). The frequency of oscillation of the crystal is determined, in this case, by the amount of metal that is deposited on it in the form of additional surface mass. The crystal is placed near the substrate and such that it is perpendicular to the evaporating metal, which it "sees". The greater the surface mass of metal deposited on the crystal, the lower the frequency of oscillation. At a frequency of 5MHz a 1Hz change corresponds to a mass increase of about 1.8×10^{-8} g/cm^2. Taking into account such factors as the density of evaporating metal and the "tooling factor" - essentially a geometrical factor which enables the amount of metal deposited on the substrate to be determined from the amount of metal deposited on the crystal - the film thickness and, when the system is duplicated for an impurity, the concentration may be determined, usually to within 10 or 20%.

As a means of getting several alloy concentrations at once the impurity metal "beam" is interrupted by two steel wire meshes each of 50% transmission factor superimposed upon each other in a way as to give transmission factors of 50 and 25%. By interposing this mesh arrangement between the impurity hearth and the substrates, ensuring that each substrate sees only one mesh portion, alloys of three concentrations could be made. In this case the rates of evaporation of Pt and Ni were arranged to give alloys of 10, 5, 2½% and pure Pt, the pure Pt obtained by positioning the substrate in such a way as it could not "see" the Ni hearth and the 10% alloy positioned so that it was in the direct beam of Ni vapour.

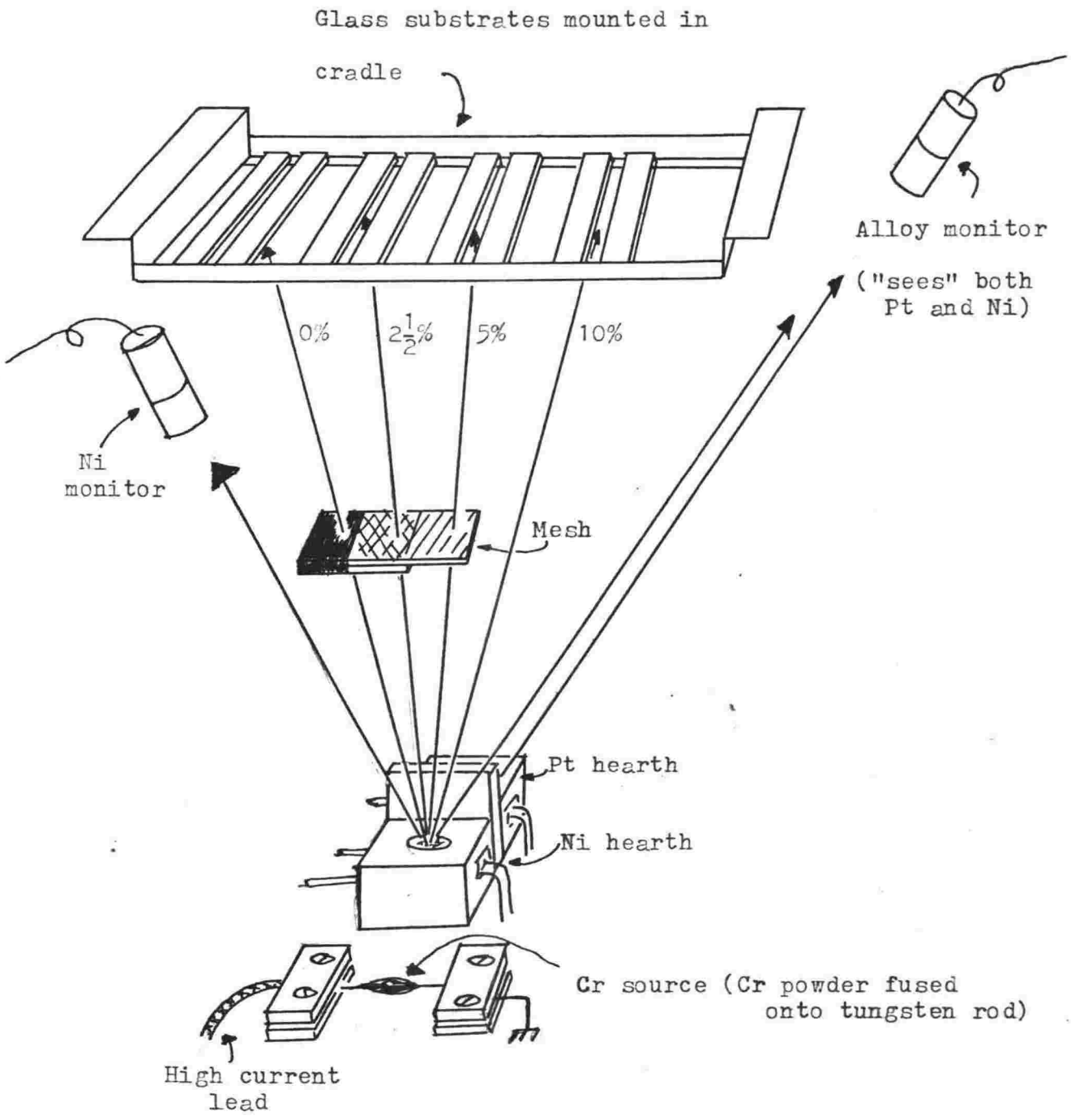

Arrangement of major components within UHV system

(shutter screening substrates from hearths not shown for clarity)

The whole operation takes place in an ultra high vacuum of better than 10^{-8} Torr, maintained by an ion pump and a titanium sublimation pump. The system is first "roughed" with a sorption pump to remove inert gases especially, such as argon, which the other pumps cannot handle.

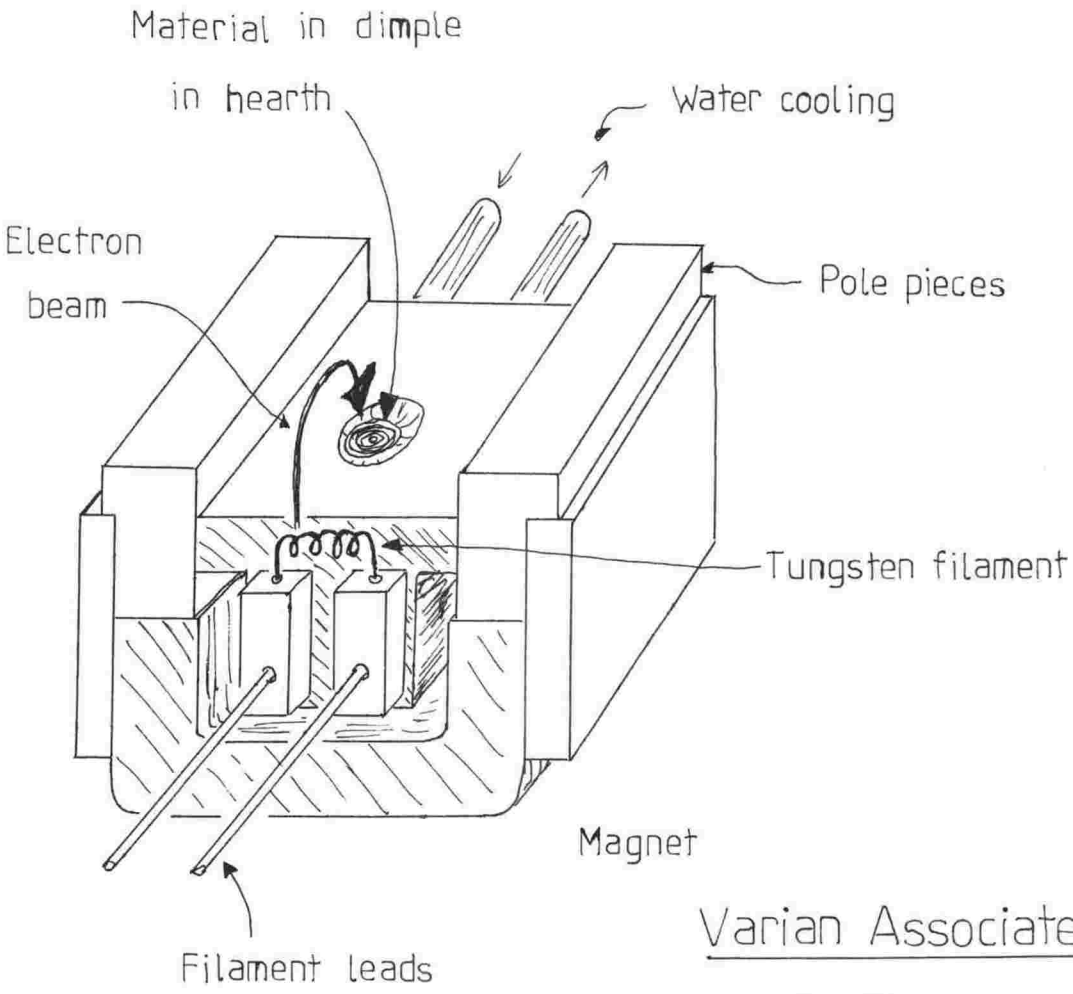

Varian Associates
e-gun

Preparation of Substrates

Glass microscope slides cut to the appropriate size were first cleaned thoroughly before being placed in the high vacuum system.

After cutting and smoothing the edges the slides were scrubbed with a very mild abrasive powder with water as lubricant. This served to polish the surface. Then followed a 15 minute wash in approx. 50% HCl solution in an

ultrasonic bath and finally a further wash in de-ionized water in the ultrasonic bath. The substrates were dried in a vapour degreaser where the vapours from boiling ethanol are allowed to condense onto the surface of the substrates and in doing so rid the surface of any remaining impurities leaving a streak-free surface. After baking the substrates at 100C for 15 minutes they were immediately placed in the vacuum system to prevent contamination.

Preparation of the Films

Altogether three runs were required to produce films that were satisfactory enough to be able to be measured.

4.1 The initial run

The substrates were placed upon a jig suspended above the two hearths and the mesh. Prior to this 99.998% Ni wire (Koch-Light Laboratories) and 99.999% Pt powder (Koch-Light Laboratories) were melted down in the system to form small globules of metal in the hearths. Pre-melting was necessary to prevent spitting of the metal (which occurred most violently in the pre-melting) when actually performing the evaporation. Of the 5 grammes of metal sitting in the hearth at the beginning of the evaporation about 2 to 3 grammes was actually used in the evaporation. Less Ni was used since the evaporation rate was only a tenth that of Pt.

It was hoped to produce films of about 1500 to 2000 Å thickness. The deposition rates onto the substrates were set at 10 Å/sec for Pt and 1 Å/sec for the Ni. Once the rates were achieved and stabilized the shutter screening the substrates, but not the rate monitor crystals of course, was opened by means of an electromagnet to allow the evaporating metals to deposit onto the substrates. The evaporation rate is automatically controlled by means of a feedback loop between the monitors and the electron gun.

Unfortunately before the monitors had even indicated that 1000 Å had been deposited the films began to disintegrate. As a result of this only two films were subsequently able to be salvaged for measurement at low temperatures. The other films, those that survived the evaporation, completely cracked up upon contact with the atmosphere which was probably at a different temperature thus causing the thermal shock (on the obviously weak films) to complete the destruction.

The alloy concentrations were calculated from the system geometry and the mesh attenuation. For the purposes of applying the modified Nordheim-Gorter rule the absolute concentrations were not required and it was felt that those deduced from geometric considerations would suffice.

4.2 The second run

Acting on a suggestion by Professor David Beaglehole the substrates were first pre-coated with a thin layer of chromium, the idea being that Pt would adhere to the Cr rather than the glass. Experimentally it is found that Pt does stick rather well to Cr. About 45 Å of Cr were deposited onto the substrates by means of a resistance-heated Cr coated tungsten rod immediately prior to the actual evaporation. The thickness of the Cr was monitored with the "alloy" monitor, account being taken of the different density of Cr when making the thickness determination. To check the actual thickness a pure Cr film was made. Although with the method available at the time this could not be done any more accurately than by the crystal monitor, low temperature resistance measurement showed that the resistance of the Cr was about 1100 ohms, or about 100 times that of the alloy films. The effect of the Cr layer upon the measured electrical properties of the alloys is expected to be negligible as most of the conduction takes place in the Pt(Ni) rather than the Cr. Likewise diffusion of Cr into the Pt is not expected to give any problems.

The evaporation then proceeded as before. The films were successfully made this time, thicknesses of about 1000 Å being aimed for. The films still did not take too kindly to heavy abuse such as being breathed upon!

4.3 The final run

A third run was also attempted as before to try to manufacture thicker films. Films of nominally 2000 Å were made although these were found to be not as robust as the 1000 Å ones. The higher concentration films (10%) were the easiest to damage. In this run the evaporation was stopped when the 10% film started to flake away.

It is interesting to note that Belser and Hicklin (1959) reported no difficulty with making Pt films. Their substrates were subjected to temperatures of 500C in some cases with no evidence of trouble such as

5. Results

After manufacture the films were placed in the resistivity and thermopower cryostats and their respective properties were measured at low temperatures. As two films of each concentration were made simultaneously, one went in the resistivity cryostat and the other in the thermopower cryostat. The results of these measurements may be seen on Graphs (5.1, 5.2, 5.3). All of the films appear to be free of Fe contamination since there is no trace of the "knee" which appeared in the Pt(Ni) wire resistivities earlier. This object, at any rate, was achieved. However total control of the alloy concentration and residual resistivities was another matter.

The first thing noticed was the rather high residual resistivity of most of the films. This can probably be attributed to the premise that the films are in a state of great strain even after annealing, which itself created new problems. The following table shows the history of the films. The film thicknesses were measured on a Varian "Å-scope". This is an interferometric method of determining film thicknesses. The ends of the films were first overcoated with Al to provide a reflective surface for the operation. The path difference between the surface of the film and the substrate surface immediately next to the end of the film causes a "step" in the interference fringes when the whole is illuminated with monochromatic light, in this case Na. The step height is directly proportional to the actual step caused by the end of the film and hence the film thickness can be calculated, knowing the wavelength of the light.

Sample	(nominal concentration) in at.%	Thickness, Å	Annealing schedule and comments
Run 1	Pure Pt	350 ± 50	not annealed
	2½%	600 ± 50	not annealed
	5%	——	Films destroyed
	10%	——	Films destroyed
Run 2	Pure Pt	350 ± 50	not annealed
	2½%	600 ± 50	not annealed
	5%	800 ± 70	Annealed in high vacuum for 15 mins at 400C
	10%	800 ± 50	Annealed in high vacuum for 15 mins at 400C
Run 3	Pure Pt	not measured	not annealed
	2½%	not measured	not annealed
	5%	1800 ± 100	not annealed
	10%	not measured	not annealed

Table (5.1). Pt(Ni) Film Sample History

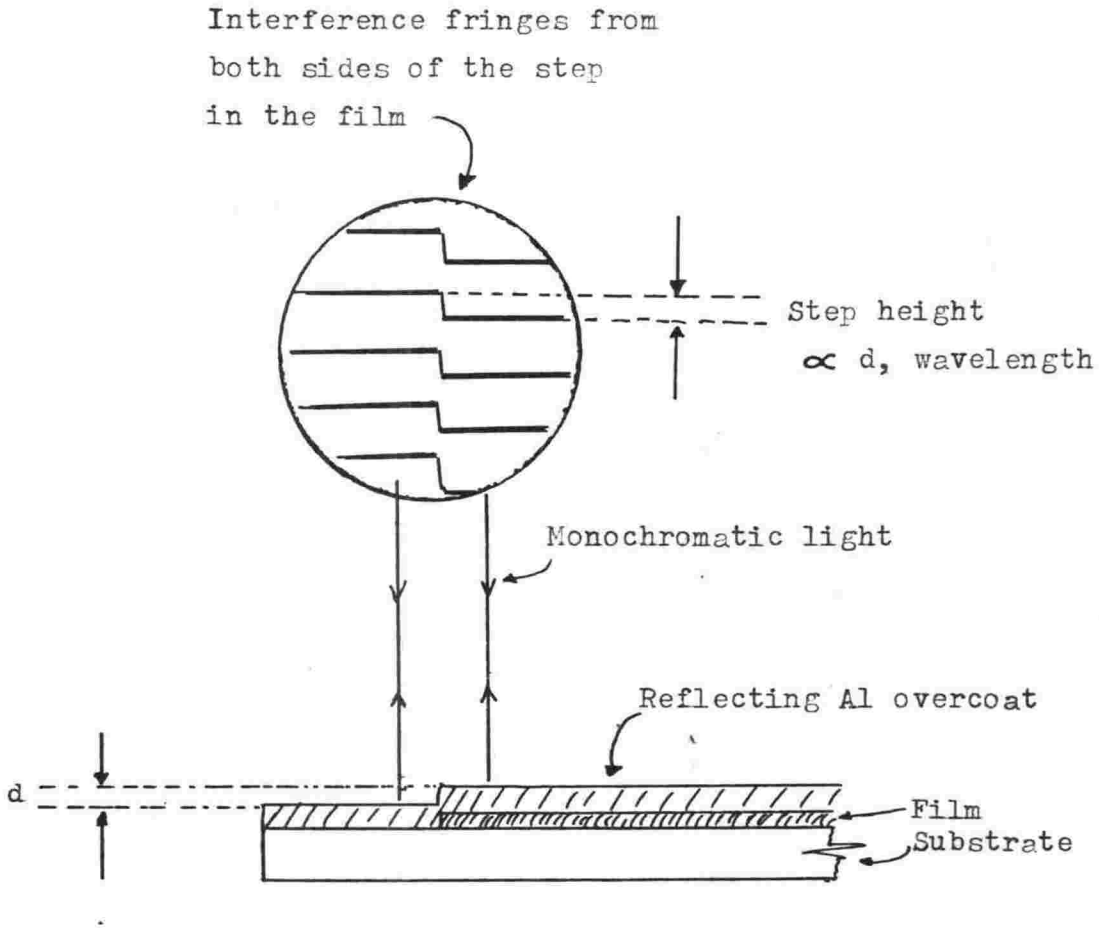

Interferometric Determination of Film Thickness

The thickness determination of the second run was assumed to be representative of the others as nothing was altered between runs.

It can be seen from the graphs of the film resistivities that some odd behaviour is taking place. Firstly, the temperature-dependent part of the resistivity of the pure Pt films is substantially higher than that of the wires. Also, we have the situation where the temperature-dependent resistivity of some of the alloy films is less than that of Pt. The discrepancies cannot be accounted for by attributing them to inaccuracies in the determination of the film thickness so we are left with the conclusion that the resistivities and the measured resistances are not directly related via the form factor l/A. In fact this is fairly obvious in the resistivities of the pure Pt and the 2½% films of the earliest run. Here the film appeared to crack up as the temperature was raised from 4.2K thus increasing the effective l and causing an increase in measured resistance over that due to electronic behaviour alone. Plugging in the measured value of l/A, determined by simple measurement, gives an enormous increase in what was initially taken to be the phonon resistivity.

It was hoped that by assuming that the phonon resistivity had the same slope in all films, and that by normalizing all the resistances to give the same high temperature slope, the low temperature resistivities could be determined. By this means any inaccuracies in determining l/A would be replaced by inaccuracies in measuring the high temperature slope which, in general, involved a much smaller uncertainty. However in view of the behaviour of the initial films it could not be guaranteed that unpredictable effects were not also occurring with the other films. In any case we still do not know for certain the behaviour of Ni in Pt at higher temperatures and any such assumption might serve to obscure the impurity effects, since it would be necessary to subtract off the pure Pt resistivity from the alloy resistivity to get the impurity contribution. Thus by assuming the high temperature resistivity slopes were all the same we would lose any possible contribution from the Ni.

In spite of the uncertainty in the magnitude of the resistivities at low temperatures pure Pt at least could be fitted to an $AT^2 + BT^5$ term anyway, the coefficients being about twice those for Pt wires, indicating a possible error in l/A, although the high temperature coefficient of the linear phonon component is not twice that of wire samples, tending thus to suggest that indeed something odd is going on in these films.

We conclude therefore that for these films the resistivities are at best uncertain and the behaviour of Ni in Pt cannot be elucidated from these data.

It is interesting to note the behaviour of the resistivity of the annealed films. These were annealed in a vacuum of about 2×10^{-5} Torr for 15 minutes at 400C and allowed to slow cool. From the shape of the low temperature resistivity i.e. the resistance minimum, it is evident that a transition to magnetic scattering has taken place. Any decrease in the residual resistivity caused by annealing out lattice imperfections (grain boundary scattering is probably the dominant scattering mechanism in these films) has probably been counteracted in part by the increase in residual resistivity due to the now present magnetic scattering. It is supposed that the Ni impurities have migrated together under annealing and formed magnetic clusters. The information from these particular films, though interesting, do not enable us to proceed with our original intention of applying the modified Nordheim-Gorter Rule to test the thermopowers as we do not have, strictly speaking, LSF alloys of the "Coles" type.

It is also interesting to see the variation of film thickness across the substrate jig in the UHV system. The pure Pt films are thinner than the higher concentration ones. This is almost certainly due to the uneven heating the Pt in the hearth due to poor positioning of the electron beam thus heating the Pt globule predominantly from one side. Since the Pt is an extended source, rather than a point source, variation in temperature across the Pt is likely to give an uneven distribution of evaporated Pt from film-to-film. The significance of this was not appreciated until after the thicknesses had been measured, of necessity after the low temperature measurements had been completed. The Ni globule appeared to be heated fairly evenly and so we can expect that the Ni was deposited evenly across the films as a consequence, allowing for geometric factors i.e. the inverse-square variation of Ni vapour concentration with distance from the source. Now, the Ni concentrations that were initially hoped for depended upon the correct amount of Pt being deposited onto the substrates; in most of the films the amount of Pt is substantially less than the amount deduced from the alloy monitor and so the relative amount of Ni is correspondingly greater. Thus the Ni concentrations are probably up to twice as great as initially calculated.

Also of note is the scatter in the resistivity data as compared with the resistivity data of wires. This is attributed to the comparatively high resistance of the films as compared with the wires creating extra thermally generated noise. The total change in the resistance "seen" by the nanovoltmeter used to measure the sample voltage is not, of course, in the same ratio as the film-to-wire resistances, but the increase is calculated to be sufficient to account for the extra noise seen on the film voltage and hence the scatter in the data. The higher resistance of the films is of little consequence when making thermopower measurements since there is already a high resistance (the manganin leads - approximately 200 ohms) in series with the sample and the slight extra resistance added by the films (about 10 ohms) causes no measurable change in the noise on the ΔV signal.

In view of the confusing resistivity results any analysis using the modified Nordheim-Gorter Rule would probably yield meaningless information and so was not even contemplated. The results of the two thermopower measurements upon a pure Pt film and a 10% alloy film may be seen in Graph (5.4) along with the results for two wires in Graph (5.5) for comparison. That the thermopower of the wires are different from those of the films is evident; unfortunately any definitive explanation is as yet lacking. Also, the wire thermopowers are not in very good agreement with some previously published data.

It could be argued that the difference between our film thermopowers and our wire thermopowers arises from the balance of scattering between phonons, surface scattering and imperfections. These effects in thin films are usually described by a "size effect" term. In the simplest case, the difference between the resistivity of a wire and that of a thin film of the same metal is that, in the latter, there exists an extra resistivity component in the form of scattering off the film surface. The ratio of resistivities of film to wire is called the size effect term. Actually we should, strictly speaking, talk of the ratio of film to bulk sample resistivities but the difference is unimportant for the purposes of our discussion. Writing

$$\rho = \rho_o f(k)$$

where ρ is the film resistivity, ρ_o is the bulk resistivity, $f(k)$ the size effect term and k is the ratio between the film thickness and the bulk mean-free-path. Inserting the film resistivity thus written into the Mott Formula for diffusion thermopower, we get

$$S = \frac{\pi^2 k^2 T}{3e} \left[\frac{\partial \ln \rho(\varepsilon)}{\partial \varepsilon} \right]_{\varepsilon_F}$$

$$= \frac{\pi^2 k^2 T}{3e} \left[\frac{\partial \ln \rho_o(\varepsilon)}{\partial \varepsilon} + \frac{\partial \ln f(k)}{\partial \varepsilon} \right]_{\varepsilon_F}$$

It can be seen that depending upon how the size effect term varies with electron energy, the film thermopower could be greater or smaller than the bulk value.

Changes in thermopower from the bulk value have been experimentally observed. Yu and Leonard (1974) observed changes in the room temperatures thermopower of Cu and Ag films which depended upon the film thickness and state of anneal. It is possible that the effects of bulk, surface and imperfection scattering in our films could be sorted out, but in view of the meaningless resistivity data and the lack of numbers of films this was not attempted. The different thicknesses of the various films would make interpretation of the thermopower a difficult business in view of the many variables involved. Yu and Leonard found that the thermopower due to imperfections (and possibly this could be extended to cover impurities) was dependent upon film thickness.

The 10% film does have a thermopower greater than that of the pure Pt film. Whether this increase is due to LSF effects is not certain. At a concentration of 10% Ni the phonon drag thermopower component may be affected and as we do not have sufficient thermopower data to positively verify this it would be unwise to draw any conclusions.

Graph (5.1)

Total Resistivities of Pt(Ni) Films

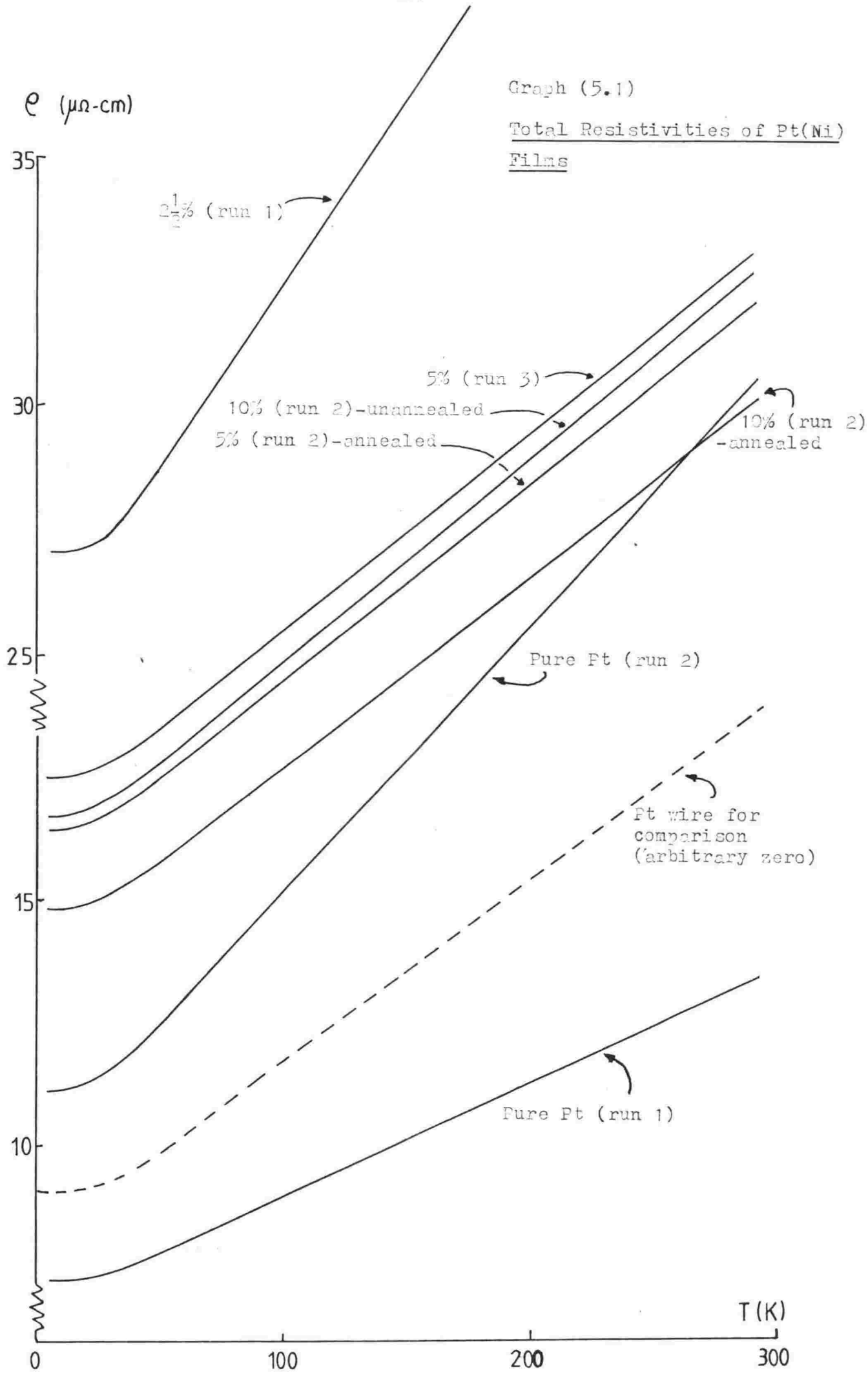

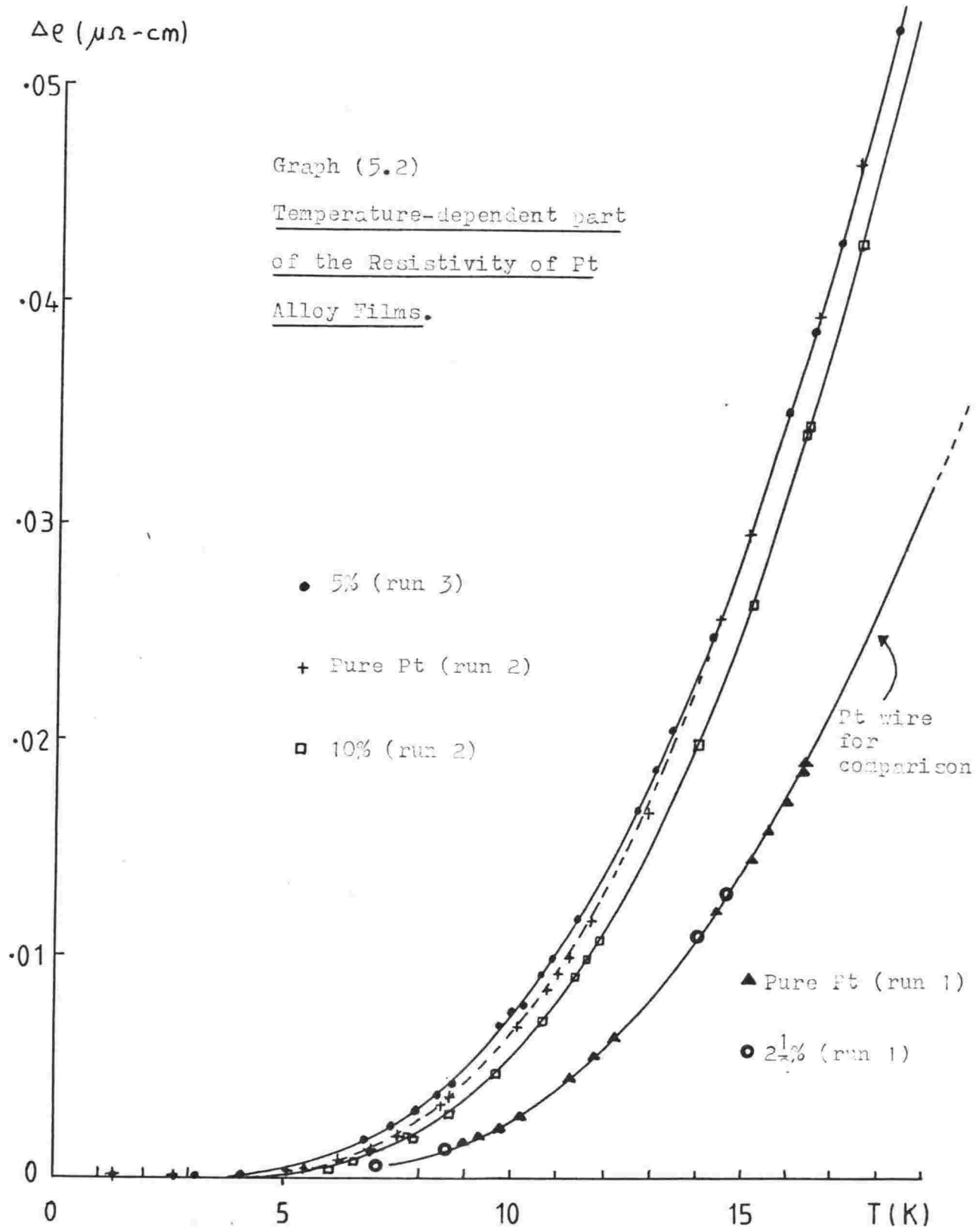
Δρ (μΩ-cm)
·05
·04
·03
·02
·01
0
0
5
10
15
T(K)
Graph (5.2)
Temperature-dependent part
of the Resistivity of Pt
Alloy Films.
● 5% (run 3)
+ Pure Pt (run 2)
□ 10% (run 2)
Pt wire
for
comparison
▲ Pure Pt (run 1)
○ 2½% (run 1)

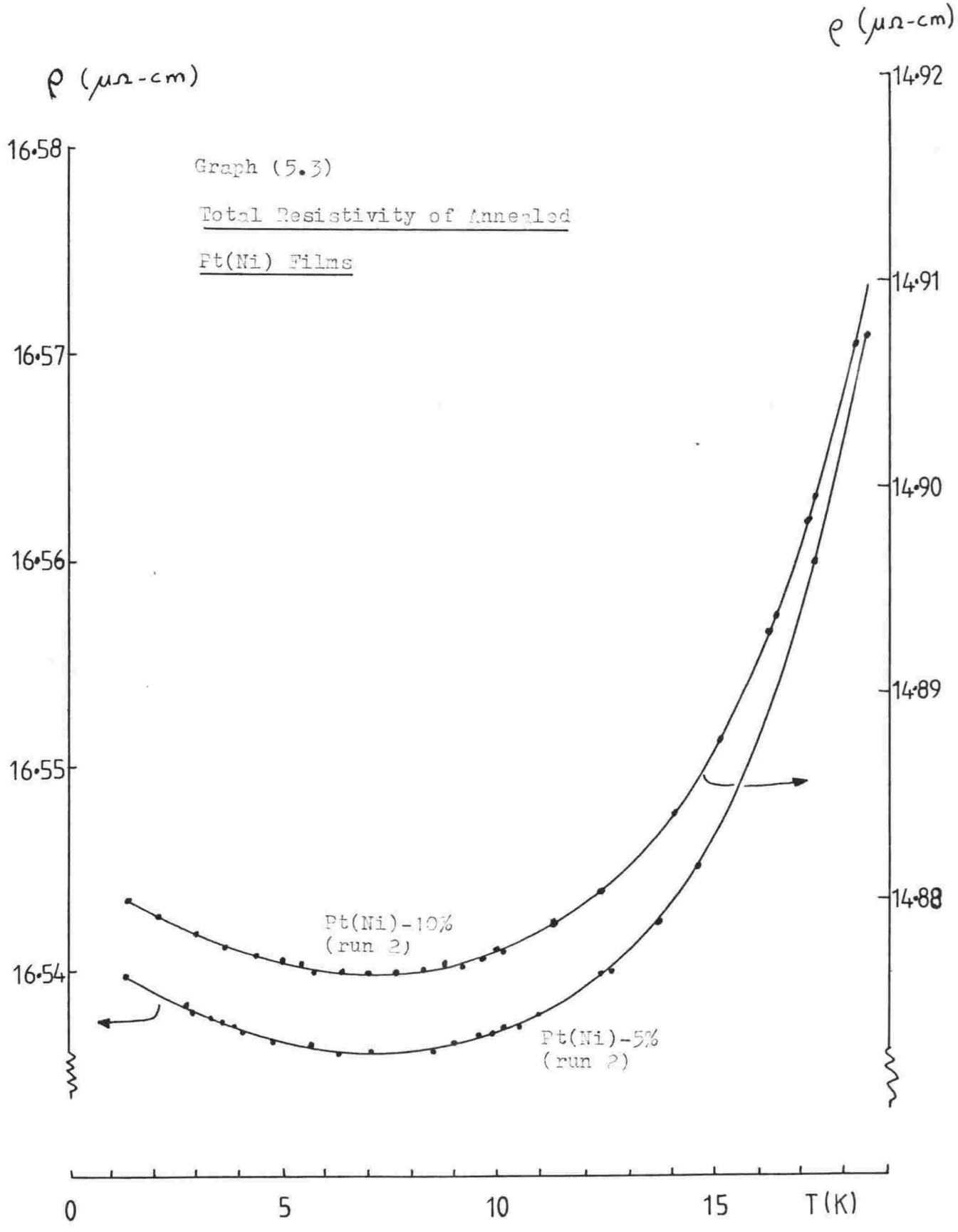
ρ (μΩ-cm)
ρ (μΩ-cm)
16·58
16·57
16·56
16·55
16·54
14·92
14·91
14·90
14·89
14·88
Graph (5.3)
Total Resistivity of Annealed
Pt(Ni) Films
Pt(Ni)-10%
(run 2)
Pt(Ni)-5%
(run 2)
0
5
10
15
T(K)

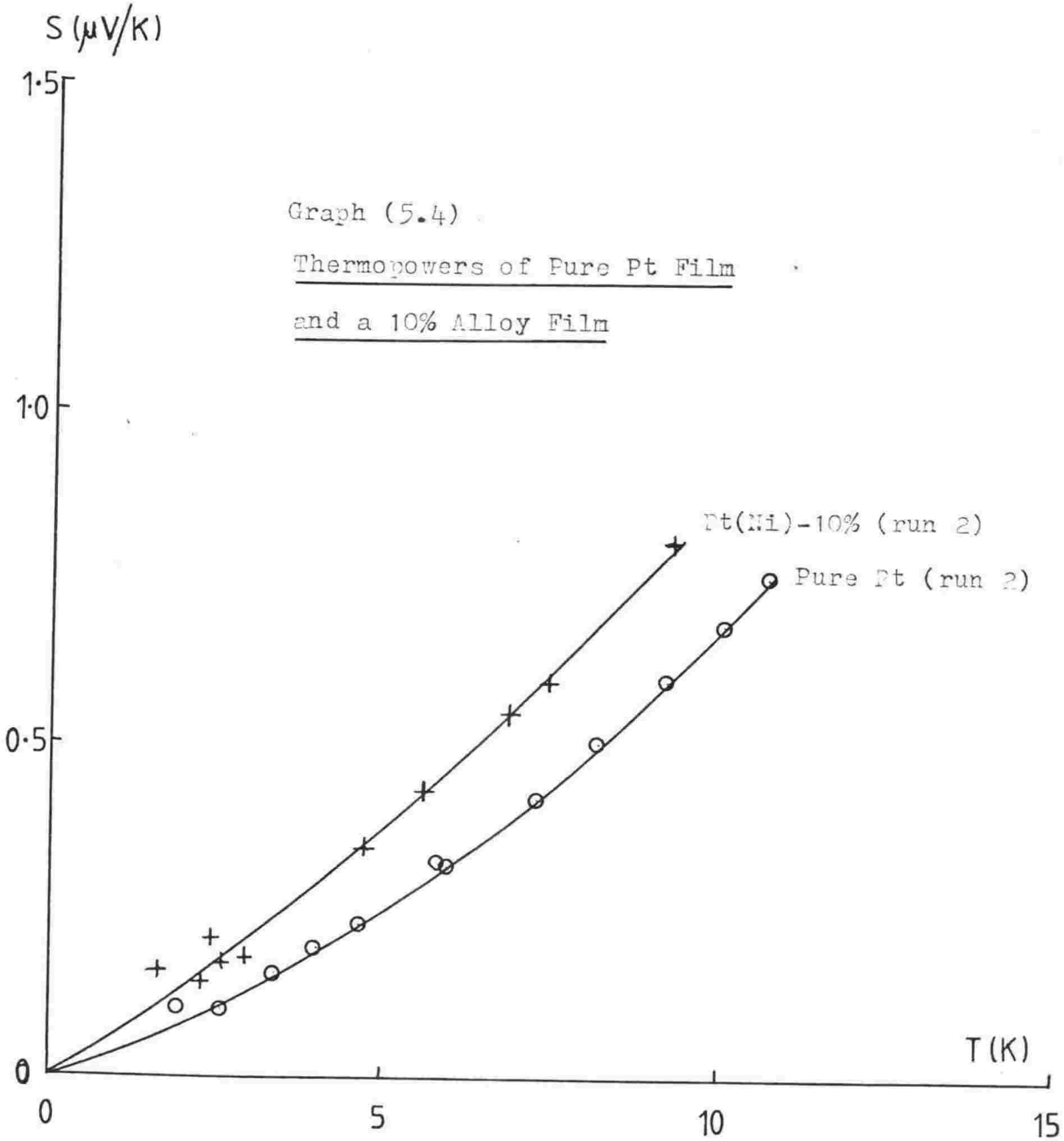

Graph (5.4)

Thermopowers of Pure Pt Film and a 10% Alloy Film

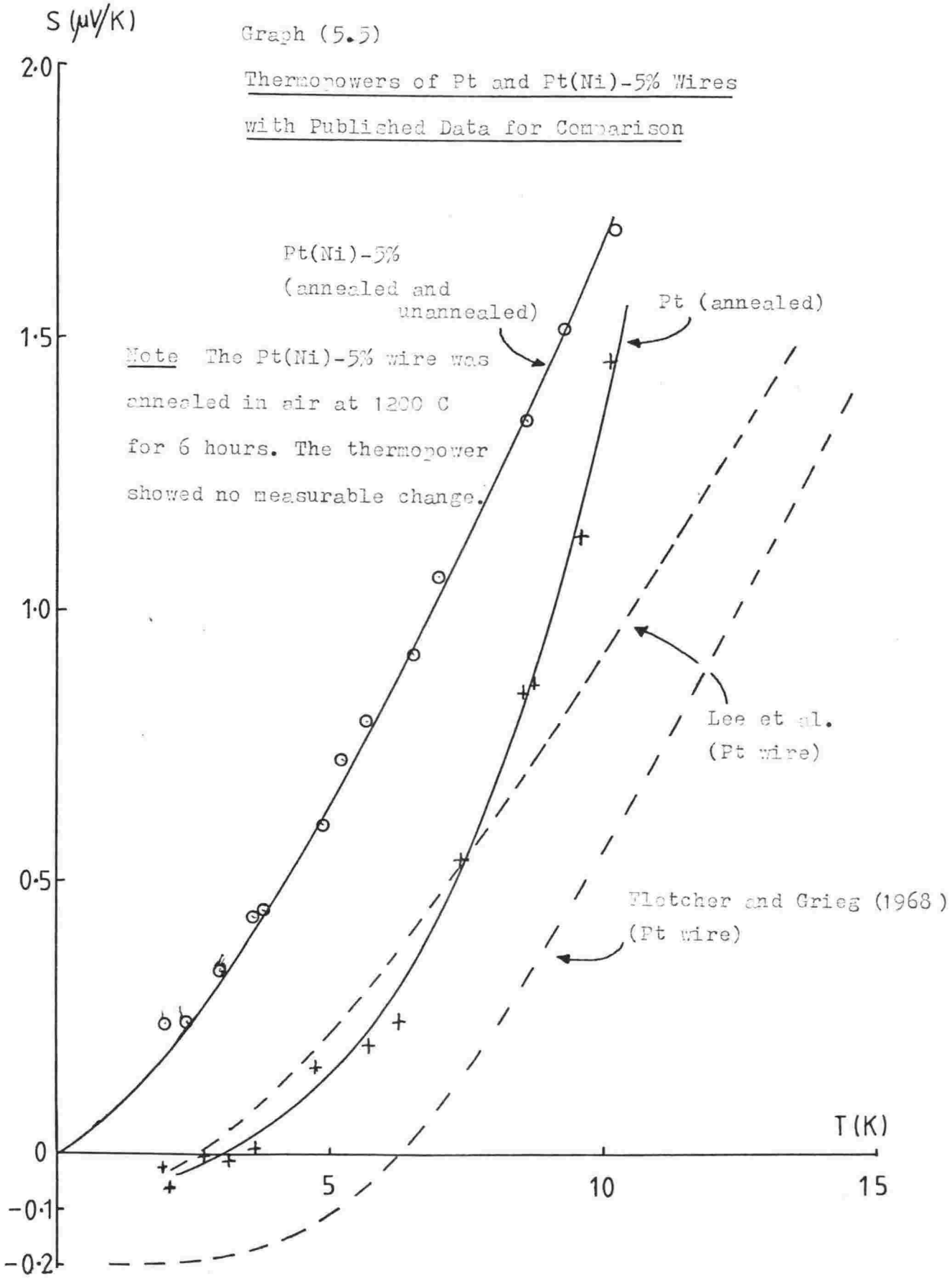

Graph (5.5)

Thermopowers of Pt and Pt(Ni)-5% Wires with Published Data for Comparison

Appendix I

Spin Fluctuation Temperature, T_{sf}, of Pt(Ni).

We will estimate T_{sf} for dilute Pt(Ni) alloys by comparing the quantities $\frac{1}{\chi}\frac{d\chi}{dc}$ and α_o with those of Pd(Ni) alloys, for which we know T_{sf}.

From Chapter One we have

$$\chi = \chi_h + c\,\frac{\delta u\,\chi_h^2}{1 - \delta u\,\chi_h}$$

where the terms have been previously defined. Writing $\Delta\chi = \chi - \chi_h$ we get

$$\frac{\Delta\chi}{c\,\chi} = \alpha\,\delta u\,\chi_h$$

for small c. In the limit of vanishing c we can write

$$\frac{1}{\chi}\frac{d\chi}{dc} = \alpha\,\delta u\,\chi_h \qquad \text{Equation 1}$$

From Kaiser (1970) we have

$$(k_B T_{sf})^{-1} = \alpha\,\delta u\,\frac{\bar{\chi}}{\omega}$$

where $\bar{\chi} = A\alpha_o^2\omega$ (Lederer and Mills 1968) where A is constant and approximately the same for both Pd and Pt. Substituting from Equation 1,

$$(k_B T_{sf})^{-1} = A\cdot\left(\frac{1}{\chi}\frac{d\chi}{dc}\cdot\frac{1}{\chi_h}\right)\cdot\alpha_o^2$$

Now $\chi_h = \alpha_o\chi_o$ where χ_o is the susceptibility calculated from the density of states. Hence,

$$(k_B T_{sf})^{-1} = A\cdot\left(\frac{1}{\chi}\frac{d\chi}{dc}\cdot\frac{1}{\chi_o}\right)\cdot\alpha_o$$

If we assume that χ_o is the same for both Pd and Pt then $(k_B T_{sf})^{-1}$ depends only upon $\frac{1}{\chi}\frac{d\chi}{dc}$ and α_o.

From Lederer and Mills (1968) we get

$$\frac{1}{\chi}\frac{d\chi}{dc} = 115 \quad \text{and} \quad \alpha_o = 10 \qquad \text{for Pd(Ni), and from}$$

Mackliet et al. (1970) we get

$$\frac{1}{\chi}\frac{d\chi}{dc} = 12 \quad \text{and} \quad \alpha_o = 5/3 \qquad \text{for Pt(Ni).}$$

Thus we have T_{sf} for Pt(Ni) = 50 T_{sf} for Pd(Ni)

= 1000 K.

CONCLUSION TO THESIS

We have developed apparatus for measuring the thermopower and resistivity of wire and thin film samples at low temperatures. We have measured the thermopower and resistivity of Rh(Fe) wire samples in order to resolve discrepancies in previous measurements and to show that the correct explanation for the observed "giant" peaks in the thermopower (at a temperature of about 3 K) is that they are a diffusion and not a spin fluctuation drag effect, which latter had been postulated as a possible explanation. Conclusive proof for the diffusion origin of the peaks was provided when we considered how the thermopower changed upon the change in the balance of electron scattering caused by rolling flat and by annealing several samples.

We have manufactured several thin film samples of Pt(Ni) by the thermal evaporation method, it being thought that better control over the samples' physical characteristics (e.g. residual resistivity) could be obtained by this method. However, at present, this is not the case and our intention of measuring the thermopower and resistivity of Pt(Ni) to see whether any possibly occurring features in the thermopower due to the Ni impurities could be interpreted as a diffusion or a drag effect was not realised, the high host residual resistivity being likely to obscure these features. Our theoretical estimate of T_{sf} for Pt(Ni) indicates that any effects in the thermopower due to the impurities are likely to extend to much higher temperatures than those seen in Rh(Fe).

REFERENCES

Anderson P W, Phys. Rev. 124, 41 (1961)

Anderson P W, Comments in Solid State Phys. 1, 31 (1968)

Anderson P W, Comments in Solid State Phys. 5, 73 (1973)

Barnard R D, "Thermoelectricity in Metals and Alloys" Taylor and Francis (1972)

Belser R B and Hicklin W H, J.Appl.Phys. 30, 313 (1959)

Blatt F J, Flood D J, Rowe V, Schroeder P A and Cox J E, Phys.Rev.Lett. 18, 395 (1967)

Calwell W and Greig D, J.Physique Coll. 39, C6-865 (1978)

Cheng L S and Higgins R J, Phys.Rev. B 19, 3722 (1979)

Christian J W, Jan J P, Pearson W B, and Templeton I M, Proc.Roy.Soc.A 245, 218 (1958)

Clogston A M, Matthias B T, Peter M, Williams H J, Corenzwit E and Sherwood R C, Phys.Rev. 125, 541 (1962)

Coles B R, Phys.Lett. 8, 243 (1964)

Cooper J R and Miljak M, J.Phys.F:Metal Phys. 6, 2151 (1976)

Fischer K H, J.Low Temp.Phys. 17, 87 (1974)

Fletcher R and Greig D, Phil.Mag. 16, 303 (1967)

Fletcher R and Greig D, Phil.Mag. 17, 21 (1968)

Foiles C L and Schindler A I, Phys.Lett. 26A, 154 (1968)

Freidel J, Nuovo Cimento Suppl. 7, 287 (1958)

Greig D and Rowlands J A, J.Phys.F:Metal Phys. 4, 232 (1974)

Graebner J E, Rubin J J, Schutz R J, Hsu F S L, Reed W A and Higgins R, AIP Conf. Proc. 24, 445 (1975)

Gruner G, Solid State Comm. 10, 1039 (1972)

Guenault A M and MacDonald D K C, Phil.Mag. 6, 1201 (1961)

Huntley D J, Can.J.Phys. 49, 2610 (1971)

Izuyama T, Kim D J and Kubo R, J.Phys.Soc.Japan 18, 1025 (1963)

Kaiser A B, Phys.Rev. B 3, 3040 (1971)

Kaiser A B, AIP Conf.Proc. 29, 364 (1976)

Kaiser A B, Calwell W and Greig D, J.Phys.F:Metal Phys. 10, 1419 (1980)

Kaiser A B and Doniach S, Int.J.Mag. 1, 11 (1970)

Kaiser A B and Gilberd P W, J.Phys.F:Metal Phys. 6, L209 (1976)

Kasuya J, Progr.Theor.Phys. 16, 58 (1956)

Kondo J, Progr.Theor.Phys. 32, 37 (1964)

Kondo J, Progr.Theor.Phys. 34, 372 (1965)

Kubo R, J.Phys.Soc.Japan 12, 750 (1957)

Lederer P and Mills D L, Phys.Rev. 165, 837 (1968)

Lederer P and Mills D L, Phys.Rev.Lett. 20, 1036 (1968a)

Lee C W, Foiles C L and Bass J, (pre-publication draft c.1980)

Loram J W, White R J and Grassie A D C, Phys.Rev. B 5, 3659 (1972)

Low G and Holden T, Proc.Roy.Soc. 89, 119 (1966)

MacDonald D K C, "Thermoelectricity, An Introduction to the Principles" Wiley (1962)

Mackliet C A, Schindler A I and Gillespie D J, Phys.Rev. B 1, 3283 (1970)

Magnetism Vol IV, Ed. Rado G and Suhl H Academic Press, New York (1966)

Matthias B T, Peter M, Williams H J, Clogston A M, Corenzwit E and Sherwood R C, Phys.Rev.Lett. 5, 542 (1960)

Mills D L and Lederer P, J.Phys.Chem.Sol. 27, 1805 (1966)

Mott and Jones, "The Theory of the Properties of Metals and Alloys" Oxford U P (1936)

Nagaoka J, Progr.Theor.Phys. 37, 13 (1967)

Nagasawa H, J.Phys.Soc.Japan 25, 691 (1968)

Napoli F and Sherrington D, J.Phys.F:Metal Phys. L53, 1 (1971)

Nielsen P E and Taylor P L, Phys.Rev. B 10, 4061 (1974)

Nozieres P, J.Low Temp.Phys. 17, 31 (1974)

Purwins H G, Talmor Y, Sierro J and Hedgcock F T, Solid State Comm. 11, 361 (1972)